Characterization of Molecular Glycerophospholipids by Quadrupole Time-of-Flight Mass Spectrometry

D I S S E R T A T I O N

zur Erlangung des akademischen Grades

Doctor rerum naturalium

(Dr. rer. nat.)

vorgelegt

der Fakultät für Biologie und Naturwissenschaften

der Technische Universität Dresden

von

Mag. Phil. Kim Ekroos

geboren am 22. September 1972 in Närpes, Finnland

Gutachter: Prof. Dr. Kai Simons (Technische Universität Dresden)

Prof. Dr. Bernard Hoflack (Technische Universität Dresden)

Prof. Dr. Konrad Sandhoff (Friedrich-Wilhelms-Universität Bonn)

Eingereicht am: 10. Oktober 2003

Tag der Verteidigung: 12. Dezember 2003

Acknowledgments

In the summer of 1999 at the European Molecular Biology Laboratory in Heidelberg, Kai Simons encouraged me to embark on an adventurous journey in lipid cell biology, my PhD. With the current lipid analysis methodologies it was not possible to dissect the molecular lipid components of lipid rafts, his vivid area of interest. My task was to change this and make it all possible, using the latest mass spectrometry techniques, under the supervision of Andrej Shevchenko. His laboratory became my outstation for the next years to come.

Reaching the finale of this magnificent and exploratory journey, I am very grateful to Kai Simons and Andrej Shevchenko for introducing me to the aspects of lipid rafts and mass spectrometry. In particular, I would like to thank Kai Simons and Andrej Shevchenko for their extraordinary support, supervision and encouragement during my thesis. Their stimulating and open-minded discussions deepened my interest for the chosen fields.

I would like to sincerely say "thank you" to all past and present members of the Simons and Shevchenko laboratories who contributed to an excellent working atmosphere. Intriguing discussions over experimental procedures and a shared interest in biological problems, and as equally important was their friendship and will remain for my future, of extraordinary value.

I thank Christer Ejsing for his unremitting help and collaboration, and of course for his friendship. I would like to thank Gustaf Selen and Eva Duchoslav for their patient and excellent expertise in the lipid software development, and Igor Chernushevich for his enormously helpful skill in QqTOF instrumentations. Moreover, I thank Sandra Jackson for sharing her intriguing research of human disorders and sample preparations. I thank Judith Nicholls for proof reading my thesis. I am grateful to Prof. Dr. Bernard Hoflack and Prof. Dr. Konrad Sandhoff for reviewing my thesis.

Finally, I would like to address my thanks to my parents, Maija and Göran, and my parents in law, Ingegerd and Ove Knekt, and last, but not least – my wife Marika for her tremendous and loving support over the past years.

Summary

The physical properties of glycerophospholipids (GPLs) are not only determined by the head group (HG), but also by their fatty acid (FA) chains, which affect their distribution and function within membranes in the cell. Understanding the microheterogenity of lipid membranes on a molecular level requires qualitative and quantitative characterization of individual lipids and identification of their FA moieties. The aim of my study was to introduce the new technology of multiple precursor ion scanning (MPIS) on a QSTAR Pulsar time-of-flight mass spectrometer (QqTOF) to analyze lipids. Detailed information on fatty acid composition of individual GPL molecules could be obtained in parallel with conventional profiling of lipid classes, and this could be done by direct analysis of total lipid extracts. This method was termed Fatty Acid Scanning (FAS) and Head Group Scanning HGS, respectively. In this way the molecular GPL composition of total lipid extracts could be charted in a single analysis accurately and rapidly at a low picomole concentration level. Furthermore, combining FAS and HGS together with ion trap MS^3 analysis allowed complete charting of the molecular composition of PCs, including quantification of their positional isomers, thus providing a detailed and comprehensive characterization of molecular composition of the pool of PCs. Development of the Lipid Profiler software allowed full automation and rapid processing of complex data, including identification and quantification of molecular GPLs.

This approach was evaluated by preliminary applications. First, the molecular composition of PCs of total lipid extracts of MDCK cells and of human red blood cells (RBC) could accurately be charted. Significant presence of positional isomers was observed increasing the total number of individual PC species close to one hundred. Secondly, the molecular PC and SM species distribution in detergent resistant membranes (DRMs) prepared by Triton X-100 DRMs were analyzed and were found to be enriched in distinct GPLs. The distribution in PCs and SMs of Triton X-100 DRMs of RBC were compared with those of the DRMs of MDCK cells. Finally, combining the use of a 96 well plate and a robotic system demonstrated that these analyses can be automated and analyzed with high throughput. This system we termed Shotgun Lipidomics. Taken together, this mass spectrometric methodology provides rapid and detailed insight into the distribution of the molecular GPLs of membranes and membrane sub-fractions.

Table of Contents

Index of Figures

Index of Tables

Abbreviations

Da   Dalton
DRM   detergent-resistant membranes
eV   electron volt
FAS   fatty acid scanning
FPV   fowl plague virus (A/strain)
HOAD   long-chain 3-hydroxyacyl-CoA dehydrogenase deficiency
HGS   head group scanning
GPL   glycerophospholipid
LysoPC   lyso-phosphatidylcholine
M   mass of an ion
MDCK II   Madin-Darby canine kidney cell strain II
MS/MS   product ion mass spectrometry
m/z   mass-to-charge ratio
OD600   optical density at 600 nm
PA   phosphatic acid
PC   phosphatidylcholine
PE   phosphatidylethanolamine
PG   phosphatidylglycerol
PI   phosphatidylinositol
PIS   precursor ion scanning
PIS *m/z* 184.1   scanning for precursor ions that produce a fragment ion with *m/z* 184.1 upon collision-induced dissociation
PS   phosphatidylserine
Q   quadrupole mass analyser
QqTOF   quadrupole time-of-flight
R Chain   respiratory chain complex 1 and 4 deficiency
RBC   red blood cells
rcf   relative centrifugal force
SM   sphingomyelin
TCM   total cell membranes
TFP   trifunctional protein deficiency
TOF MS   time-of-flight mass spectrometry
VLCAD   very long-chain acyl-CoA dehydrogenase deficiency
VSV   vesicular stomatitis virus
X/Y-GPL   GPL molecule with X fatty acid moiety at *sn*-1 position of the glycerol backbone, and Y fatty acid moiety at *sn*-2 position
{X;Y}-GPL   GPL molecule (or a mixture of isomeric molecules) comprising fatty acids X and Y at unidentified position of the backbone

1 INTRODUCTION

1.1   Cell biology and cell polarization

A fundamental problem in cell biology is to understand the architecture and characteristics of a particular cell type and its distinct differences to other cell types. This is approached by thoroughly elucidating the complex cellular morphogenesis involving diverse interplay between signal transduction, gene expression, organelle biogenesis, membrane trafficking and dynamic cytoskeleton networks. Insight is gained by dissecting individual processes down to the molecular level and then integrated into their cellular context for understanding how the cell architecture might be established.

Particular interest and effort has been, over past years, concentrated on understanding the mechanisms behind biogenesis of cell polarity. This has thoroughly been investigated in epithelial cells. These cells form a barrier between the exterior and the interior milieu. The tight junctions divide the cells in two distinct plasma membrane domains; an apical domain facing the outside and a basolateral domain facing the underlying extracellular matrix and blood supply (Rodriguez-Boulan and Nelson 1989). Both domains comprise a distinct set of proteins (Balcarova-Stander, Pfeiffer et al. 1984) and lipids (Hansson, Simons et al. 1986). To mimic the organization of the cell sheets formed in vivo, a major part of these investigations was performed on cells grown on permeable filter supports. By infecting cells with enveloped viruses they distribute their glycoproteins either to the apical or the basolateral membrane domain. The vesicular stomatitis virus (VSV) preferably selects a basolateral route (Fuller, von Bonsdorff et al. 1984) whereas influenza virus, as the fowl plague (FPV) strain, selects the apical route (Matlin and Simons 1984). The glycoproteins of these viruses have therefore become essential tools in investigating the mechanisms behind polarized sorting and segregation. Furthermore, studies on the delivery of newly synthesized sphingolipids in epithelial MDCK cells showed that a simple glycosphingolipid, glucosylceramide, was preferentially transported to the apical membrane (Simons and van Meer 1988). Together with this, it was suggested that clusters of sphingolipid domains function as platforms for cargo as glycosylphosphatidylinositol (GPI) -linked proteins (Brown and Rose 1992) and influenza hemagglutinin (HA) proteins but not the G protein of VSV (Scheiffele, Roth et al. 1997; Scheiffele, Rietveld et al. 1999). The sphingolipid microdomains enriched in cholesterol

(Simons and Ikonen 1997) – termed rafts- are insoluble to nonionic detergents, such as Triton X-100 (Brown and Rose 1992). Therefore, detergents have become a valuable tool for investigating the protein and lipid composition of rafts.

Taken together, these thorough studies have clearly enabled detailed knowledge of the mechanisms behind biogenesis of cell polarity in epithelial cells. Still, there is not sufficient capacity of the tools, especially the ones used for lipid analysis, used to dissect the machinery involved. This should be approached by comprehensive lipid analysis that enables fast and sensitive quantitative information of the molecular species present. In this way, new insights into how the individual lipid molecules are involved in different biological events could be revealed. Furthermore, it will be essential to analyse lipids in concert with the proteins involved.

1.2   Cell membranes and lipid rafts

Contrary to the classical view of the plasma membrane as a homogenous glycerophospholipid (GPL) assembly that is loaded with proteins, proposed by Singer and Nicholson (Singer and Nicolson 1972), it is now accepted that the plasma membrane is heterogeneous. Biological membranes are structurally and compositionally complex. The structural complexity is the result of the physicochemical properties of the individual membrane components, which is governed by its composition and chemical environment. Compositional complexity arises through chemical diversity of the membrane constituents. In general, eukaryotic membranes are mainly composed of glycerophospholipids (GPLs), sphingolipids and sterols (Figure 1). Sterols show little structural variation, compared to that of GPLs and sphingolipids, in which structural diversity originates through variability of the polar head groups and the apolar hydrocarbon chains (e.g. carbon chain length, degree of saturation, hydroxylation, branching). This structural variation yields a multitude of similarly built molecules with diverse physical properties, which in concert with membrane proteins, regulate membrane properties in a dynamic fashion.
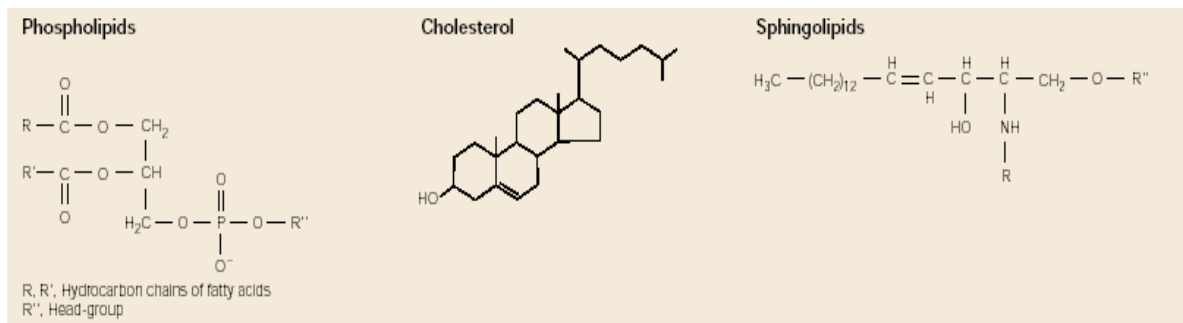
Figure 1. Chemical structures of phospholipids, cholesterol and sphingolipids. From (Simons and Toomre 2000).

Various explanations of the compositional complexity of biological membranes exist. One interesting concept today is the existence of membrane rafts (Figure 2) (Simons and Ikonen 1997). Lipid rafts are enriched in sphingolipids, sterols, and are mainly comprised of saturated GPLs (Brown and London 1998; Brown and London 2000). Lipid rafts have been implicated in processes such as transmembrane signal transduction (Simons and Toomre 2000), sorting and trafficking through the secretory and endocytotic pathways (Ikonen 2001), prion diseases, Alzheimer's disease and cancers (Anderson 1998; Ehehalt, Keller et al. 2003). In addition to the diverse role of rafts, many viruses, bacteria and protozoan parasites exploit host microdomains to infect target cells (Manes, del Real et al. 2003). Host rafts are hijacked by intracellular pathogens at different points in the infective process as gateways for entry into the cell, to create sheltered environments in which to replicate, to prevent host immune responses by co-opting signalling pathways or to generate areas in which new pathogens can be assembled efficiently.
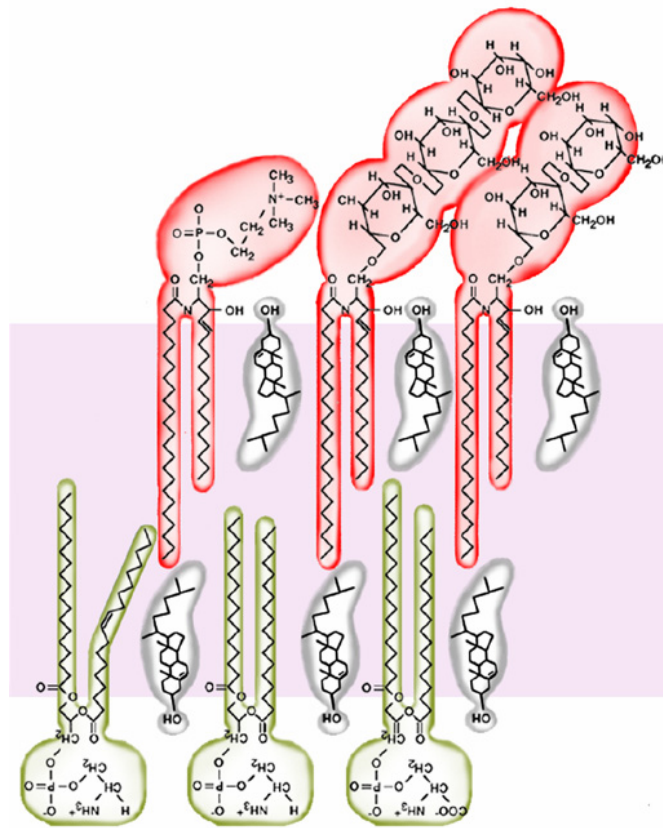
Figure 2. Model of a raft microdomain. From (Simons and Ikonen 1997).

It is most likely that different rafts exist. A common biochemical method to analyze the domain organization of membranes is extraction with mild detergents like Triton X-100. Although detergent treatment disrupts most lipid–lipid interactions, a minor fraction of cell membranes is preserved and can be isolated as detergent-resistant membranes (DRMs). DRMs prepared with Triton X-100 probably originate from the cholesterol- and sphingolipid-rich liquid-ordered (l_o) phase, which resists extraction due to its tight lipid packing (Brown and London 1998). Detergent extraction also disrupts lipid–protein interactions, so that most membrane proteins are solubilized. Only a few proteins retain their association with lipids and are recovered in DRMs. Thus, DRM association of a protein is indicative of a strong interaction with highly ordered domains in the l_o phase. However, DRMs may only imperfectly reflect the distribution of membrane components between the l_o and liquid disorder (l_d) phases (London and Brown 2000), and it is unknown how well the composition of DRMs correlates with the components of native lipid rafts in cell membranes. DRMs have mainly been prepared with Triton X-100 (Brown and Rose 1992) and 3-(Bohuslav, Cinek et al.)-1-propanesulfonate (CHAPS) (Kurzchalia, Dupree et al. 1992), but other detergents such as Brij 58 (Bohuslav, Cinek et al. 1993), Brij 96

(Madore, Smith et al. 1999), Lubrol WX (Roper, Corbeil et al. 2000), and Brij 98 (Drevot, Langlet et al. 2002) have also been used. Yet, it is unclear whether DRMs of different cell types prepared with Triton X-100 similarly reflect the same aspect of membrane organization, *i.e.*, segregation of cholesterol- and sphingolipid-rich domains in the l_o phase from the l_d phase rich in unsaturated glycerophospholipids.

Another biochemical method to analyze the raft domain organization is the use of enveloped viruses. It is known that the GPL composition of the viral envelope closely reflects that of the plasma membrane of the host cells (Pessin and Glaser 1980). The influenza hemagglutinin (HA) protein is shown to be associated with rafts, whereas the G protein of VSV is not raft-associated by using DRM behaviour as a criterion (Scheiffele, Roth et al. 1997; Scheiffele, Rietveld et al. 1999). Lipid composition of the FPV envelope should therefore closely mimic the lipids of raft domains. On the other hand, the lipid composition of the VSV envelope should thus be different. Several studies have shown that FPV and VSV have different lipid composition (van Meer and Simons 1982; Blom, Koivusalo et al. 2001). However, caution has to be taken in how the viruses are produced since this might affect the lipid composition of the viral envelope. So far, it is unclear from these approaches how the individual molecular lipid species are distributed within the viral envelope and to what extent they reflect the host membranes.

1.3   Glycerophospholipids

GPLs are the main constituents of cellular membranes, consisting of a polar headgroup with a phosphate moiety and two fatty acids that are attached to the glycerol backbone. Many structural variants are therefore possible within each class of lipids since the headgroup can be combined with a large pool of fatty acids that vary in both chain length and degree of saturation. This yields a multitude of similarly built molecules having a large diversity of physical properties, which allows the living cell to regulate the intrinsic heterogeneity of membranes in a dynamic fashion.

Phosphatidylcholines (PC) (Figure 3) are the most abundant GPLs in mammalian cells, accounting for more than 30% of the total lipid content (Kawai, Fujita et al. 1974) and are mainly located on the outer leaflet of the plasma membrane (Renooij, Van Golde et al. 1976). In mammalian cells PCs are synthesised *via* the CDP-choline pathway or *via* the phosphatidylethanolamine methylation pathway (Cui, Vance et al. 1993; Kent 1995; Walkey, Yu et al. 1998). Further metabolism involves remodelling processes, which are

controlled by a coordinated action of acyltransferases, transacylases, and lipases (Yamashita, Sugiura et al. 1997). Inhibiting the CDP-choline pathway is lethal (Cui, Houweling et al. 1996; Baburina and Jackowski 1998) and is not compensated by the alternative phosphatidylethanolamine methylation pathway, presumably because different PC species are produced (DeLong, Shen et al. 1999; Waite and Vance 2000). The majority of *de novo* synthesized PCs are believed to comprise of saturated fatty acids at the position *sn*-1 and unsaturated fatty acids at the position *sn*-2 (Arvidson 1968; Akesson, Elovson et al. 1970), although they might be altered by subsequent remodeling (Lands and Hart 1965; Okuyama, Yamada et al. 1975; van Heusden, Reutelingsperger et al. 1981). Certain cellular compartments and membrane microdomains are distinguished by a characteristic composition of PCs, in which very long chain, or saturated, or highly unsaturated fatty acid moieties prevail (Ramanadham, Hsu et al. 2000; Simons and Toomre 2000; Brooks, Clark et al. 2002; Igbavboa, Hamilton et al. 2002). One main function of PC is to serve as a reservoir for several lipid messengers: it is the source of the bioactive lipids diacylglycerol, phosphatidic acid, lysophosphatidic acid, platelet-activating factor and arachidonic acid (Exton 1994; Brindley, Abousalham et al. 1996; Vance and Vance 1996).

Phosphatidylethanolamine (PE) and phosphatidylserine (PS) (Figure 3) are two other major GPLs in mammalian cells. These aminophospholipids are mainly localized in the inner leaflet of the plasma membrane. Biosynthesis of PE in eukaryotes can occur via several pathways. The main one is the CDP-ethanolamine pathway constituting the de novo synthesis of PE first described by Kennedy and Weiss in 1956 (Kennedy and Weiss 1956). PE can also be generated by decarboxylation of PS. On the other hand, PS is generated by a base-exchange reaction in which the headgroup of the pre-existing GPL is exchanged for serine. As for PC, both PE and PS undergo similar remodelling processes, which are controlled by a coordinated action of acyltransferases, transacylases, and lipases (Yamashita, Sugiura et al. 1997). Aminophopsholipids have been shown to take part in the regulation of several processes such as blood coagulation (Bevers, Comfurius et al. 1983), cell adhesion (Tanaka and Schroit 1983; McEvoy, Williamson et al. 1986), and endocytosis (Devaux 1991). Furthermore, PS has been exposed as a hallmark of apoptosis (Fadok, Voelker et al. 1992) and is enriched in the HIV envelope functioning as a cofactor for infection of monocytic cells (Callahan, Popernack et al. 2003).

Phosphatidylinositol (PI), phosphatidylglycerol (PG) and phosphatidic acid (PA) (Figure 3) are minor GPL constituents of mammalian cells. PI is located predominantly on the inner leaflet of the plasma membrane and is mainly synthesised via the CDP-

diacylglycerol (CDP-DG) pathway from PA. PI kinases further phosphorylate sequentially 4, 5 and 3 positions of the inositol ring of the phosphatidylinositols to form PI-4-phosphate, PI-4,5-bisphosphate and PI-3,4,5-trisphosphate. Other permutations are also possible. These products have been implicated as active intracellular regulatory factors and signalling molecules. In general PG comprise less than 1 % of total GPL in mammalians and are mainly located in mitochondria. Synthesis of PG also uses the CDP-DG pathway. PG is usually further converted into diphosphatidylglycerol (DPG), also named cardiolipin.

Sphingosine-based lipid sphingomyelin (SM) is comprised of a choline headgroup as PC and therefore is a phosphosphingolipid (Figure 1). As in the case of PC, SM is predominantly located on the outer leaflet of the plasma membrane. SM is particularly relevant for the cellular physiology because of the property to cluster cholesterol in the plane of the membrane. These clusters make up the basis for rafts in the plasma membrane. Furthermore, SM has a regulatory role in the cells and participates in cellular signalling (Huwiler, Kolter et al. 2000).

R₁ : hydrocarbon chain of *sn*-1 fatty acid
R₂ : hydrocarbon chain of *sn*-2 fatty acid
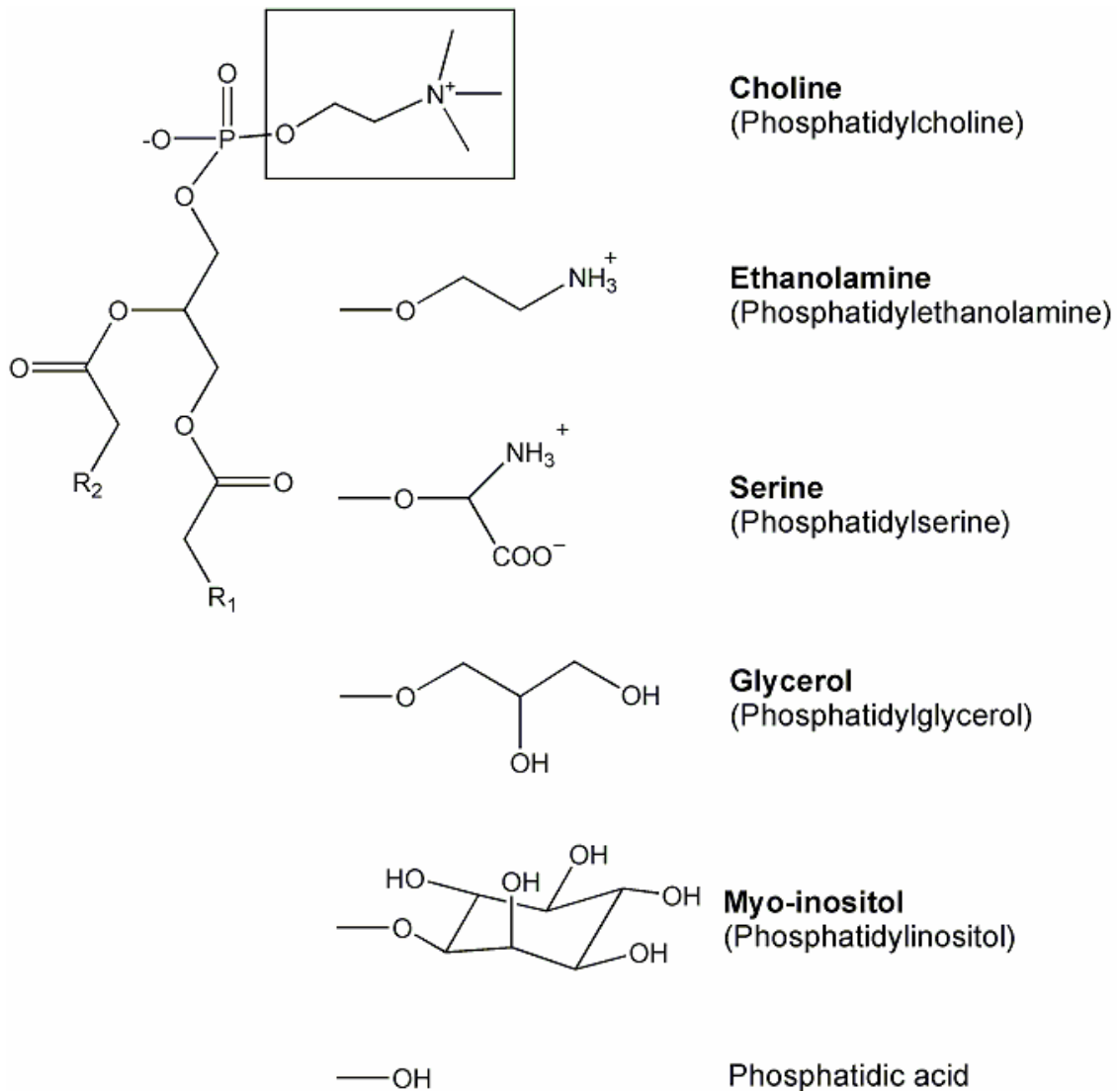
Figure 3. Structural overview of the major GPL classes. Head groups for the other classes of GPL are shown.

GPL biosynthesis and distribution are firmly regulated qualitatively and quantitatively and are coordinated within the cell allowing particular events to take place spatially and temporally. This requires that the large pool of molecular species constantly undergoes rearrangements inside the living cell. The composition of molecular GPL species changes with the state of the cell and their total levels are similar to neighbouring cells of the same type. Thus, similar profiles and levels in total molecular GPL species can be expected between two cells of the same kind. Defects and/or disturbances in the lipid and/or protein pathways might lead to cellular dysfunctions and lead to disease states. On the cellular level, such dysfunctions are often observed as particular changes in certain GPL classes

and/or molecular species. In the case of certain forms of cancer (Ramanadham, Hsu et al. 2000; Ivanova, Cerda et al. 2001; Xiao, Schwartz et al. 2001; Xie, Gibbs et al. 2002) elevated levels in distinct GPLs are observed. Therefore, a complete GPL profile showing the quantitative abundance of different molecular species could potentially be used to predict the state of a cell.

1.4   Analysis of GPLs

In order to gain further insight into the compositional basis of microdomains and other membrane-related phenomena, analytical methodology is needed which can quantify individual lipid species and subtle compositional changes. Conventional analytical technologies for lipid analysis, such as high-performance liquid chromatography, thin-layer chromatography, and gas chromatography are mostly used for characterization of global perturbations of lipid composition (Blank, Robinson et al. 1984; Kuypers, Butikofer et al. 1991; Connor, Lin et al. 1997). These techniques are time-consuming, labor-intensive, require a relatively large amount of sample, and can be prone to biased losses of certain types of lipids (DeLong, Baker et al. 2001).

Improvements in mass spectrometric technology have made it possible to quantify lipid species in unprocessed extracts by electrospray ionisation mass spectrometry (Han and Gross 1994; Kerwin, Tuininga et al. 1994; Han and Gross 1995). This analytical methodology is less time-consuming compared to that of conventional methods, and requires less sample amount because of its high sensitivity. The specificity and reliability of the methodology has been further improved by the use of precursor ion scanning (PIS) (Brugger, Erben et al. 1997). This method allows the specific detection of molecular ions (precursor ions) that, upon collision-induced dissociation (CID) through collision with neutral gas molecules in the collision cell of a mass spectrometer, generate characteristic product ions. For example, when performing analysis in positive ion mode, PC and SM are readily detected as molecular ions due to the positively charged quaternary amine of the choline head group (Figure 8). Upon CID these ions generate a characteristic fragment ion of the phosphorylcholine head group with mass-to-charge ratio (m/z) of 184.1. This property allows quantitative profiling of PC and SM species by PIS m/z 184.1 (Brugger, Erben et al. 1997). Furthermore, this could be performed at the low picomole concentration level of the analyte. In the same way, other GPL classes generate characteristic fragment

ions upon CID which later on can be selected for PIS (Table 6). Notably, in precursor ion scanning mode, all GPLs, except for PC, are preferentially detected as negatively charged molecular ions. Upon CID, these ions produce acyl anions of corresponding fatty acid moieties attached to the glycerol backbone of the glycerophospholipids (Hsu and Turk 2000; Hsu and Turk 2000; Hsu and Turk 2000; Hsu and Turk 2000; Hsu and Turk 2001). Depending on the nature of the GPLs, the acyl anions are differently produced. For acidic GPLs, as PA and PS, dissociation of the *sn*-1 fatty acid is preferential in respect to the *sn*-2 fatty acid, thus generating a more abundant acyl anion (Hsu and Turk 2000). This is presumably due to the closer distance of the phosphate group to the *sn*-1 fatty acid in these GPLs. For more basic GPLs, as PE, PI and PG, this is reversed. Here, dissociation of the *sn*-2 fatty acid is preferential over the *sn*-1 fatty acid (Hsu and Turk 2000; Hsu and Turk 2000; Hsu and Turk 2001; Larsen, Uran et al. 2001), so this information allows position determination of the attached fatty acids. The mechanisms behind this are mainly depending on the head group characteristics and the balance between the neutral loss as fatty acid and as ketene ions, generated upon CID of the intact lipid molecule ions.

Electrospray ionisation mass spectrometry has already been applied in several studies on lipid composition (Fridriksson, Shipkova et al. 1999; Blom, Koivusalo et al. 2001), lipid trafficking (Heikinheimo and Somerharju 2002), lipid metabolism (DeLong, Shen et al. 1999; Schneiter, Brugger et al. 1999; Brooks, Clark et al. 2002; Hunt, Clark et al. 2002; Boumann, Damen et al. 2003), and for structural characterisation of lipids (Levery, Toledo et al. 2001; Beckedorf, Schaffer et al. 2002). The studies on lipid metabolism have been able to address issues such as enzyme substrate specificity and fatty acid remodelling in vivo. Use of stable isotope labeled precursors for PC metabolism has shown that the two pathways that synthesised PCs produce different molecular species (DeLong, Shen et al. 1999; Boumann, Damen et al. 2003).

Importantly, so far no identification and quantification software for individual GPL species exists. All evaluation of the mass spectrometric data has, in general, been manually performed. Therefore, identification of GPL species of small pools of data can already be very time consuming, which, furthermore, dramatically extends if a quantitative approach is required. To this point, no significant effort has been taken to overcome this by making mass spectrometric data analysis more automated and high-throughput directed.

1.5   Electrospray ionization mass spectrometry (ESI-MS)

Mass spectrometry is a method that determines the mass-to-charge ratios (*m/z*) of ions and detects their intensity. A mass spectrum is a plot of ion abundance versus *m/z* (*q.v.* Figure 8), where the *m/z* axis can be presented in Dalton (Da) per unit charge. By using mass spectrometry, accurate mass estimates of a given molecular ion, the abundance, and, in case of tandem mass spectrometry (excluding any orifice fragmentation), the structural information can be obtained.

There are three main components of a mass spectrometer: an ionization source, mass analysers, and a detector (Figure 4). By various physical mechanisms (electron impact, or electrospray ionization etc.) the ion source generates ions in gas phase, which are then focused and transported by ion optics into mass analysers that separate ions of different *m/z* for final registration by a computer-assisted detection system. This analysis is performed by operating the mass analyzers and detector at pressures the range of 10^{-5} to 10^{-7} Torr[1].

Figure 4. The basic components of a mass spectrometer. The collision cell is typically not an analyzer, and normally located between mass analyzers or directly after.

The following sections outline some basic features of mass spectrometric techniques pertinent to this thesis. Electrospray ionization, the basic features of mass analysers, and the operational modes of mass spectrometers are highlighted.

Regardless of the ionization method applied, a successful ionization requires that energy is transferred to the analyte. This turns out to be extremely important, because the applied energy and the way it is applied determine the produced mass spectrum. Ionization methods can be termed hard and soft. Hard ionization methods (e.g. electron ionization) occur in two steps: the analyte is first volatilized and then ionized. This type of ionization process limits the scope of molecules that can be analyzed to relative low molecular mass compounds that are thermally stable and volatile. Not surprisingly, hard ionization methods have a limited applicability to biological studies because of high molecular mass and polarity of biological compounds. Soft ionization techniques allow larger, non-volatile

and thermally labile compounds to be transferred into gas-phase. Electrospray ionization is one type of soft ionization method that has proved highly valuable in biological studies. This ionization method produces analyte ions primarily via protonation (in positive ion mode) or deprotonation (in negative ion mode), or via formation of adduct cations of alkaline metals (e.g. Li^+) or adduct anions (e.g. Cl^-). The development of electrospray ionization was recognized by the 2002 Nobel Prize in Chemistry awarded to John B. Fenn.

The basics tenets of electrospray ionization are reviewed in (Cole 2000). Electrospray ionization generates molecular ions at atmospheric pressure by passing a liquid sample through a small capillary, which is subjected to potential and pressure gradients. As a result of electrolytic processes occurring in the capillary, liquid emerges at the exit of the capillary and elongates in the direction of the gradients. The elongated surface of the liquid is termed a Taylor cone. From the apex of the Taylor cone a 'jet' of liquid droplets forms because the charge density at the apex attains such a high value that the surface tension of the liquid can no longer hold together the emerging fluid. Droplet formation is favored because the excess charge can be spread over a larger surface area, thereby reducing the Coulomb energy. By this process a fine spray of charged droplets of a single polarity is formed and directed along the potential gradient. As solvent evaporates from charged droplets, the size of the droplets becomes smaller. Since the charge of the droplets remains constant, increasing electrostatic stress at the surface of the droplet will result. As a consequence, droplets will undergo 'Coulomb fission', a process that makes the droplets disintegrate into even smaller droplets (Figure 5). The droplet fission process may repeat itself upon further shrinkage of a droplet.
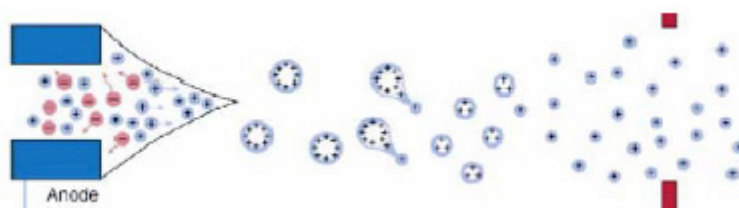
Figure 5. Schematic overview of electrospray ionization.

Two mechanisms have been suggested to explain the process by which gas-phase ions originate from small, highly charged droplets. The charged residue model depicts a series of fission events that ultimately lead to the production of smaller droplets that bear an excess charge and a single analyte molecule. As the remaining solvent molecules

evaporate, the excess charge will rest on the analyte thereby producing a gas-phase analyte ion. The evaporation mechanism model depicts solvated analyte ions being directly emitted from charge droplets after the radii of the droplets decrease to a suitable size. Research has indicated that both processes occur, and that a critical parameter in determining the mechanism is the mass of the analyte. Larger analyte ions seem to be produced via the charged residue model (i.e. >3.3 kDa), whereas smaller analyte ions can be generated by both mechanisms.

Depending on the flow rate of the electrosprayed liquid, electrospray ionization can be subdivided into microelectrospray (Emmett and Caprioli 1994) and nanoelectrospray (Wilm and Mann 1996). Microelectrospray ion sources maintain flow rates over 500 nL/min, whereas nanoelectrospray are of approximately 30 nL/min.

The function of mass analyzers is to separate ions according to their *m/z*. Quadrupole mass analyzers (Qs) are ion beam analyzers. These devices are usually composed of four rods with cylindrical geometry arranged in a specific three-dimensional fashion (Figure 6A). By applying a combination of direct current and relative frequency voltages to the rods, ions can be transmitted through the analyzer. The analyzer can be operated in three modes, depending on the selection of voltages and frequencies: (i) all ions with *m/z* within a certain interval (e.g. 200 to 1000 Da per unit charge) can be transmitted simultaneously, (ii) ions of a given *m/z* ratio can traverse the analyzer, whereas ions with different *m/z* ratios collide with the rods and are lost, or (iii) ions of increasing *m/z* can be made to pass successively through the analyzer in small intervals (e.g. 0.1 to 0.2 Da). In the last mentioned operation mode, the quadrupole mass analyzer is said to be scanning, and is a feature that is essential for PIS experiments, as outlined below.
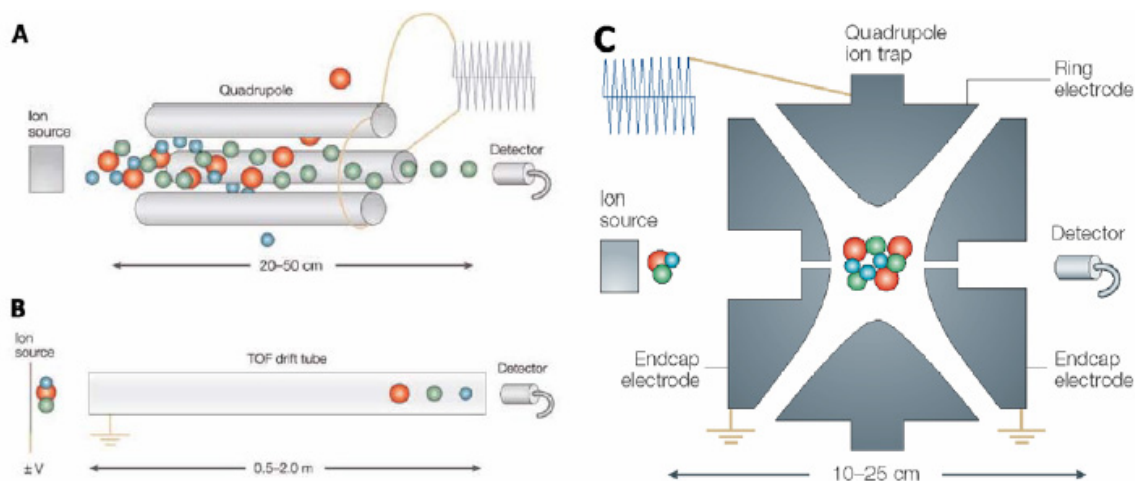
Figure 6. Schematic overview of mass analyzers. **(A)** Schematic of a quadrupole mass analyzer. The top rod is not shown since the view is from above. **(B)** Schematic of a time-of-flight analyzer. **(C)** Schematic of a quadrupole ion trap mass spectrometer. The ion trap analyzer is composed of the two end-cap electrodes and the ring electrode. From (Glish and Vachet 2003).

The time-of-flight analyzer is a relatively simple device (Figure 6B). In this type of analyzer, ions are pulse-accelerated into a field-free time-of-flight drift tube. Based on difference in obtained velocity, ions will be separated according to *m/z*. Since all ions acquire the same energy during the pulse, ions of lower *m/z* ions achieve higher velocities than the higher *m/z* ions. Thus, the *m/z* of ions can be determined by measuring the time it takes for the ions to travel a fixed distance.

Quadrupole ion trap mass analyzers are composed of two end-cap electrodes and one ring electrode (March 1997; Glish and Vachet 2003) (Figure 6C). Ions are injected in the trap over a short period of time and are then maintained in stable orbits within the trap by means of electrostatic fields. By changing the voltages on the electrodes, and thereby the electric fields, the orbits of ions can be made unstable in an *m/z* selective manner. By correct choice of voltages, ions can be ejected for either detection, or the isolation of ions of a given *m/z*. Isolated ions can subsequently be subjected to collision-induced dissociation, and produce fragment ions that can then be trapped in the analyzer (MS^2). Fragment ions can be ejected for either detection or for another round of ion isolation and collision-induced dissociation (MS^3). This operational feature can be repeated virtually an unlimited number of times (MS^n), and therefore make quadrupole ion trap mass analyzers suitable for detailed structural characterization of analyte ions, e.g. for protein sequencing.

1.6 QSTAR Pulsar *i* hybrid quadrupole time-of-flight mass spectrometer (QqTOF)

The mass spectrometer used for most experiments presented in this thesis is a hybrid quadrupole time-of-flight (QqTOF) mass spectrometer. These instruments were introduced a few years ago (Morris, Paxton et al. 1996; Shevchenko, Chernushevich et al. 1997) and revolutionized the field of structural characterization of biomolecules by acquiring tandem mass spectra with high resolution, mass accuracy, and sensitivity provided by parallel detection of all ions (no scanning). The basic features of this instrument are a ionization source (*i.e.* nanoelectrospray and liquid chromatography (LC)), three quadrupoles, a reflecting time-of-flight analyzer, and a multiple anode detector combined with a multichannel time-to-digital converter (Figure 7) (Chernushevich, Loboda et al. 2001). The configuration of the mass analyzers can be regarded as the replacement of the third analytical quadrupole (Q3) in a triple quadrupole mass spectrometer by a time-of-flight analyzer.

The three quadrupoles of the QqTOF mass spectrometer have independent functions. The first quadrupole (Q0) serves to focus and transfer ions originating from the ionization source, the second (Q1) is a mass filter quadrupole that can separate ions, and the third quadrupole (Q2) functions as a collision cell where analyte ions can be fragmented by the process of collision-induced dissociation through collision with neutral gas molecules (i.e. N_2 or Ar).
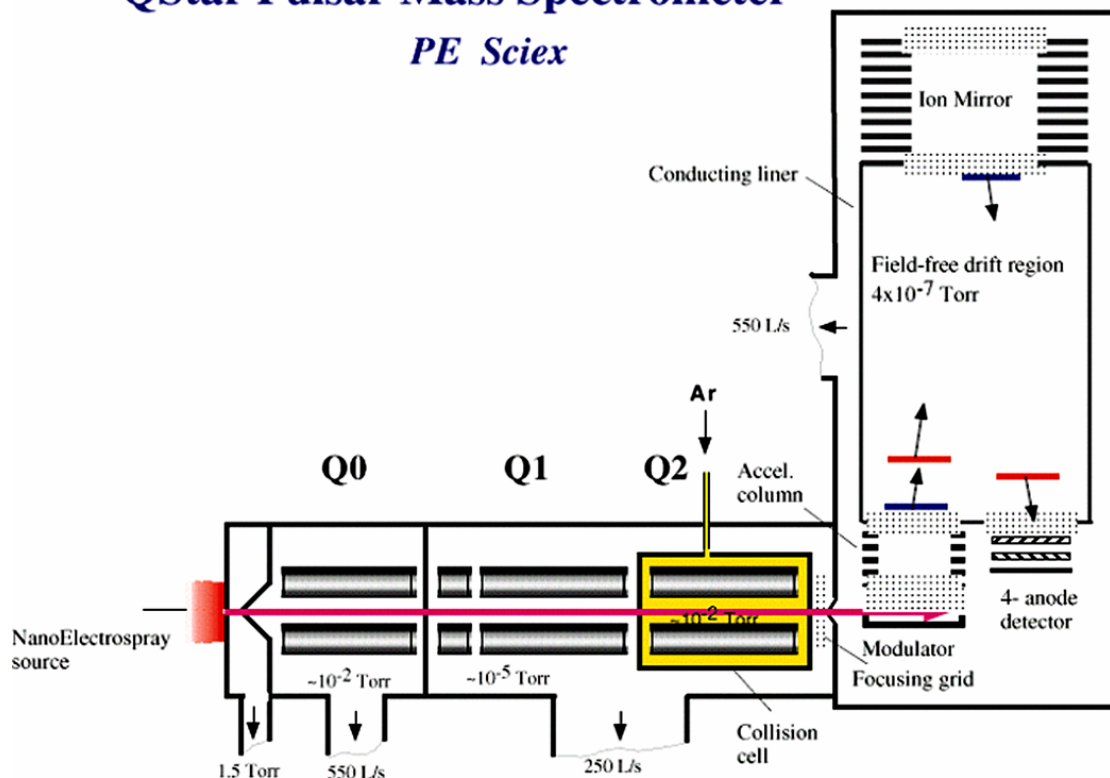
Figure 7. Schematic overview of the QqTOF mass spectrometer. From the Operator Manual of QSTAR Pulsar-i.

In the time-of-flight section, ions entering from Q2 are detected. The basic components of the time-of-flight analyzer in the QqTOF mass spectrometer are an ion accelerator, an ion mirror, and the ion detector. The ion accelerator serves to accelerate ions, which are then separated in the drift tube based on difference in obtained velocity. The ion reflector functions to reverse the direction of the ion. This instrumental feature improves spectral mass resolution by reducing variation in kinetic energy of obtained ions in the modulator.

Practically, a QqTOF mass spectrometer can be operated in three modes: (i) time-of-flight mass spectrometry (TOF MS), (ii) product ion mass spectrometry (MS/MS), and (iii) precursor ion scanning (PIS).

In TOF MS mode, the mass filter quadrupole (Q1) is operated in rf- (radio frequency) only mode, *i.e.* all ions having a broad range of *m/z* is transmitted simultaneously, and the time-of-flight section is used to record spectra. This yields a mass spectrum of all ionizable compounds present in the electrosprayed analyte (*q.v.* Figure 15). The obtained TOF MS spectrum only provides information regarding molecular mass and

number of charges of a given analyte ion, no information regarding the structure can be obtained.

In MS/MS mode, Q1 is operated in the mass filter mode to transmit only a precursor ion of interest within a certain mass window (typically of 1-3 Da). Precursor ions are then accelerated into the collision cell (Q2) where they undergo collision-induced dissociation through multiple collisions with gas molecules. Resulting product ions (and remaining precursor ions) then pass into the time-of-flight section for detection. The obtained MS/MS spectrum reflects a fragmentation pattern from which structural information about the specific precursor ion can be derived (*q.v.* Figure 9A).

In PIS mode, precursor ions that generate a specific product ion are detected. In this mode, the Q1 is scanning over a mass range of interest. Sequentially, ions are accelerated into the collision cell where they undergo collision-induced dissociation. Generated fragment ions are then transmitted into the time-of-flight section for detection. Any precursor ion of a given *m/z* ratio that produces a specific product ion will be recorded. In this way a Q1 mass spectrum is generated that shows all precursor ions which produce a product ion of interest.

The advantage of PIS has made it very attractive in the analysis of GPL species (Brugger, Erben et al. 1997). However, no efficient precursor ion scanning has been possible on QqTOF machines (Bateman 1998). In PIS mode, the analysis does not benefit from a non-scanning acquisition of spectra by the TOF analyzer. On the contrary, the sensitivity of detecting a selected fragment ion (the very essence of precursor ion scanning) is limited by the duty cycle that can be as low as 5% for low molecular weight species. The breakthrough emerged when the ion trapping and bunching technology was introduced in QSTAR Pulsar mass spectrometers (Chernushevich 2000). Fragment ions of a given *m/z* can be trapped temporarily in the collision cell and then released as a short ion packet into the TOF analyzer. In this way, 100% duty cycle can be achieved for any fragment ion, and it is improved significantly for ions with *m/z* close to the specified one (Chernushevich, Loboda et al. 2001).

This makes QSTAR Pulsar instruments attractive for lipid analysis because inherent features of the TOF analyzer, such as high mass accuracy, resolution, and non-scanning acquisition of spectra, can help to overcome the limitations imposed by conventional quadrupole mass filters. This would allow performing a virtually unlimited number of PIS - termed Multiple Precursor Ion Scanning (MPIS) – that can be acquired at

the same time. In addition, each product ion of interest can be detected with high mass accuracy (0.1 Da). These features make the performance of PIS on QqTOF mass spectrometers superior to those of triple quadrupole mass spectrometers. First of all, triple quadrupole mass spectrometers can only perform one PIS a time due to single ion recording of the third analytical quadrupole (Q3). Secondly, PIS can only be performed using relatively poor mass selection (4 Da) due to the otherwise insufficient number of ions required for detection.

1.7   The aim of the present study

The objective of the work underlying this thesis was to evaluate the multiple precursor ion scanning technology on a quadrupole time-of-flight mass spectrometer for characterization of molecular glycerophospholipids, and how to enhance the complete lipid analysis

Another objective was to examine how to determine positional isomers of phosphatidylcholine (PC) of total lipid extracts using multiple precursor ion technology on a quadrupole time-of-flight mass spectrometer and MS^n analysis on an ion-trap mass spectrometer.

A further objective was to evaluate the mass spectrometric approach to characterize the molecular glycerophospholipids of detergent-resistant membranes.

Finally, a perspective in how to manage an automatic high throughput analysis of molecular glycerophospholipids is evaluated.

2   RESULTS

2.1   Detection and quantification of molecular GPLs of total lipid extracts by MPIS

2.1.1   HGS accurately detects species based on their brutto composition

The QqTOF instrument was always calibrated and optimized by performance before any mass spectrometric analysis. We found it particularly convenient to use a synthetic lipid PC standard for calibrating the TOF analyzer in positive ion mode. Regardless of the employed ion source (conventional- or nanospray) PCs are always detected as singly charged species. PCs are easy to fragment and the characteristic fragment of the head group, that contains the tertiary amino-group, is obtained with high yield (fragmentation mechanisms are reviewed in Cheng and Gross 2000). For calibration we typically used 250 fmol/µL solution of 1,2-dilignoceroyl-*sn*-glycero-3-phosphocholine (DGPC) in methanol/chloroform 2:1 (v/v), containing 5 mM ammonium acetate. The solution is stable for months at -20º C. To avoid possible overlap of the low *m/z* reference peak with peaks of background, the instrument was calibrated in MS/MS mode. First analytical quadrupole (Q1) was operated under low resolution settings that enabled unperturbed transmission of the entire isotopic cluster of the precursor. Peaks of the intact precursor and of the head group fragment were used as the high *m/z* and low *m/z* reference masses, respectively. Applying medium collision energy (38 eV) allowed us to balance the intensity of both peaks (Ekroos and Shevchenko 2002). On the other hand, synthetic standards of PE, PS or PG that are detected as anions were used as standards for calibrating the QqTOF instrument in negative ion mode.

By accurately selecting the *m/z* of the characteristic head group fragment ion in precursor ion scanning mode enables, in general, specific detection of one particular lipid class. This was termed H̲ead G̲roup S̲canning (HGS).

Next, the performance of HGS on the QqTOF instrument was evaluated. Since different lipid types have the same head group conformation, both classes are simultaneously detected. For example, selection in PIS of the characteristic phosphorylcholine fragment ion *m/z* 184.1 (PIS *m/z* 184.1) detects not only PC species but

also SM species (Figure 8) (Brugger, Erben et al. 1997). By trapping the ions temporarily in the collision cell, Q2, a 6 to 8-fold increase in the intensity was observed. After 10 acquired scans (summed), an intensity of the SM 16:0 reached close to 3500 counts per second (cps). By non trapping this was approximately 700 cps. The same thing was observed with the 32:0-PC. Even in a wider *m/z* range the ratio between peaks was constant using with and without the ion trapping conditions. This clearly indicated extreme reliability and enhancements in the trapping conditions. Notably, similar results were obtained in analysis of other GPL classes and, importantly, by performing multiple precursor ion scans (MPIS) simultaneously.

From the PC species detected in HGS, the fatty acid composition of the molecular species can not directly be determined, but rather the total number of carbon atoms and the total number of double bonds in fatty acid moieties. On the other hand, since mammalians contain mainly sphingosine in their ceramide backbone, fatty acid composition of SM species can be determined. Notably, due to existence of other ceramide backbones in mammalians, the exact species determination is not absolute (Huwiler, Kolter et al. 2000). The typical selected fragment ions of GPLs in HGS are illustrated in Table 6.
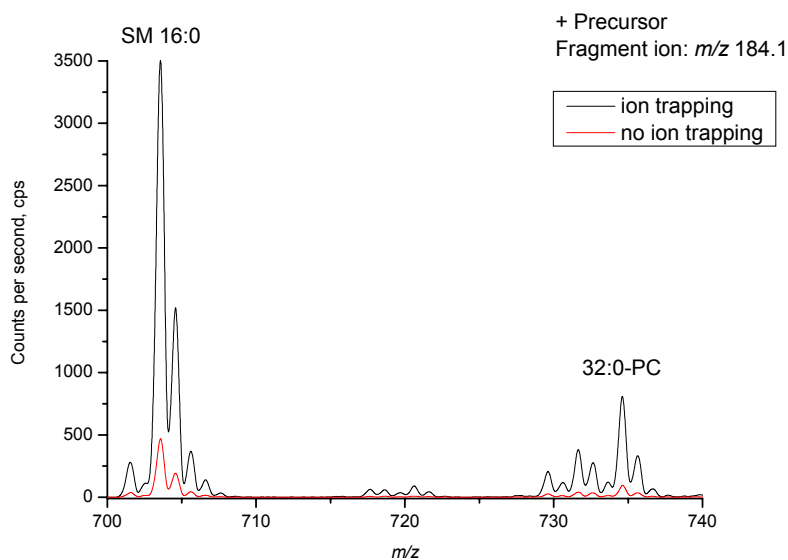
Figure 8. Detection of PC and SM by PIS m/z 184.1 using ion trapping. A 6 to 8-fold increase in both SMs and PCs is observed by using ion trapping (black line) in comparison to no ion trapping (red line). The collision energy was set to 40 eV.

2.1.2   FAS accurately detects anionic molecular species

However, HGS scan does not reveal what fatty acid radicals are present in the particular lipid molecule and the intensity of detected peaks merely reflects "average" concentration of a pool of isobaric molecules, rather than the concentration of the chemically individual lipid.

Hsu and Turk demonstrated previously that, in negative ion mode, low energy CID of major GPLs, *i.e.* PE, PS, PI, PG and PI, might produce acyl anions of their fatty acid constituents (Hsu and Turk 2000; Hsu and Turk 2000; Hsu and Turk 2000; Hsu and Turk 2000; Hsu and Turk 2001). Indeed, fragmenting of a PG with *m/z* 719.5 at moderate (40 eV) collision energy completely destroyed the precursor ion and yielded peaks of acyl anions of both fatty acids moieties, along with the peak of the fragment of the head group. Importantly, intensity of acyl anions was 5 to 10-times higher than that of the head group fragment (Figure 9A). This result encouraged me to evaluate if the characteristic masses of the produced acyl anions can be selected in precursor ion scanning for detection of the intact molecules. 18:0/18:1-PG standard, analyzed in negative ion mode by selecting the acyl anion fragments *m/z* 281.2 and *m/z* 283.2 in PIS, corresponding to oleic and stearic acid respectively, clearly enabled detection of the particular species (Figure 9B). As in analysis of PC by HGS illustrated in Figure 8, the intact molecular ions are readily detected as singly charged peaks. Furthermore, no "ghost" peaks arising from chemical noise are observed in the spectra, thus showing the high accuracy of the ion selection. Similar observations were done for PEs, PSs, PIs and PAs (data not shown). Notably, hardly any signal of the precursor ion could be detected by HGS on the same PG standard by selecting the characteristic fragment ion *m/z* 153.0. The higher sensitivity by FAS in comparison to HGS correlates well to the intensity differences in the characteristic fragment ions observed in the MS/MS spectrum (Figure 9B). Moreover, both MS/MS and FAS show a more abundant *sn*-2 acyl anion in comparison to the *sn*-1 acyl anion and at similar ratios. This is according to previous tandem mass spectra studies of GPLs (Hsu and Turk 2000; Hsu and Turk 2000; Hsu and Turk 2000; Hsu and Turk 2000; Hsu and Turk 2001), and thus suggests that the position of fatty acid moieties at the glycerol backbone can be determined from FAS spectra. This is evaluated and outlined in detail in section 2.2.
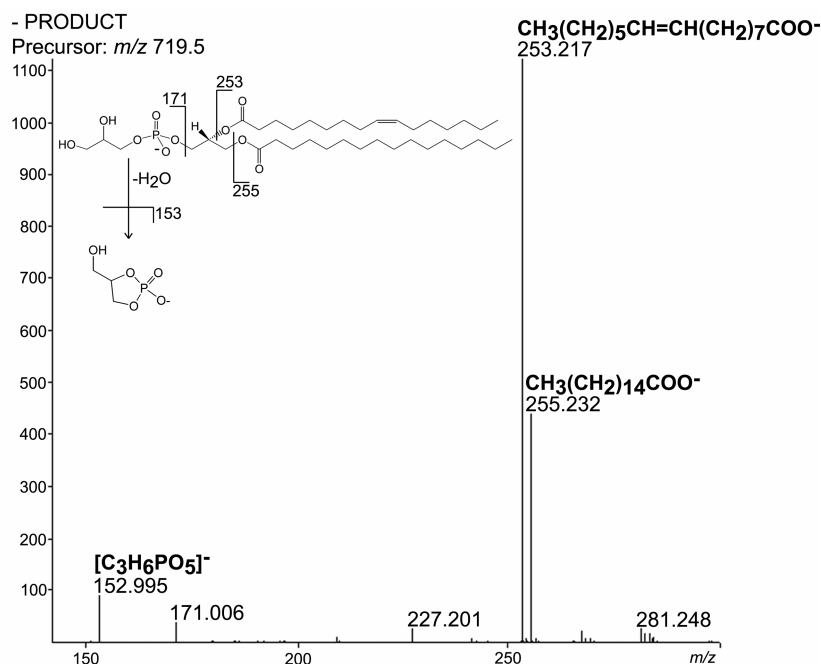
Figure 9A. Tandem mass spectrum of PG with *m/z* 719.5 acquired in negative ion mode. Peaks of acyl anions of the fatty acid moieties and the peak of a characteristic fragment of the head group are labeled.
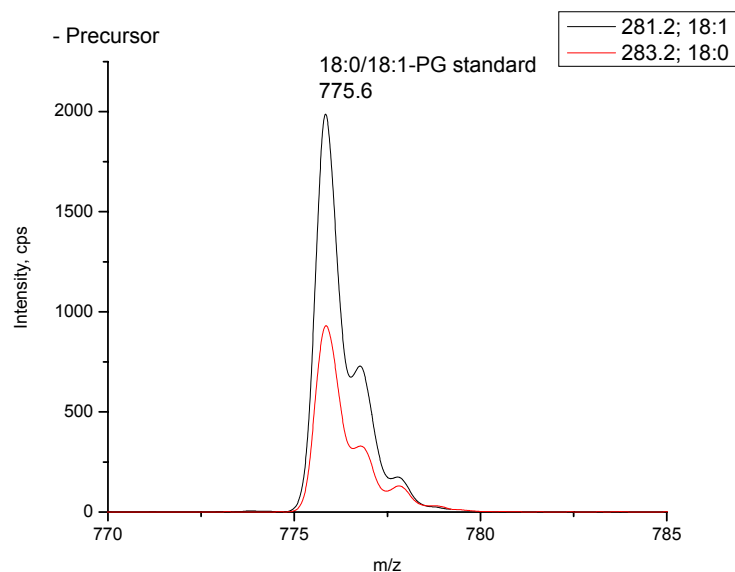
Figure 9B. Multiple profile overlay of 18:0/18:1-PG standard monitored by FAS. The intensity difference in the acyl anion signals allows position determination of the attached fatty acids. Collision energy was set at 40 eV.

Furthermore, masses of FAs are typically in 200–300 Da range, close to the masses of the head group fragments (Table 6), and thus can be enhanced together under the same trapping settings (Chernushevich 2000; Chernushevich, Loboda et al. 2001). We therefore reasoned that, in a single experiment, MPIS could detect lipids by simultaneous monitoring

acyl anions of all major fatty acids, which may (or may not) be present in a particular sample. This was termed Fatty Acid Scanning (FAS) and would complement monitoring of characteristic fragments of lipid head groups. Notably, the ion trapping efficiency was similar in HGS and FAS, thus producing a 6 to 8-fold increase in ion intensities.

Since MPIS can be performed on QqTOF instruments, HGS and FAS analysis could be done simultaneously. Moreover, the reliability of identification and quantification of lipids by precursor ion scanning depends on the accurate selection of fragment masses and may be compromised if other molecules (of lipid and nonlipid origin) yield fragments of similar mass. Therefore, in ambiguous cases, complementing HGS by FAS may provide independent verification of the identity of lipids. Profiling of *P. pastoris* lipid extract may serve as an example (Figure 10). Peaks at *m/z* 833.7 and 835.7 were detected independently at the precursor ions scans specific for PGs and for PIs (Table 6). However, taken together with FAS spectra, these peaks were unambiguously identified predominantly as PI 16:0/18:2 and PI 16:0/18:1, respectively. Subsequent inspection of data revealed that the fragment ion with *m/z* 153.0 is yielded upon collisional fragmentation of PGs, PIs, and PSs but not of PEs or PCs.
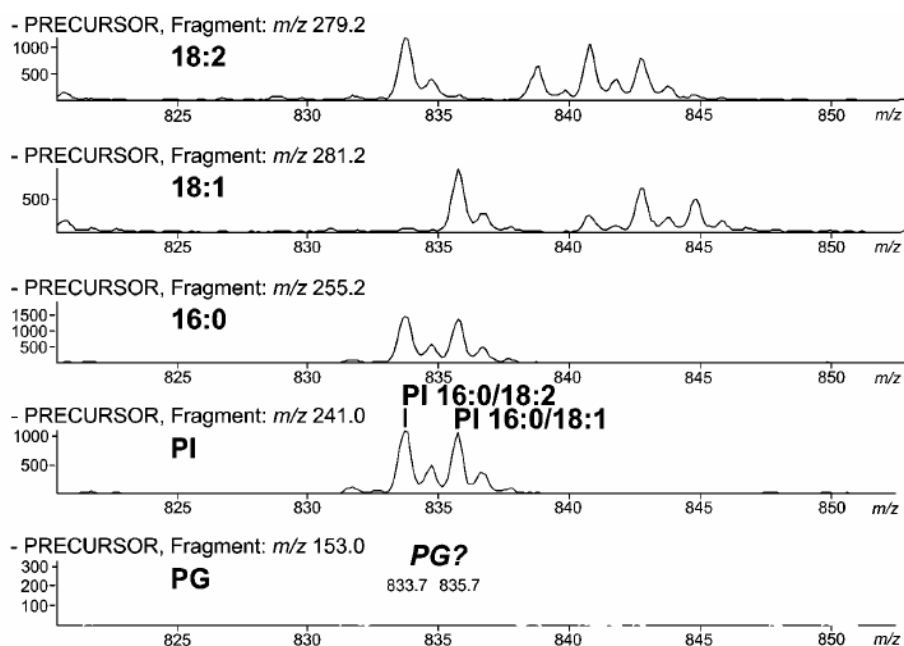
Figure 10. Complementing HGS by FAS verifies the lipid identity. A segment of precursor ion scan spectra in the *m/z* 820-850 range, acquired in parallel for PG (*m/z* 153.0), PI (*m/z* 241.1), 16:0 (*m/z* 255.2), 18:1 (*m/z* 281.2), and 18:2 (*m/z* 279.2). Overlaying of multiple precursor ion scan spectra reveals the identity of individual lipid species.

In conclusion, FAS readily allows accurate detection of molecular GPL species of PE, PS, PI, PG and PA. The intensity difference in the acyl anion signals allows position determination of the attached fatty acids (evaluated in more detail in section 2.2). Combining HGS and FAS clearly verifies the identity of a particular lipid species. Together with the accurate detection, this significantly increases the reliability in identification and quantification of lipids of total lipid extracts (see Figure 25). Since virtually unlimited number of precursor ion scans can be performed simultaneously, only a single analysis is required for detection and quantification of all molecular species.

2.1.3 Detection of GPLs as salt adducts by HGS and FAS

Sensitivity in detection of PE and PS species in HGS is particular low because of the low abundance in their head group fragment ions upon CID. The sensitivity can be increased dramatically by performing neutral loss scanning (Brugger, Erben et al. 1997). Currently, this option is only available on triple quadrupole instruments and not available on QqTOF MS. To replace it, salt sources have to be used to form lipid salt adducts. For instance, in 1 mM LiCl positively charged lithium adducts of the neutral fragments of PS and PE (Hsu and Turk 2000) are formed and can be selected as characteristic fragment ions in HGS (Table 6). This increases the sensitivity dramatically and still enables accurate determination of the particular GPLs. Thus, complementary HGS and FAS can be done with high accuracy.

Furthermore, since phosphorylcholine moiety comprises a quaternary amino group, high sensitivity detection of PCs in negative ion mode is problematic. Spiking 5 mM ammonium acetate or chloride into an electrosprayed solution of PCs rendered anion adducts $[M+CH_3COO]^-$ and/or $[M+Cl]^-$ (Kerwin, Tuininga et al. 1994; Han and Gross 1995; Larsen, Uran et al. 2001) (Figure 11A). Upon collision-induced dissociation, anion adduct of PC ions lose both a methyl group from the choline moiety and the counter ion, yielding a fragment ion (designated as $[M–15]^-$) with m/z 15 Th smaller than the mass of the zwitterionic form of the intact PC (Figure 11B). The $[M–15]^-$ ions undergo further fragmentation either *via* formation of low abundant intermediates by neutral loss of free fatty acid $[M–15–R'CH_2COOH]^-$ or by neutral loss of ketene $[M–15–R'CH=C=O]^-$, or yielding acyl anions of fatty acids directly (this is described more in detail in section 2.2.4). A similar pattern of fragment ions was observed in MS/MS analysis of PCs (Han and

Gross 1995) as well as other glycerophospholipids on a triple quadrupole instrument (Hsu and Turk 2000; Hsu and Turk 2000; Ramanadham, Hsu et al. 2000; Hsu and Turk 2001).
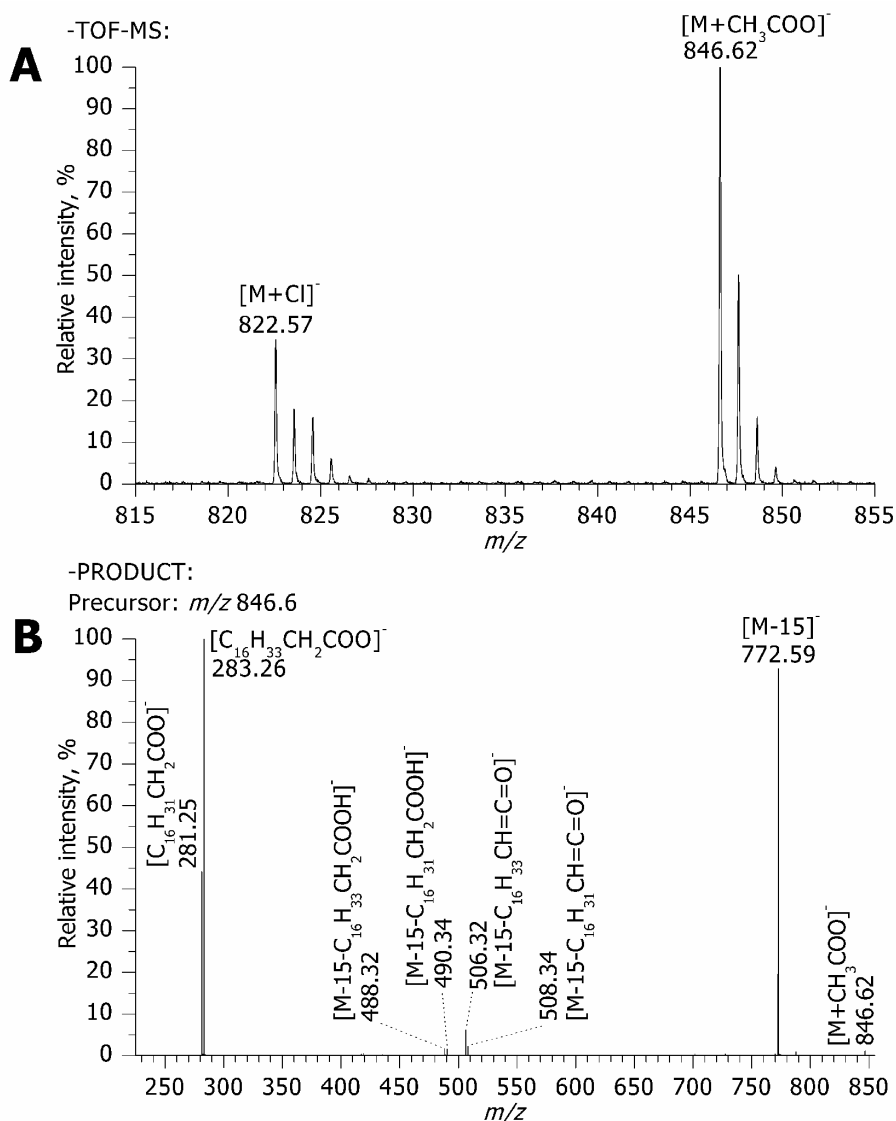
Figure 11. Analysis of PC acetate adducts in negative ion mode. A: TOF MS spectrum of synthetic 18:1/18:0-PC standard in chloroform/methanol (1:2) containing 5 mM ammonium acetate. PC was detected as anions of acetate and chloride adducts at m/z 846.62 and m/z 822.57, respectively.

B: MS/MS spectrum of the acetate adduct at m/z 846.62 acquired at collision energy 40 eV. Peaks at m/z 772.59, 283.26 and 281.25 correspond to the fragment ion of de-methylated PC ([M–15]$^-$) and acyl anions of stearic and oleic acid, respectively. Low abundant fragments were produced by the loss of fatty acids as ketenes [M–15–$C_{16}H_{31}CH$=C=O]$^-$ (m/z 508.34) and [M–15–$C_{16}H_{33}CH$=C=O]$^-$ (m/z 506.32), and by neutral loss of free fatty acid [M–15–$C_{16}H_{31}CH_2COOH$]$^-$ (m/z 490.34) and [M–15–$C_{16}H_{33}CH_2COOH$]$^-$ (m/z 488.32).

How the intensity of fragments depends on the applied collision energy was further examined (Figure 12). At low collision energy (~30 eV) MS/MS spectra were dominated

by the intact precursor ion and [M–15]⁻ fragment of the de-methylated PC. With increasing collision energy the intensity of both precursor and [M–15]⁻ ions decreased, with concomitantly increasing intensity of acyl anion fragments. The intensity of acyl anions peaked at ~50 eV and then decreased, presumably because high collision energy compromised focusing and steering of the ion beam in the mass spectrometer. In the range of 40-60 eV, altering the collision energy had almost no impact on the yield of acyl anions and, consequently, no tuning of the collision energy was required for optimizing the sensitivity.
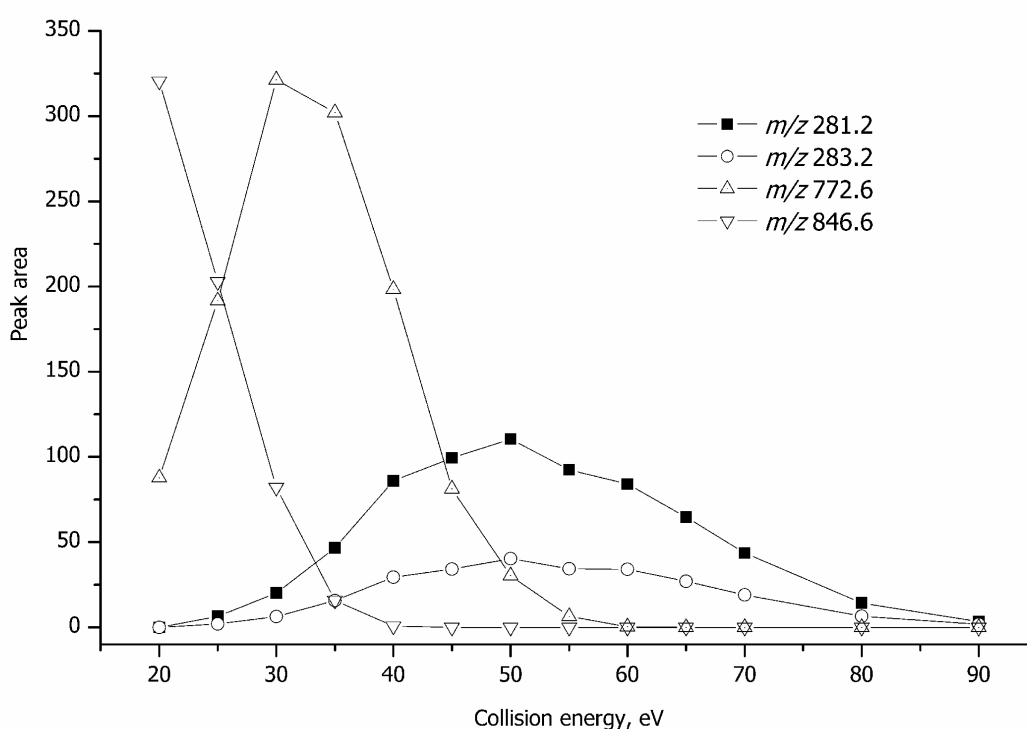
Figure 12. Collision energy dependence on the PC adduct fragmentation. Intensity of peaks of fragments of the acetate adduct of 18:1/18:0-PC change with increasing the collision energy. *m/z* 846.6 - [M+CH₃COO]⁻; *m/z* 772.6 - [M–15]⁻; *m/z* 281.2 and *m/z* 283.2 - acyl anions of stearic and oleic acids, respectively.

Since acyl anions of fatty acid moieties are efficiently produced by collision-induced dissociation of anion adducts of PCs they could be directly profiled by FAS, similar to other classes of glycerophospholipids. FAS analysis of 16:0/18:1-PC and 18:1/16:0-PC standards was performed by selecting *m/z* 255.2 and 281.2, corresponding to acyl anions of palmitic acid (16:0) and oleic acid (18:1), respectively, and precursor ions of acetate and chloride adducts were detected (Figure 13).

A 16:0/18:1-PC

B 18:1/16:0-PC
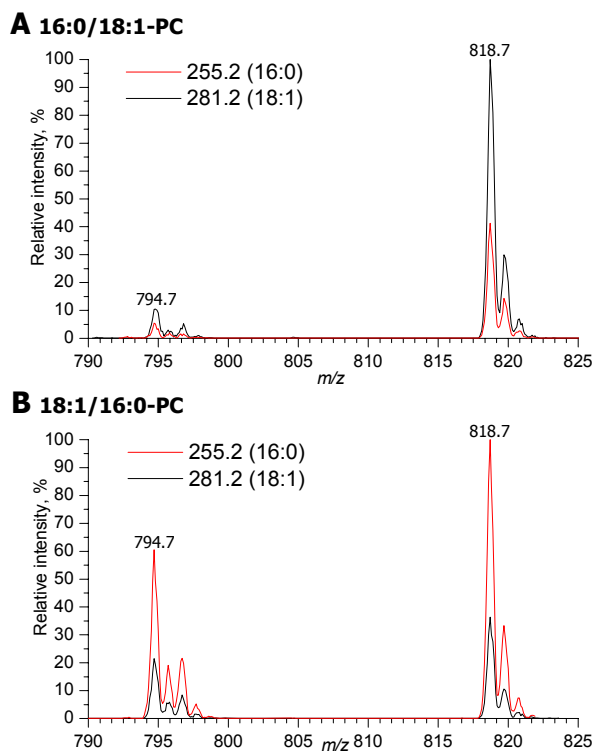
Figure 13. FAS spectra of synthetic 18:0/18:1-PC standard. Acyl anions of stearic and oleic acid (*m/z* 283.25 and *m/z* 281.25) were selected as fragment ions identifying precursor ions of acetate (*m/z* 818.9) and chloride (*m/z* 794.9) adducts.

B: FAS spectra of synthetic 18:1/18:0-PC standard, acquired in the same way as the spectrum in panel A. Note reversed intensities of peaks of the precursor, compared to panel A.

As expected, in the fragment patterns in MS/MS spectra of adducts (Figure 11B), the peak of the precursor ion was more abundant in FAS for the acyl anion fragment of *sn*-2 fatty acid, than of *sn*-1 fatty acid. Thus, this clearly shows that by applying FAS on anionic PC adducts enables molecular composition analysis of PCs. FAS complements the previously established method of PIS *m/z* 184.1 and not only increases the specificity and the dynamic range of detection, but also allows identification of the fatty acid moieties of individual PC molecules.

2.1.4 Reduction in chemical background by accurate mass selection

In contrast to triple quadrupole instruments, a TOF analyzer of the QSTAR Pulsar can precisely select masses of fragment ions without compromising the sensitivity in PIS mode (Steen, Kuster et al. 2001). This feature drastically reduces chemical background, increases

the specificity of PIS and is therefore important for the analysis of lipids enriched by extraction with non-ionic detergents - a common method of isolating membrane rafts (Brown and Rose 1992). We were able to profile endogenous PCs and SMs in a detergent-insoluble fraction enriched by flotation of a total extract of membrane lipids in cold 1 % Triton X-100 containing 1 mM LiCl. No additional clean-up or extensive washing steps were included in the sample preparation routine. TOF MS spectrum, acquired from the sample, contained only a series of clusters of the detergent with sodium and lithium ions that were detected at overwhelming intensity (Figure 14A). The same series of detergent ions appeared even in precursor ion scan for m/z 184.1 when recorded with a relatively wide m/z-window of 0.2 Da (panel B in Figure 14). Lithium adducts of Triton X oligomers produced a fragment ion with m/z 184.129 (its possible structure is $[H(C_2H_4O)_4Li]^+$), which accidentally almost coincide with the mass of the fragment of the head group of PCs, $i.e.$184.075 Da. Therefore the m/z window had to be narrowed down to 0.1 Da around m/z 184.05 in order to record lipid ions only (panel C in Figure 14). Note that neither 0.1 nor 0.2 Da isolation of fragment ions is achievable on conventional triple quadrupole mass spectrometers.
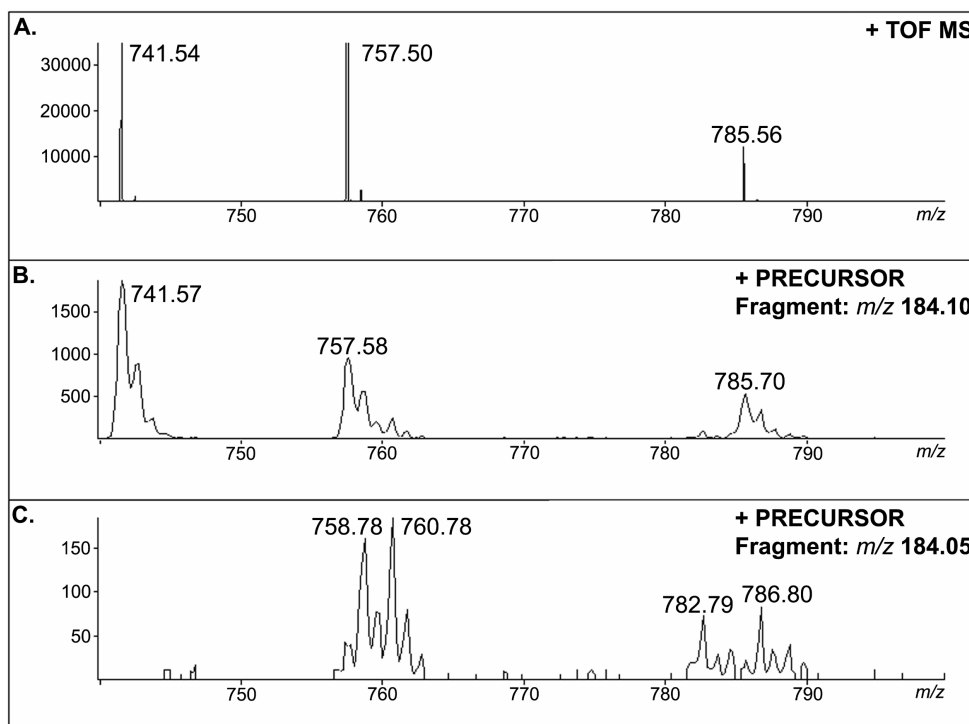
Figure 14. HGS of PC in samples containing 1% Triton X-100. Segments of TOF MS (A) and precursor ion spectra (fragment m/z 184.1) (B, C) acquired from a fraction of lipids floated in 1% Triton X 100. In panel B, the characteristic fragment ion was recorded within an m/z window from 184.00 to 184.20, thus including the "parasitic" fragments of the detergent and recording the same peaks as in TOF MS. In (C), the fragment ion was recorded within a narrower window from m/z 184.00 to 184.10. Only PCs were detected in (C).

38

Thus, this demonstrates that enhanced precursor ion scanning capability of a QSTAR Pulsar mass spectrometer makes it a valuable tool in qualitative analysis of total lipid mixtures since GPLs can be specifically detected at the level below chemical noise. Furthermore, superior specificity of the fragment ion selection may provide a crucial advantage in analyzing mixtures of lipids, isolated by detergent-assisted extraction or flotation.

2.1.5 Comparable sensitivity in HGS and FAS

Previous studies have clearly demonstrated that electrospray ionisation mass spectrometry is a sensitive and specific tool for the characterization of PCs in total lipid extracts (Han and Gross 1994; Kerwin, Tuininga et al. 1994; Han and Gross 1995; Brugger, Erben et al. 1997). Because of the positively charged quaternary amine of the choline head group, PCs are readily detected in positive ion mode with the femtomole sensitivity (Brugger, Erben et al. 1997). Therefore, I set out to evaluate the sensitivity of a QqTOF in PIS mode. A solution of 1,2-dilauroyl-*sn*-glycero-3-phosphatidylcholine, having a concentration of 6 fmol/μL, was analyzed by PIS *m/z* 184.1. The isotopically resolved singly charged peak of the lipid was reliably detected (Figure 15). The same lipid was barely distinguished from chemical background in the TOF MS spectrum, and thus demonstrating the advantage of PIS. The obtained sensitivity is directly comparable to the sensitivity of a conventional triple quadrupole instrument (API III from MDS Sciex, Toronto).
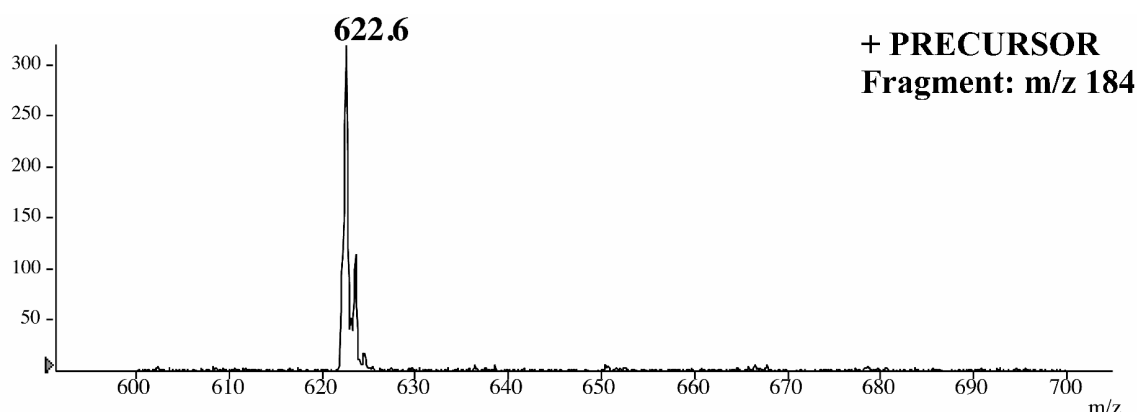
Figure 15. Detection sensitivity of PC in HGS. 6 fmol/μL of the synthetic standard PC 24:0 on a QqTOF was analyzed by PIS *m/z* 184.1. The peak of the PC 24:0 is readily detected.

It is not surprising that the detection of PCs is reduced in FAS, since their detection requires formation of salt adducts (Figure 16). As in HGS, linear correlation was observed in the 0.4-10 µM concentration range and was not affected if PC standards were spiked into a lipid extract (data not shown). Samples are usually analyzed inside this concentration range and thus the linearity is fundamental for any quantitative analysis. Thus, this shows that the sample concentration can be kept constant for detection of PCs in both analysis modes. This does not only decrease sample preparation time, but also directly improves the speed and reliability in data comparison between FAS and HGS.
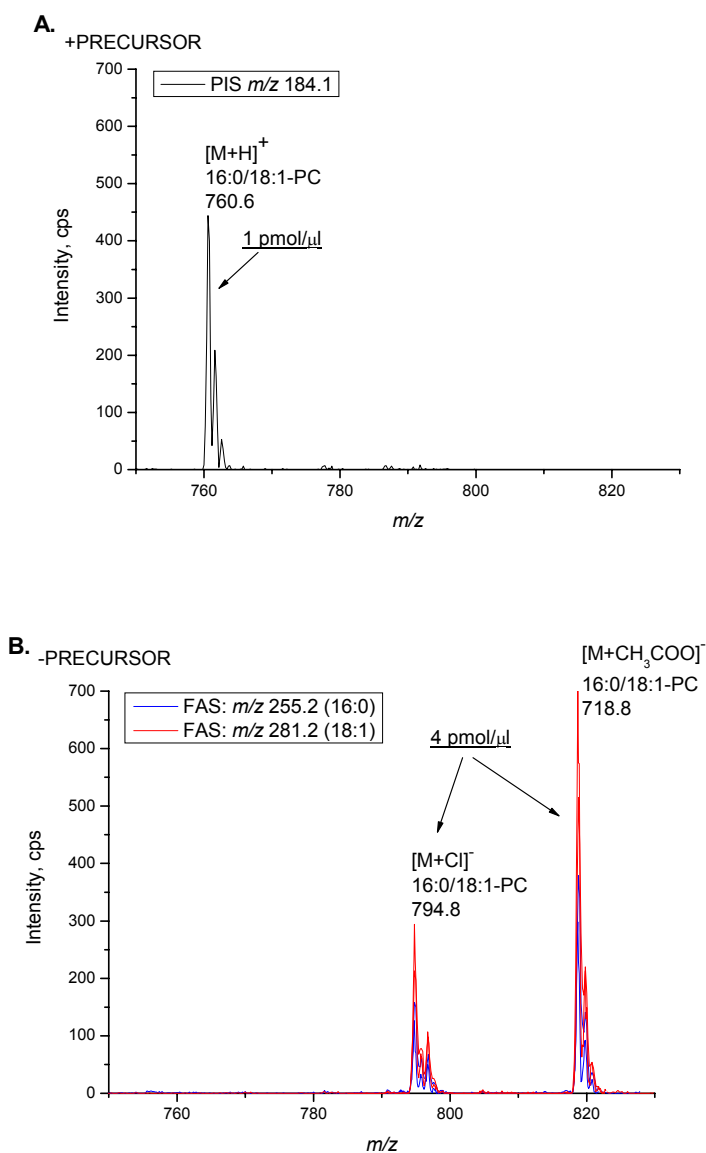
Figure 16. Sensitivity comparison of PC by HGS and FAS. A. 1 pmol/µl of the 16:0/18:1-PC standard was analyzed by PIS *m/z* 184.1. B. 4 pmol/µl of the same standard was analyzed as acetate adducts in FAS by selecting *m/z* 255.2 (16:0) and *m/z* 281.2 (18:1). Collision energy was set to 40 eV and the same number of scans was acquired in both ion modes.

Furthermore, PE and PG are detectable at similar sensitivities by FAS. Notably, PA (two-fold) and in particular PS (five-fold) are not detectable to the same extent at fixed collision energy of 40 eV (Figure 17). Detection of PS is directly comparable to the sensitivity of PC adducts. Importantly, all detected species showed linear correlation in the 0.4-10 μM concentration range, as in the case for PCs, which is important for their absolute and relative quantification. All GPL standards comprise the same fatty acid moieties, 18:0/18:1, to normalize ionization efficiency. Notably, generation of acyl anions is collision energy-dependent and faintly different among the different GPL classes (described in section 2.2). Using fixed collision energy will only enable maximal detection of a particular lipid class, whereas lipid classes with different collision energy dependency are only partly detected. By changing the collision energy, the maximal detection (sensitivity) of these lipids can be reached. Therefore, by careful ramping (stepwise increasing dependent on *m/z* window) of the collision energy optimization should be achievable and thus produce similar intensities in the different molecular species at the same concentrations shown in Figure 17. This is only important for absolute quantification of molecular species, but is not as crucial for relative quantification where their changes are measured. Therefore this was not further explored. In conclusion, this setup shows that a fixed sample concentration enables analysis of all GPLs simultaneously, both in positive and negative ion mode. Furthermore, all GPLs, irrespective in which mode they are analyzed, show linear correlation (Figure 18) in the normal working concentration range, crucial for any quantification approach. The detection threshold of total lipid extracts analysis can be as low as 200-300 cells per μL.
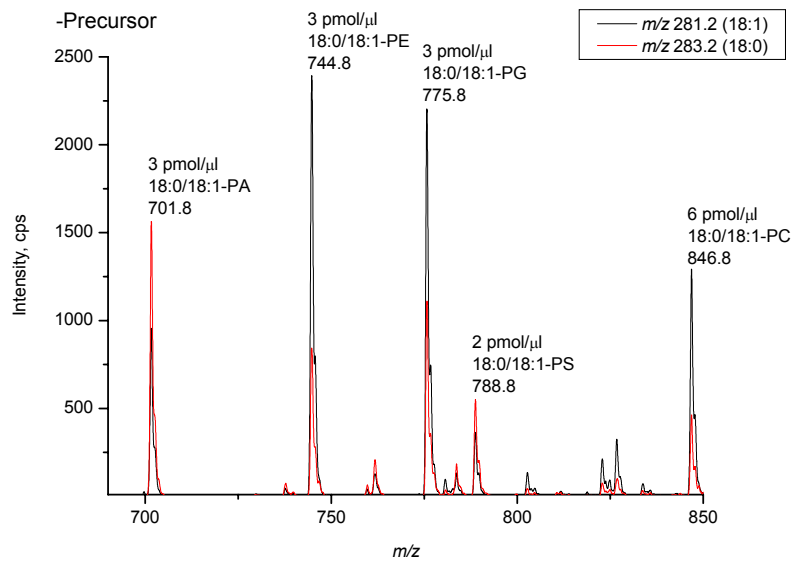
Figure 17. Sensitivity comparison of GPL classes by FAS. Analyzed GPL species comprise the same fatty acid backbones (18:0/18:1). Similar concentrations of all molecular species were analyzed in FAS by selecting *m/z* 283.2 (18:0) and 281.2 (18:1). Collision energy was set to 40 eV and the same number of scans was acquired in both modes.
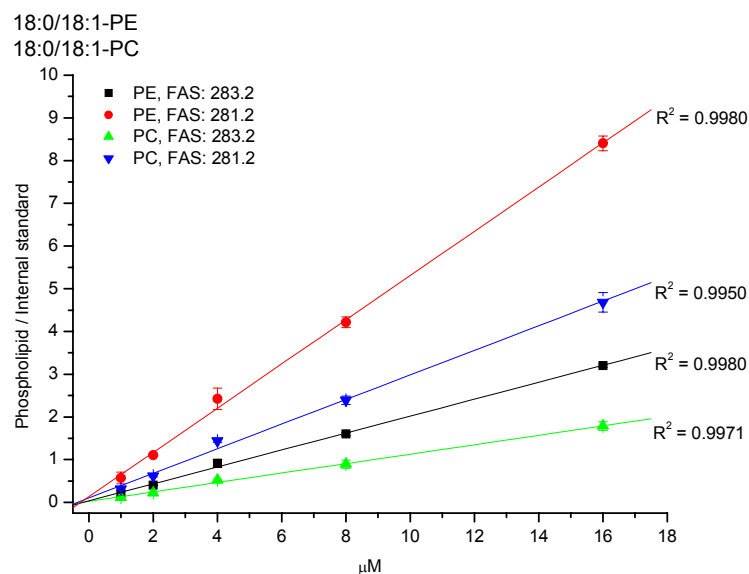
Figure 18. Linear correlation. 18:0/18:1-PC and 18:0/18:1-PE standards were spiked into a total lipid extract of *E. coli.* at concentrations ranging from 0.5 to 16 μM and monitored by FAS (*e.g. m/z* 281.2 (18:1) and *m/z* 283.2 (18:0)). Peak area of individual fatty acid signal was related to the peak area of the internal standard 14:0/14:0-PE (*e.g. m/z* 227.2 (14:0)). Linear regression coefficient (R^2) is presented. Collision energy was 40 eV and 10 scans were acquired.

2.1.6 Minimizing losses by defined lipid extraction

Reliable and reproducible results are required in both qualitative and quantitative analyses. In the sample preparation process, losses in lipid species and/or lipid classes should therefore completely be avoided. At the same time this preparation should be simple, robust and fast. The Bligh & Dyer (Bligh and Dyer 1959) and the Folch (Folch 1957) methods are the most widely used and established lipid extraction methods. The former one is more suited for samples in solution whereas the latter one is suited directly for tissue samples. Therefore, the latter one requires a higher percentage of organic solvent to enable efficient extraction. The Folch extraction method is suitable for a wider lipid type spectrum as, for instance for glycosphingolipids (Rauvala 1976). The extraction recovery of the Folch's procedure is more efficient and robust over a wider lipid concentration range compared to the Bligh & Dyer procedure (Iverson, Lang et al. 2001).

We therefore set out to evaluate the efficiency and robustness of the extraction recovery, to methodically monitor various lipid types extracted by the Bligh & Dyer and by the Folch method. A mixture, A, of synthetic standards containing 14:0/14:0-PC, 18:0/18:0- PE, lactosyl ceramide (C8) and G_{M1} ganglioside was directly subjected to lipid extraction and a second mixture , B, containing the molecular species 12:0/12:0-PC and 14:0/14:0-PE, and glucosyl ceramide (C8) and G_{M3} ganglioside was used as internal standards. Mixture A was spiked into water, a Chinese hamster ovarian (CHO) cell extract and into a 30% Optiprep solution. In the case of spiking into the Optiprep solution, both methods showed similar lipid recovery (Table 1). Slightly better recovery of lactosyl ceramide was observed using the Folch method. By spiking the mixture into water or a cell extract significant changes in lipid recovery was observed. The Bligh & Dyer method resulted in larger losses in all analyzed lipid species in comparison to the Folch method. PC and PE species were approximately 90 and 80% respectively, recovered by Folch extraction. Furthermore, this method also enables extraction of gangliosides. This result shows that approximately 85 % of the analyzed phospholipids can be recovered using Folch extraction method. Using the Bligh & Dyer method this is at least 10 % less. Therefore, from these results it was decided to use, from this point on, Folch extraction method instead of Bligh & Dyer method.

Table 1. Increased lipid recovery by Folch extraction. Lipid recovery was compared between the Folch and Bligh & Dyer extraction methods. Mixture A containing; 18:0/18:0-PE, 14:0/14:0-PC, G_{M1} and Lactosyl ceramide was spiked into either 30 % optiprep, water or CHO cells and subjected to Bligh & Dyer and Folch extractions. Mixture B containing; 14:0/14:0-PE, 12:0/12:0-PC, G_{M3} and Glucosyl ceramide was spiked into the lipid extracts upon mass spectrometric analyses and used as internal standards. The lipids of mixture B was used to monitor the extraction recovery of the lipids of mixture A (*e.g.* 14:0/14:0-PE was used to monitor 18:0/18:0-PE). Mixture B was spiked directly into mixture A to monitor the maximal signal of individual lipids of mixture B.

Sample spiking	18:0/18:0-PE	14:0/14:0-PC	G_{M1} ganglioside	Lactosyl ceramide (C8)
Optiprep, B&D[b]	31.3 ± 0.8	63.0 ± 0.4	$0.0 \pm$ n.d.[a]	43.6 ± 1.5
Optiprep, Folch	46.6 ± 4.2	65.4 ± 1.2	$0.0 \pm$ n.d.[a]	62.1 ± 4.5
dH$_2$O, B&D[b]	42.7 ± 0.3	67.7 ± 1.7	$0.0 \pm$ n.d.[a]	57.0 ± 1.5
dH$_2$O, Folch	59.0 ± 0.3	74.8 ± 0.4	7.8 ± 1.4	97.4 ± 5.2
CHO cells, B&D[b]	70.7 ± 2.0	75.8 ± 5.0	$0.0 \pm$ n.d.[a]	65.1 ± 5.2
CHO cells, Folch	93.7 ± 1.0	83.9 ± 1.6	4.0 ± 0.7	70.3 ± 3.8

[a] not determined

[b] Bligh & Dyer's

2.2   Determination of positional isomers pf PC in total lipid extracts

2.2.1   *Quantification of isomers in synthetic PC standards*

To quantify isomers of endogenous PCs, we first established the isomeric purity of available synthetic standards. PLA$_2$ hydrolyses the *sn*-2 ester bond in PCs, yielding 2-lysoPCs. We tested PLA$_2$ specificity by hydrolyzing 15 mg of synthetic 16:0/18:1-PC standard and analyzing the reaction mixture by 1H-NMR. We only detected the signal from hydrogen atoms of the secondary alcohol and not from the primary alcohol, which indicated that *sn*-1 ester bond was not hydrolyzed to any noticeable extent (data not shown). We therefore concluded that, under the applied reaction conditions, the hydrolysis of the *sn*-2 ester bond by PLA$_2$ is specific.

Mass spectrometric analysis of PLA$_2$-treated PC standards on a QqTOF mass spectrometer by TOF MS and by PIS *m/z* 184.1 suggested that they contained a noticeable amount of corresponding positional isomers (Table 2).

Table 2. Isomeric purity of synthetic lipid standards.

Lipid Standard	[a,b] Abundance of isomeric species, mol%			
	PLA$_2$ hydrolysis and QqTOF			[c]Ion trap MS^3
	TOF MS	PIS *m/z* 184.1	FAS	
16:0/18:1	88/12	87/13	88/12	83/17
18:1/16:0	83/17	82/18	81/19	79/21
16:0/18:0	88/12	85/15	88/12	83/17
18:0/16:0	94/6	95/5	93/7	93/7
18:0/18:1	96/4	96/4	95/5	89/11
18:1/18:0	81/19	81/19	84/16	75/25

[a]coefficient of variation for QqTOF measurements was 1.6 %, and for ion trap measurements 3.6%. [b]mol% of the indicated structure/mol% of the isomer, *e.g.* 16:0/18:1-PC vs. 18:1/16:0-PC. [c]MS^3 fragmentation of chloride adducts in negative ion mode.

2.2.2 *Determination of positional isomers by FAS*

The next task was to evaluate whether FAS enables determination of positional isomers. Since the fatty acid dissociation is position-dependent, as shown for PCs above and previously for other GPLs (Hsu and Turk 2000; Hsu and Turk 2000; Hsu and Turk 2000; Hsu and Turk 2000; Hsu and Turk 2001) the signal ratio of the precursor ions obtained from each individual FAS data was investigated. First, the yield of acyl anions of the corresponding fatty acids was collision energy-dependent. Interestingly, the release of the *sn*-2 fatty acid was about 3-fold higher than the *sn*-1 fatty acid for PE and PC whereas for PS and PA this was reversed, now with a 2-fold higher *sn*-1 fatty acid (Figure 18). This correlates well to the previous studies by Hsu et al (Hsu and Turk 2000; Hsu and Turk 2000; Hsu and Turk 2000; Hsu and Turk 2000; Hsu and Turk 2001). According to them the fatty acid yield is dependent on the nature of the head group, and therefore acidic GPLs, as PA and PS, show higher abundance in *sn*-1 fatty acids in comparison to *sn*-2 fatty acids, whereas for more basic GPLs, this is reversed. Note that in MS/MS of different GPLs, comprising the same backbone, PC requires 50 eV for maximum dissociation whereas for PE this is 40 eV. For PA and PS this is 45 and 60 eV respectively (Figure 19). The maximum collision energy difference is 20 eV (PE and PS). This is due to the characteristic nature of ethanolamine and serine head groups and their interactions with the glycerol backbone and fatty acids. Presumably, both lipids undergo, upon CID, different dissociation mechanisms with a diverse balance between the neutral loss as fatty acid and as ketene from the precursor ion, and thus directly resulting in different abundances in

generated acyl anions. Since enhancement in FAS brings about 5 eV more to the collision energy due to the ion trapping, the used collision energy in FAS has been standardized to 40 eV to enable coverage of all GPLs without ramping.
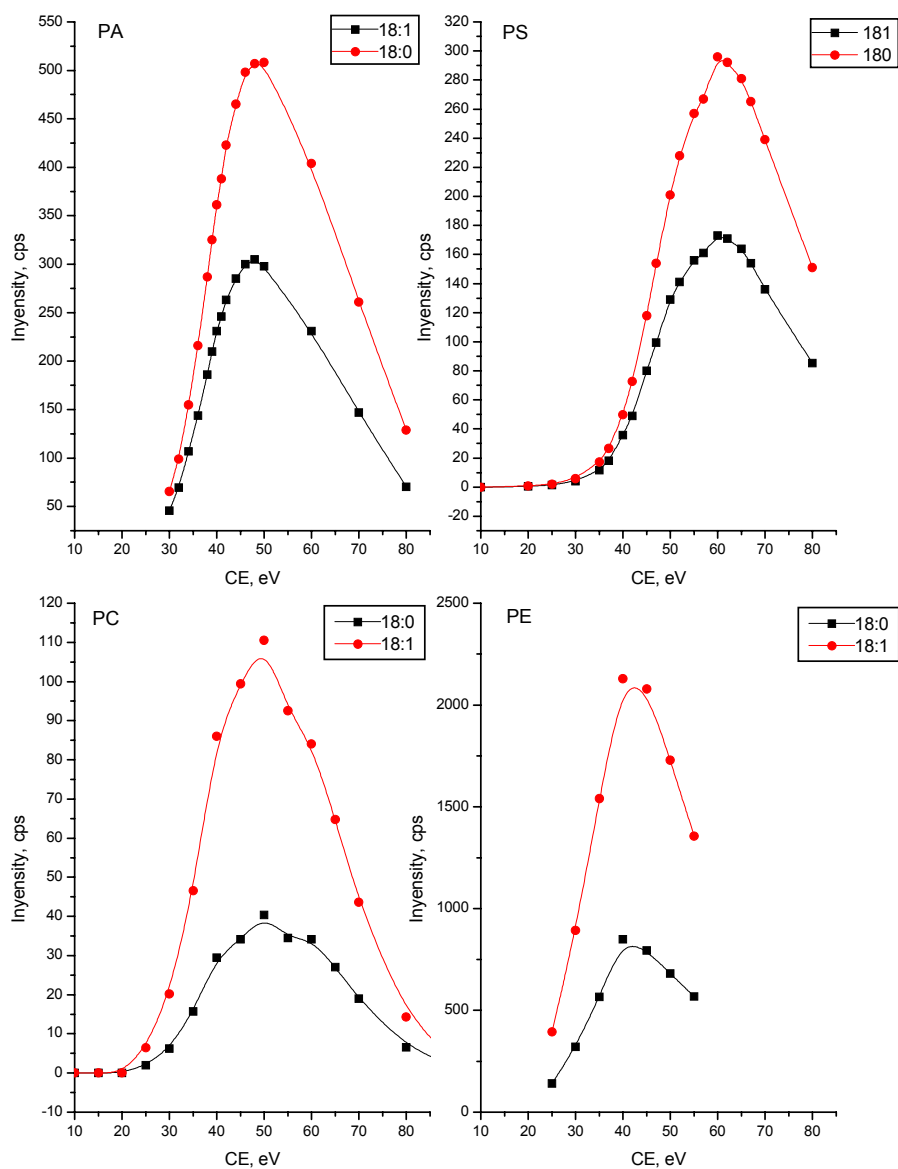
Figure 19. Acyl anion release from GPLs. All analyzed standards are comprised of the same backbone, 18:0/18:1, and at a concentration of 3 pmol/µl. 40 scans were acquired for each data point and the Q1 quadrupole set at high resolution.

Quantification of isomers of the commercially available PS and PA standards could not be obtained by the PLA$_2$ hydrolysis due to incomplete hydrolysis by the enzyme. The results shown in Table 2, 18:0/18:1-PC is determined to contain 4% of its positional isomer.

Performing FAS by selecting *m/z* 281.2 and 283.2 fragment ions and calculating the percentage of the precursor ion obtained in FAS of *m/z* 281.2 (*sn*-2) to the sum of both precursor ions (*m/z* 281.2 + *m/z* 283.2), is about 75%. Performing similar experiments on the 16:0/18:1-PC standard a value of 71% was obtained. Notably, this standard contains 12% of its positional isomer. From these results it is difficult to determine whether the difference in 4% of the obtained values is due to differences in purity or/and differences in the fatty acid backbone. Therefore, similar FAS experiments on PLA$_2$-determined molar mixtures of the same standards were performed. Both molar mixtures linearly correlated and generated the same linear regression values (slope value, B, and intercept, A) and therefore suggested that the dissociation is independent of the *sn*-1 fatty acid in this range (Figure 20).
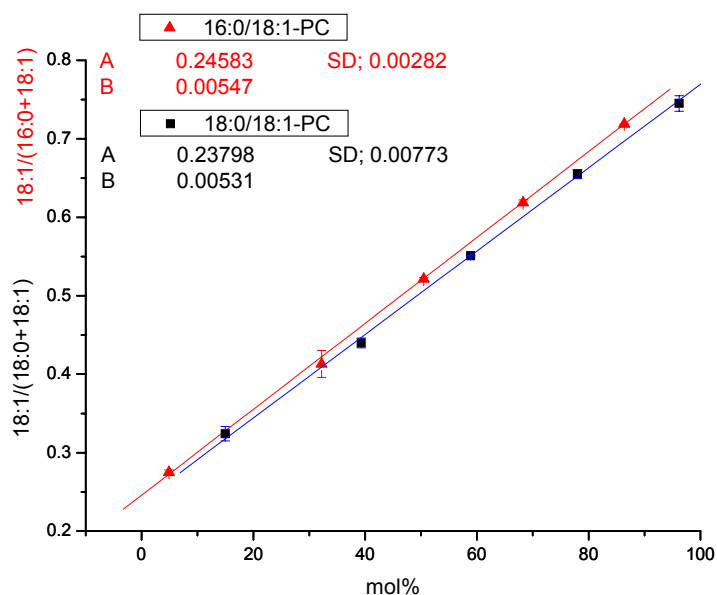
Figure 20. Positional isomer determination of PC by FAS. Molar mixtures of 16:0/18:1 and 18:1/16:0-PC and 18:0/18:1 and 18:1/18:0-PC were analysed by FAS. Precursor ion obtained by FAS of *m/z* 281.2, for both standard mixtures, linearly correlates to the purity obtained by PLA$_2$ hydrolysis. Linear regression of both standards generates the similar slope values, B, and intercept values, A. Collision energy was 40 eV.

Due to lack of standards, similar experiments were not performed on other mixtures comprising of different fatty acid backbones to evaluate whether the dissociation is fatty acid and/or position dependent (e.g. effect of length of fatty acid and degree of saturation attached at either *sn* position).

PC can be converted to PA by phospholipase D hydrolysis (Kovatchev and Eibl 1978). This allowed us to evaluate whether the fatty dissociation is head group-dependent or not. First, mol% of mixtures of 18:0/18:1 and 18:1/18:0-PC standards was determined by PLA$_2$ hydrolysis. Afterwards, an aliquot of the mixture was converted completely to PAs, and monitored by FAS. Thereafter, the PA and PC mixtures were subjected to FAS experiments as described above. The FAS data were linearly correlating to the determined PLA$_2$ purity for both mixtures. On the other hand, significant differences were observed in the linear regression results showing different slope, B, and intercept, A, values of both mixtures (Figure 21). Due to the flipped dissociation behaviour of PA the abundance in the precursor ion monitored by in m/z 283.2 (sn-1) was related to the total precursor ion signal. This clearly shows that the fatty acid dissociation is head group-specific.
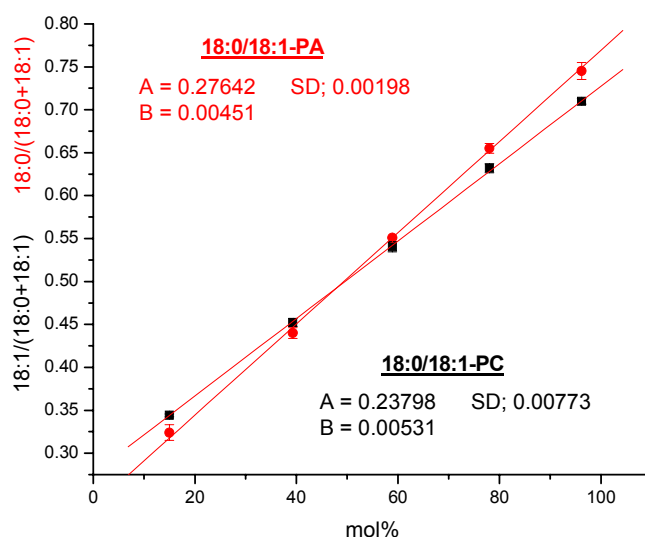
Figure 21. Positional isomer determination comparison of PC and PA by FAS. FAS of molar mixtures of 18:0/18:1 and 18:1/18:0-PC and 18:0/18:1 and 18:1/18:0-PA. Linear correlation of the precursor ion obtained by FAS of m/z 281.2 for PC and by FAS of m/z 283.2 to the purity obtained by PLA$_2$ hydrolysis. Linear regression of both standards generates significantly different slope values, B, and intercept values, A. Collision energy was 40 eV.

In conclusion, molecular positional isomers presumably could directly be determined from the FAS data if the linear regression values of its molecular molar mixture were known. This has still to be evaluated in analysis of total lipid extracts. Even though if both molar mixtures of 16:0/18:1- and 18:0/18:1-PC had a similar linear regression value it would not be sufficient from this to conclude that the fatty acid dissociation is fatty acid and position-

independent. This can only be done by performing similar experiments on molar mixtures comprising of different types of fatty acids, both in length and degree of saturation. Since mammalian cells comprise of a wide molecular species variety this will be very demanding and difficult to generate. Furthermore, this gets even more difficult since the fatty acid dissociation is head group dependent for PC and PA and presumably is also in other classes. It means that molar mixtures need to be generated in all analyzed GPL classes, which is not feasible.

2.2.3 *Fragmentation of phosphatidylcholine adducts by ion trap MS^3*

Since FAS did not allow direct determination of positional isomers and, regardless of the applied collision energy, fragmentation of anion adducts of PCs on the quadrupole time-of-flight mass spectrometer did not produce ions which could directly characterize the relative abundance of isomeric PC species (Figure 11B). In contrast to tandem mass spectrometers equipped with a linear collision cell (e.g. triple quadrupole or QqTOF instruments), ion trap mass spectrometers fragment a precursor ion by applying an *m/z*-dependent resonance excitation voltage, which leaves product ions unaffected. If necessary, any product ion can be further trapped and fragmented in another cycle of the tandem mass spectrometric experiment (MS^n experiments) (reviewed in March 1997).

We tested whether fragmenting anion adducts of PCs in an ion trap mass spectrometer would enable direct quantification of positional isomers. MS^2 fragmentation of the chloride adduct of 16:0/18:1-PC standard produced abundant ion of a de-methylated fragment of PC [M–15]$^-$ at *m/z* 744 (Figure 22A). Subsequently, MS^3 fragmentation of [M–15]$^-$ resulted in neutral loss of the fatty acids as ketene [M–15–R'CH=C=O]$^-$ rendering product ions of de-methylated lysoPCs at *m/z* 480 and 506, with the peak of the former product most abundant. Acyl anion fragments [R'CH$_2$COO]$^-$ were observed at *m/z* 255 and 281, although they were less abundant than in QqTOF spectra. Minor fragments formed by neutral loss of free fatty acid [M–15–R'CH$_2$COOH]$^-$ from [M–15]$^-$ were detected at *m/z* 462 and 488. As expected, MS^4 fragmentation of the de-methylated lysoPCs produced the acyl anion fragment and corresponding products of ketene and free fatty acid losses at *m/z* 242 and 224, respectively (data not shown). Ion trap MS^n analysis of other PC standards followed the same fragmentation pathways (data not shown).
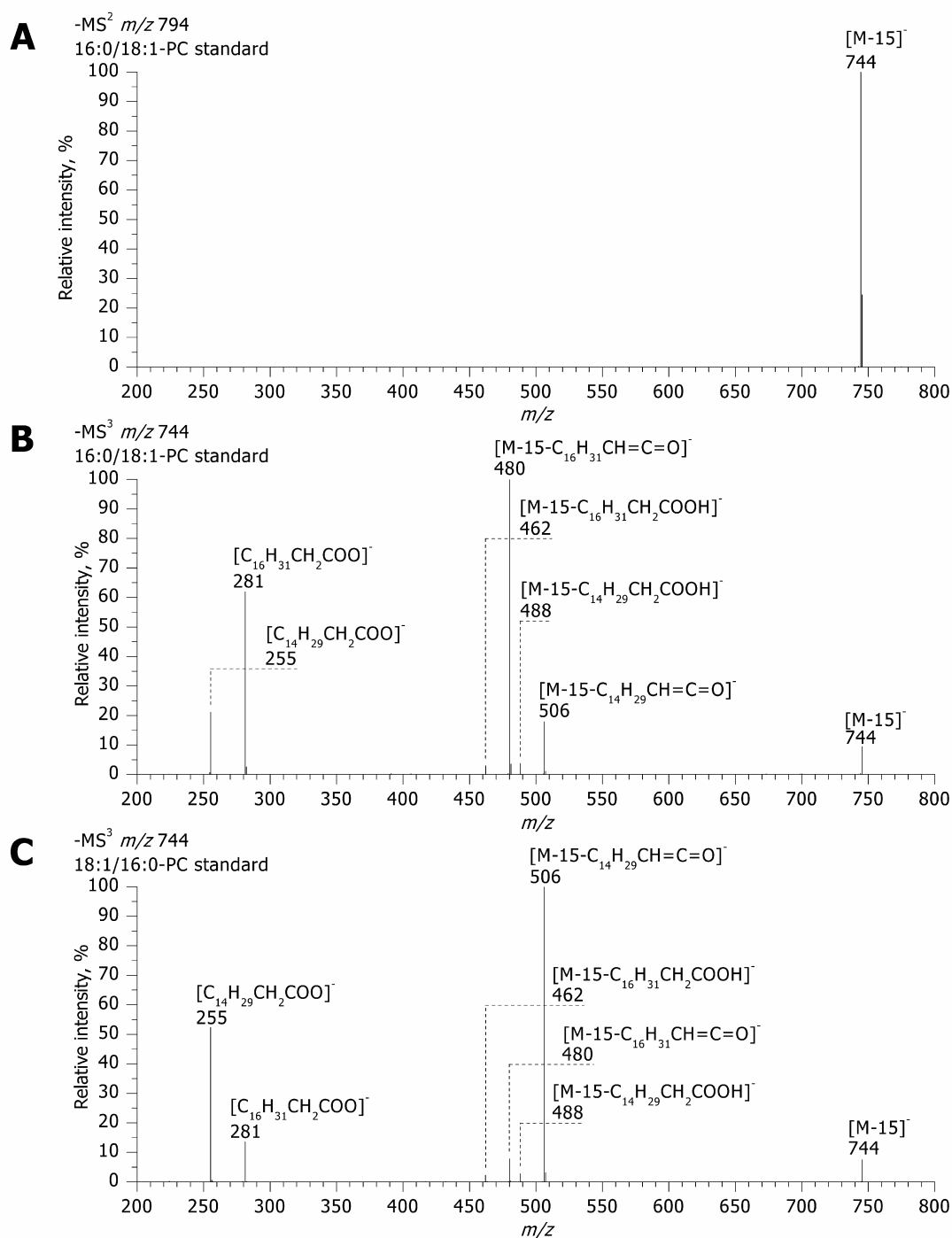
Figure 22. Ion trap MS^n analysis of PC adducts. A: MS^2 spectrum of a chloride adduct of synthetic 16:0/18:1-PC standard. Abundant fragment at m/z 744 corresponds to de-methylated PC $[M–15]^-$. B: MS^3 spectrum of m/z 744. The observed fragments are the products of ketene loss $[M–15–C_{14}H_{29}CH=C=O]^-$ (m/z 506) and $[M–15–C_{16}H_{31}CH=C=O]^-$ (m/z 480), corresponding to ions of de-methylated 18:1-lysoPC and 16:0-lysoPC, respectively; acyl anions of oleic (m/z 281) and palmatic (m/z 255) acids; loss of free fatty acid $[M–15–C_{14}H_{29}CH_2COOH]^-$ (m/z 488) and $[M–15–C_{16}H_{31}CH_2COOH]^-$ (m/z 462). C: MS^3 spectrum of $[M–15]^-$ ion (m/z 744) obtained by MS^2 fragmentation of a chloride adduct of synthetic 18:1/16:0-PC standard. The spectrum is similar to the one in panel B, but the intensities of fragments at m/z 506 and 480, as well as at m/z 281 and 255 are reversed.

50

MS^3 fragmentation of the isomeric standard 18:1/16:0-PC produced a spectrum in which the intensities of fragment ions were reversed compared to the spectrum of 16:0/18:1-PC standard (Figure 22C), suggesting that fragmentation pathways in ion trap and QqTOF mass spectrometers are similar (Figure 23), implying that release of fatty acids as either acyl anions or as neutral ketenes are position-dependent processes.
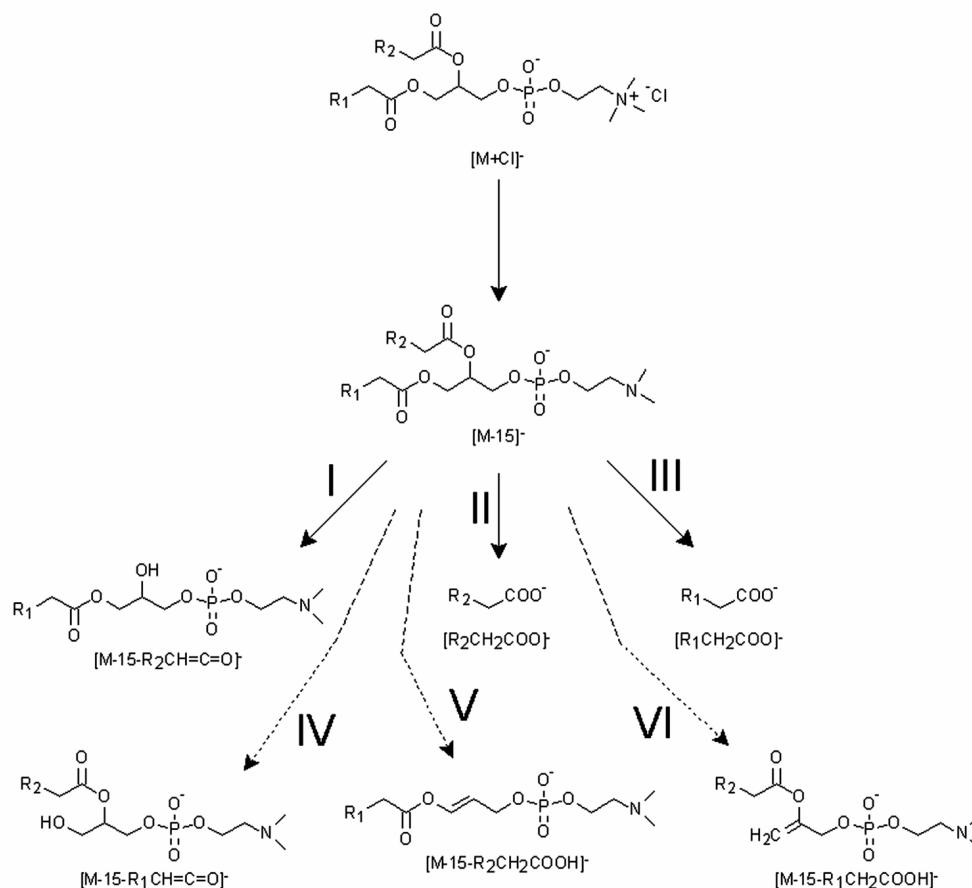
Figure 23. Fragmentation pathways of anion adduct of PC. Fragmentation pathways are under low-energy collision-induced dissociation. In the first step of collision-induced dissociation of the PC adduct anion (*e.g.* [M+Cl]$^-$) the de-methylated fragment ion [M–15]$^-$ is produced. Fragmentation of the [M–15]$^-$ ion proceeds along three major pathways: (I) loss of *sn*-2 fatty acids as a ketene yields a de-methylated 2-lysoPC; (II) and (III) - formation of acyl anions of *sn*-2 and *sn*-1 fatty acids; and three minor pathways: (IV) loss of *sn*-1 fatty acid as a ketene; (V) and (VI) - loss of neutral fatty acids from *sn*-2 and *sn*-1 positions.

In conclusion, regardless of the type of the instrument, collision-induced dissociation of an anionic adduct first generates abundant [M–15]$^-$ fragment, whose subsequent fragmentation pathways are common for negatively charged glycerophospholipids (Hsu and Turk 2000; Hsu and Turk 2000; Hsu and Turk 2000; Hsu and Turk 2000; Hsu and Turk 2001; Larsen, Uran et al. 2001).

2.2.4 *Quantitative analysis of positional isomers by MS³ fragmentation*

MS³ fragmentation of PC adducts yielded abundant de-methylated lysoPC fragment ions matching the neutral loss of *sn*-2 fatty acid as ketene, which might be employed in direct quantification of isomeric and isobaric species. We therefore evaluated if the relative intensity of these ions correlated with the estimates of mol% of isomeric species determined by PLA_2 hydrolysis of synthetic standards. The ratio of intensities of de-methylated lysoPCs fragment ions rendered *via* neutral loss of fatty acids as ketenes (*i.e.* [M−15−R'CH=C=O]⁻) correlated with the estimates of mol% determined by the other three independent methods of detection (Table 2). To further validate the method, we mixed pairs of isomeric standards in various molar ratios, digested the mixtures by PLA_2 and determined the content of positional isomers on the QqTOF mass spectrometer. Aliquots of the mixtures of standards were analysed directly by MS³ fragmentation, and the results were compared. Linear regression demonstrated a statistically confident correlation between the obtained mol% estimates (Figure 24). The same experiment was performed using another pair of isomeric standards: 16:0/18:0-PC and 18:0/16:0-PC and produced similar results (data not shown). Taken together, the data indicated that neutral loss of fatty acid as ketene predominantly occurs at the *sn*-2 position.
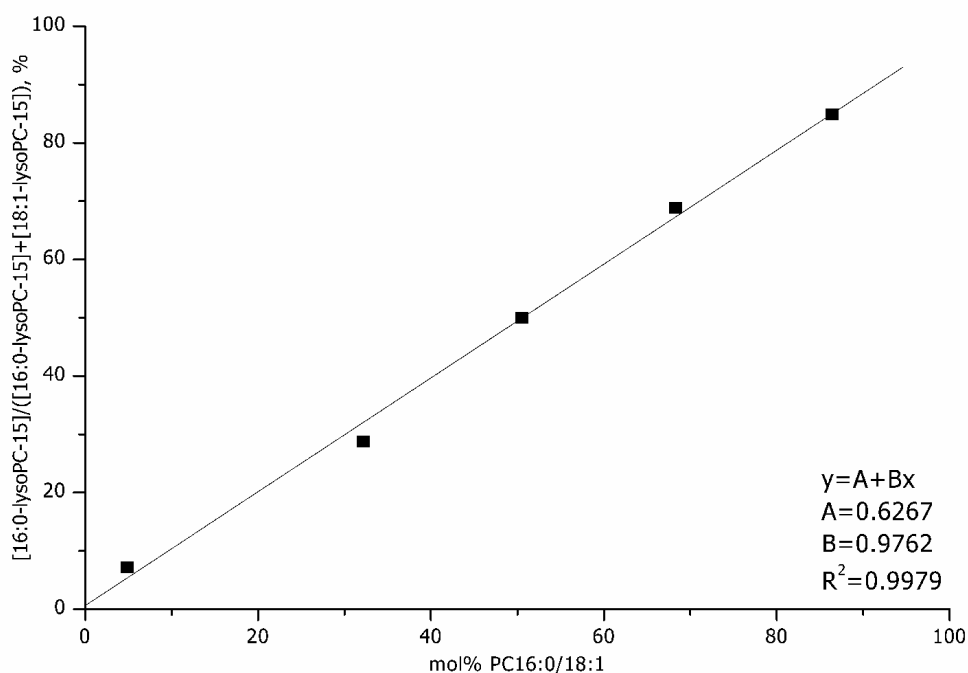
Figure 24. Linear correlation of ion trap MS^3 and PLA_2 analysis of PC. Quantification of mixtures of 18:1/16:0-PC and 16:0/18:1-PC standards by ion trap MS^3 fragmentation. X-axis: mol% of 18:1/16:0-PC in the mixture determined by PLA_2 hydrolysis and PIS *m/z* 184.1; Y-axis: the peak intensity of de-methylated 16:0-lysoPC divided by the sum of peak intensities of de-methylated 18:1-lysoPC and 16:0-lysoPC in acquired MS^3 spectra.

The intensity of other fragments, or a combination of intensities of fragments, observed in MS^3 spectra, did not correlate well with the mol% of the isomers, most likely because the yield of fragments from other fragmentation pathways is less position-specific than that of ketene loss. Further supporting this notion, it was found that lyso-phosphatic acid fragments formed by loss of ketene from *sn*-2 position enabled accurate estimates of mol% in mixtures of 16:0/18:1- and 18:1/16:0 phosphatic acid, although they were much less abundant than fragment ions produced by neutral loss of free fatty acid (data not shown).

Thus, relative (in mol%) quantification of isobaric and isomeric PC species by ion trap MS^3 fragmentation is direct and does not require internal standards. The determination is very specific because of the accurate selection of precursor masses at MS^2 and MS^3 stages, and therefore is reliable even if applied to total lipid extracts.

2.2.5   Quantification of positional isomeric PCs in MDCK II cells

The MDCK II cell line is an established model to study the biogenesis of epithelial surface polarity and the mechanisms of polarized protein and lipid sorting. Here, we applied a combination of FAS and MS[3] fragmentation to characterize the molecular composition of PCs in a total lipid extract.

Lipid extracts of MDCK II cells were first analysed in positive ion mode by PIS *m/z* 184.1 to detect PCs. The total number of carbon atoms and double bonds in fatty acid moieties was calculated from intact masses of detected precursors (Table 3). The same sample was further analysed by FAS in negative ion mode. 50 precursor ion scan spectra of acyl anions of fatty acids were matched to the spectrum of PIS *m/z* 184.1 by Lipid Profiler 1.0 software (described in the next section) and allowed me to determine the fatty acid composition of all detected PC species (Table 3).

Table 3. Molecular composition of PCs from MDCK II cells.

PIS m/z 184.1			FAS		Ion trap MS[3]		
+Precursor ion, *m/z*	Relative content, %	[a]Brutto composition	[b]-Precursor ion, *m/z*	Fatty acid moieties	[c]-Precursor ion, *m/z*	Molecular species	mol %
692.6	<1	29:0	750.8	14:0;15:0			
704.6	2	30:1	762.8	14:0;16:1			
706.6	1	30:0	764.8	14:0;16:0			
718.6	1	31:1	776.8	14:0;17:1			
				15:0;16:1			
720.6	<1	31:0	778.8	14:0;17:0			
730.6	1	32:2	788.8	16:1/16:1			
732.6	6	32:1	790.8	14:0;18:1	766	14:0/18:1	3
				15:0;17:1		18:1/14:0	6
				16:0;16:1		15:0/17:1	3
						16:0/16:1	55
						16:1/16:0	33
734.6	2	32:0	792.8	16:0;16:0			
744.6	2	33:2	802.8	16:1;17:1			
746.6	8	33:1	804.8	15:0;18:1			
				16:0;17:1			
				17:0;16:1			
748.8	1	33:0	806.8	15:0;18:0			
				16:0;17:0			

756.6	<1	34:3	814.8	16:1;18:2			
758.6	7	34:2	816.8	16:0;18:2			
				16:1;18:1			
760.6	23	34:1	818.8	16:0;18:1	794	16:0/18:1	89
				17:0;17:1		18:1/16:0	10
						17:1/17:0	1
772.6	5	35:2	830.8	15:0;20:2	806	15:0/20:2	6
				16:1;19:1		16:1/19:1	2
				17:1;18:1		19:1/16:1	4
						17:1/18:1	70
						18:1/17:1	18
774.6	2	35:1	832.8	16:0;19:1			
				17:0;18:1			
				18:0;17:1			
782.6	<1	36:4	840.8	16:0;20:4			
784.6	3	36:3	842.8	16:1;20:2			
786.6	17	36:2	844.8	16:0;20:2			
				18:0;18:2			
				16:1;20:1			
				18:1/18:1			
788.6	9	36:1	846.8	18:0;18:1			
				16:0;20:1			
800.6	2.7	37:2	858.8	17:0;20:2			
				18:1;19:1			
				17:1;20:1			
802.6	<1	37:1	860.8	17:0;20:1			
812.6	2	38:3	870.8	18:1;20:2			
814.6	3	38:2	872.8	18:0;20:2			
				18:1;20:1			
816.6	<1	38:1	874.8	18:0;20:1			

[a] total number of carbon atoms : total number of double bonds
[b] detected as acetate adduct
[c] detected as chloride adduct

Complementing PIS *m/z* 184.1 by FAS allowed specification of ambiguous precursor ion assignments. For example, a minor peak at *m/z* 748.5 was detected by PIS *m/z* 184.1. It was not obvious whether the peak belonged to 33:0-PC, since it overlapped with the second isotopic peak of abundant 33:1-PC at *m/z* 746.5 (Figure 25). Nevertheless, FAS

identified 33:0-PC species as {16:0;17:0}-PC and {15:0;18:0}-PC. In total lipid extract of MDCK II cells we identified 15 PC species (not including positional isomers) comprising fatty acid moieties with an odd number of carbon atoms, although this was rather unexpected from the known pathways of de novo lipid biosynthesis in mammalian cells.
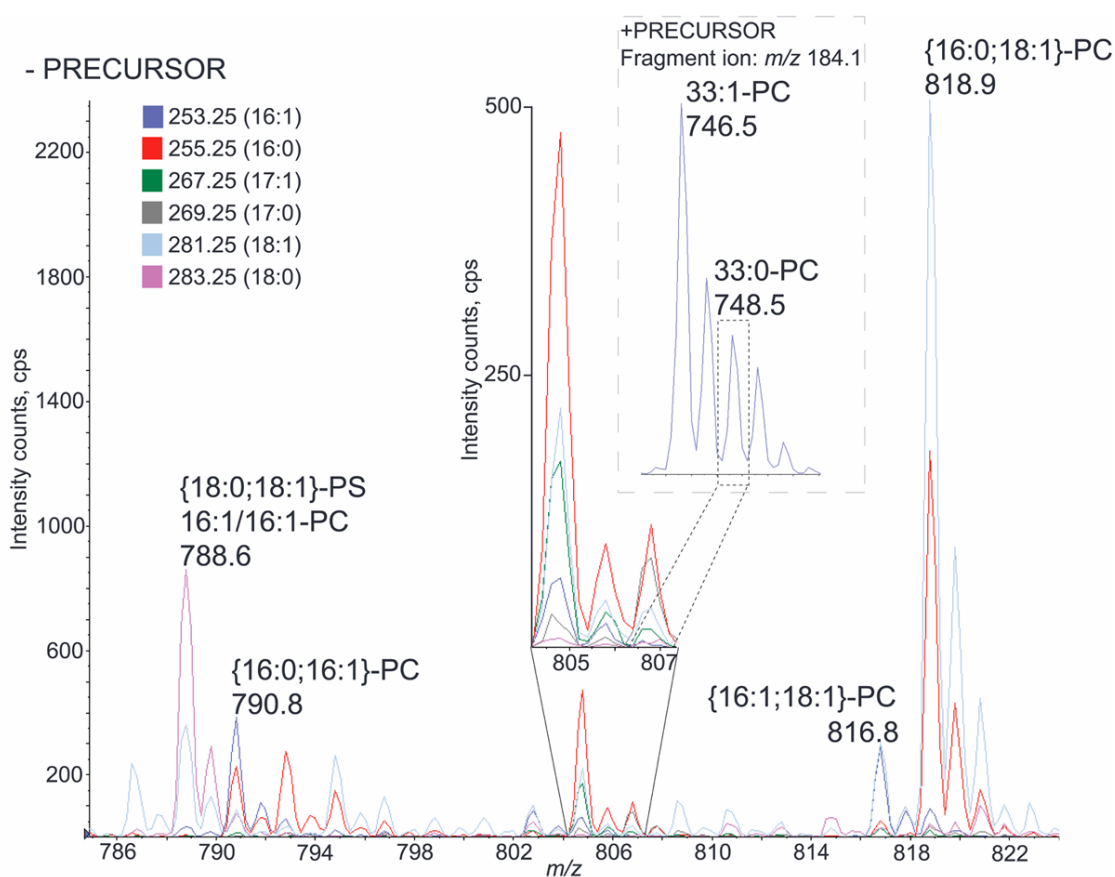
Figure 25. Resolving ambiguous precursor ion assignments by FAS. In PIS *m/z* 184.1, the peak of 33:1-PC (*m/z* 748.5) overlaps with the second isotope peak of abundant 33:0-PC (*m/z* 746.5)(inset). FAS (zoomed) suggested that 33:0-PC is a mixture of {15:0;18:1}-, {16:0;17:1}- and {17:0;16:1}-PCs (only representative precursor scans are presented in the figure). At the same time, FAS identified 33:1-PC as {16:0;17:0}- and {15:0;18:0}-PCs. 50 precursor ion scan spectra were simultaneously acquired in the FAS experiment.

Ion trap MS^3 analysis was further performed on the most abundant PCs (Table 3). For example, FAS indicated that 34:1-PC (*m/z* 766.8) consists of {16:0;16:1}-PC, {15:0;17:1}-PC and {14:0;18:1}-PC. MS^3 analysis confirmed the fatty acid assignment and enabled us to determine that 16:0/16:1-PC and 16:1/16:0-PC constitute 33 and 55 mol% of the total 34:1-PC, respectively, with other species accounting for 3 to 6 mol% (Table 3).

It should be noted that *m/z* of PC species with fatty acids having an odd number of carbon atoms might coincide with *m/z* of ether PCs in which an alkyl chain is linked to the

56

glycerol backbone *via* an ether, rather than an ester, bond. However, in MS/MS spectrum of synthetic 1-O-hexadecyl-2-arachidonoyl-*sn*-glycerol-3-PC standard, no corresponding alkoxide ion at *m/z* 241.25 was observed (data not shown). Therefore alkoxide anions of ether lipids will not be detectable by FAS and will not compromise the confidence of peak assignment in FAS spectra. Taken together, PIS *m/z* 184.1, FAS, and ion trap MS[3] fragmentation revealed high complexity of the molecular composition of PCs, represented by a variety of isomeric and isobaric species.

In conclusion, combination of FAS and MS[3] was applied to profile PCs in a lipid extract from MDCK II cells. The conventional analysis by PIS *m/z* 184.1 detected 25 peaks of isobaric PCs (Table 3). Further analysis of the same sample by FAS revealed that they represent 46 species with unique fatty acid composition. MS[3] fragmentation of the most abundant peaks suggested that they are mixtures of positional isomers and therefore the total number of molecular species is close to one hundred. Although we detected no sizeable amount of ether PCs, we could not exclude the possibility that they might be present in the extract (Daniel, Huang et al. 1993), but were masked by more abundant species.

2.2.6   *Quantification of positional isomeric PCs in human red blood cells*

The lipid composition and major molecular species of glycerophospholipids of human red blood cells were previously rigorously characterized (Connor, Lin et al. 1997) by a sophisticated analytical routine that involved several TLC separations, hydrolysis of lipids by phospholipase C, derivatization of diradylglycerols by benzoic anhydride followed by quantification of diradylglycerolbenzoates by reversed-phase HPLC (Blank, Robinson et al. 1984). Diradylglycerolbenzoates were separated into 20 chromatographic peaks (some of them contained a few co-eluted species), however separation of positional isomers was not achieved (Blank, Robinson et al. 1984).

To further validate our mass spectrometric approach and the results obtained in MDCK cells, we determined the molecular composition of PCs from human red blood cells (Table 4) and compared it with previously reported results by Connor et al (Connor, Lin et al. 1997). Connor et al identified 26 molecular species of PCs and 22 species were identified by mass spectrometry. It must be noted that we did not acquire precursor ion spectra for acyl anions of a few minor fatty acids (*e.g.* 22:6) although Connor et al found corresponding lipids. Within two independent data sets 14 molecular species overlapped.

All non-overlapping species were at low abundant and their relative content was less than 3 mol%. All 8 major PC species with relative content > 3 mol%, which were reported by Connor et al, were also detected by mass spectrometry with very similar relative abundance. Furthermore, ion trap MS[3] analysis of major PC species suggested that positional isomers (remained undetected by Connor et al) are common in human red blood cells (Table 4). For example 20:4/16:0-PC, having a highly unsaturated arachidonic acid at *sn*-1 position, constitutes about 13 mol% of the total 36:4-PC.

Table 4. Molecular composition of major PCs from human red blood cells.

PIS m/z 184.1			FAS		Ion trap MS[3]		
+Precursor ion, m/z	Relative content, %	[a]Brutto composition	[b]-Precursor ion, *m/z*	Fatty acid moieties	[c]-Precursor ion, *m/z*	Molecular species	mol %
706.6	1	30:0	764.8	14:0;16:0			
732.6	2	32:1	790.6	16:0;16:1			
734.6	5	32:0	792.6	16:0/16:0			
746.6	1	33:1	804.8	16:0;17:1			
748.6	<1	33:0	806.8	16:0;17:0			
756.6	<1	34:3	814.8	16:1;18:2			
758.6	20	34:2	816.8	16:0;18:2	792	16:0/18:2	94
						18:2/16:0	6
760.6	22	34:1	818.8	16:0;18:1	794	16:0/18:1	85
						18:1/16:0	15
762.6	3	34:0	820.8	16:0;18:0			
772.6	1	35:2	830.8	17:0;18:2			
774.6	<1	35:1	832.8	17:0;18:1			
782.6	7	36:4	840.8	16:0;20:4	816	16:0/20:4	87
						20:4/16:0	13
784.6	4	36:3	842.8	18:1;18:2	818	18:1/18:2	42
				16:0;20:3		18:2/18:1	16
				18:0;18:3		16:0/20:3	31
						20:3/16:0	6
						18:3/18:0	5
786.6	8	36:2	844.8	18:0;18:2	820	18:0/18:2	71
				18:1/18:1		18:2/18:0	7
						18:1/18:1	23
788.6	6	36:1	846.8	18:0;18:1			
				16:0;20:1			

790.6	<1	36:0	848.8	18:0/18:0			
808.6	1	38:5	866.8	18:1;20:4			
810.6	2	38:4	868.8	18:0;20:4			

[a] total number of carbon atoms : total number of double bonds
[b] detected as acetate adduct
[c] detected as chloride adduct

Connor et al detected one PC species comprising a fatty acid with an odd number of carbon atoms - {17:0;18:1}-PC. Mass spectrometry confirmed that 17:0 and 17:1 are major fatty acids with an odd number of carbons that are present in PCs from red blood cells and also detected them in another three molecular species (Table 4). We therefore concluded that qualitative and quantitative concordance of the molecular composition of PCs determined by us and, independently, by Connor et al validates the mass spectrometry based approach.

2.3   Identification and quantification of molecular GPL species

2.3.1   *Identification of GPLs using Calculus software*

To enable automated identification of molecular species, detected by FAS and HGS, we decided to build a software called Calculus, to speed up the identification process. This was done in collaboration with Gustaf Selen (Åbo Akademi University, Turku, Finland). Our strategy was to calculate what brutto compositions match the *m/z* determined with given mass accuracy. Since GPLs are detected as singly charged lipids, the determined *m/z* value directly corresponds to their monoisotopic mass.

We set out to evaluate how such calculations could efficiently be performed. The monoisotopic masses of the various head groups and fatty acids were first inserted into a database. An algorithm was built that combined the masses of a head group (with the glycerol backbone) and two fatty acids, and that matched the calculated total mass with the determined *m/z*. Depending on the way the molecular species are detected, additional information needed to be included for the calculation. In positive-ion mode the lipids are either detected as protonized (H^+) ions $[M+H]^+$ or as lithiated (Li^+) adducts $[M+Li]^+$, and therefore subtraction of the monoisotopic masses of these ions are required for the calculations. Similar additional calculations were performed for lipids detected in negative

ion mode. Here, the monositopic mass of hydrogen was added. The monoisotopic masses of isotopic labeled head groups and fatty acids, either with ^{15}N or ^{13}C, were also added to the database, to enable identification of metabolically labeled lipids generated in *E.coli* and *P. pastoris* (see section 2.4). The matching results were treated as a true value and finally displayed by their head group and pair of fatty acids including the monoisotopic masses and the mass error (calculated *vs.* submitted).

We further evaluated whether this setup enabled identification of the correct lipid species. *M/z* 758.8 detected by PIS *m/z* 184.1 was submitted for identification. Before, the mass was set to correspond to an unlabeled protonized lipid (Figure 26A). No match could be determined in this fashion. This was due to the low mass accuracy in the determined *m/z* coming from the set resolution of the Q1 quadrupole. Therefore it was necessary to introduce a mass window option, *e.g.* mass accuracy, in the calculations. With the mass window set to 0.4 Da the *m/z* 758.8 could be correctly detected as PC 34:2. The identified PC was displayed as a molecular species including its monoisotopic mass and mass error (Figure 26B). From this we defined that, if the calculated masses were outside the submitted *m/z* value but inside the selected mass window, they should be treated as true hits. As default this mass window was set to a total of 0.4 Da which clearly enabled detection of the right molecular species.

Figure 26. Overview of the Calculus software. A. *m/z* value submit page for lipid identification in the Calculus software. 0.4 Da accuracy (mass window) is set as default. Isotope calculations, 13C and 15N, selection as protonated/deprotonated (+/- H) ions (negative and positive ion mode selection) and detection as Li$^+$ adducts in positive ion mode are set as user defined additional options. B. *M/z* 760.9 recorded in PIS *m/z* 184.1 is identified as PC 34:1 and the suggested molecular species are displayed.

Calculus software was programmed in the Phyton programming language and run in a web browser under the Linux computer system. This permits very fast calculations and identification of molecular species. By submission of all detected *m/z* values and performing the identification process through web pages, run from a separate server, the Calculus software becomes flexible and powerful. Neither special software is required nor is a separate installation on different computers needed. Furthermore, the software can be installed on the same computer if no network is available and still enables a complete identification process. Thus, this significantly increases the automation and speed in the identification process of molecular species.

2.3.2 Lipid Profiler 1.0 software

Calculus software only allows manual identification of single peaks. There is no automation option included that would enable identification of multiple peaks in a single run. Furthermore, the peak information data, as peak area and peak intensity, can not be extracted by the software, thus making, for instance, quantification analysis very time consuming due to all manual manipulations. Therefore, large sets of data generated in a single MPIS experiment on a total lipid extract are not amenable to the analysis using this software.

To overcome this we set out to develop together with Eva Duchoslav at MDS Sciex (Concord, Canada) a software that we named Lipid Profiler. This software facilitates data processing in support of qualitative and quantitative profiling of lipids by TOF MS and MPIS (HGS and FAS) on QqTOF instruments. Lipid Profiler is compatible with the MS acquiring software Analyst QS 1.0 SP6 and later versions. Microsoft Office (Microsoft Access), version XP is recommended. While Microsoft Access is not needed for data processing, it is required for any customizing of the supporting lipid database. The workflow and possibilities of this software is described in detail in the next two sections.

2.3.3 Analysis of TOF MS, FAS and HGS spectra by Lipid Profiler 1.0

We first evaluated how to perform and handle the identification of multiple molecular GPLs simultaneously. The strategy was to match all determined *m/z* values, above a certain threshold, obtained from a single MPIS experiment to the calculated brutto and molecular lipid compositions. We decided to store the monoisotopic masses of isotopically labeled

and unlabeled head group and fatty acid fragments in separate tables, including their analysis information. For positive ion mode analysis, separate tables for the protonized (H^+) and lithiathed (Li^+) head groups were generated. For negative ion mode analysis, separate tables for deprotonized head groups and chlorine and acetate head group adducts were generated. The monoisotopic mass of the glycerol backbone was included in the head group masses.

Next, depending on which mode GPLs are analyzed in, the identification of molecular species should proceed in different ways. The monoisotopic masses of head groups and fatty acids should be combined and matched to the detected m/z value in the TOF spectrum. In HGS and FAS, since one fragment ion is already known (selected fragment ion) the identification process is slightly different. In FAS, monoisotopic masses of head groups should be combined with the monoisotopic mass of one fatty acid. On the other hand, in HGS the monoisotpoic masses of two fatty acids should be combined and matched to determined m/z value. The latter combinations demand less calculation and thus increase the identification throughput in comparison to TOF analysis. In this approach lipids are identified, in TOF and HGS, based on their brutto composition (*e.g.* total number of carbon atoms and total number of double bonds of the attached fatty acids) whereas in FAS lipids are identified as molecular species. To optimize and accelerate the identification procedure we needed to implement a user-defined threshold for minimum peak area and/or peak intensity. This clearly decreases the number of m/z values to be matched and therefore speeds up the identification process. Furthermore, due to the low mass accuracy in the MPIS data a mass tolerance option of Q1 quadrupole was implemented. The identification process was further optimized by enabling smoothing of MPIS and TOF data. We realized that this was critical for data acquired at low resolution.

We next evaluated the workflow of the data processing. Here, we wanted to enable identification processing directly on an opened data file in Analyst QS. Therefore, a script – termed Find Phospholipids - was integrated in the software. This script extracted the determined m/z values and submitted them for identification. This script could be run from the Script menu in Analyst QS (Figure 27). To increase flexibility in the identification process, we decide to keep the manipulations of the threshold for minimum peak area and/or peak intensity, mass tolerance and smooth spectrum options user-defined. Furthermore, to accelerate the identification time the total number of double bonds in the sum of fatty acids, and only in the second fatty acid, was also implemented in the script menu. This clearly minimizes total number of combinations in the calculation.
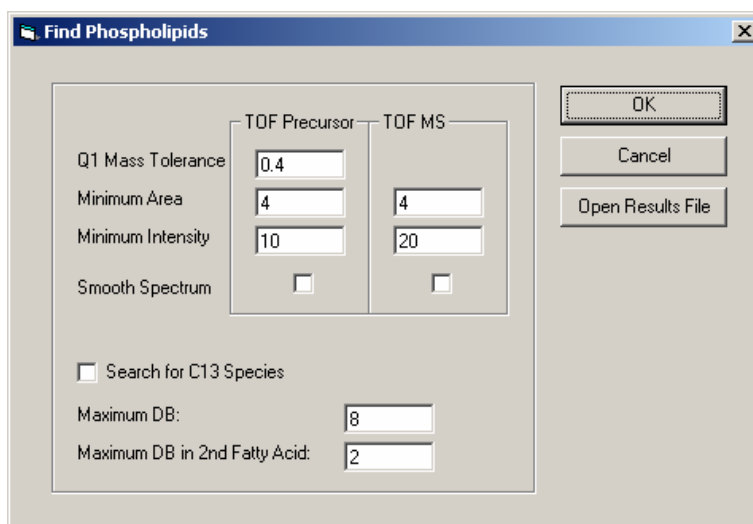
Figure 27. Screen shot of the Find Phospholipids script. Q1 mass tolerance, minimum area, minimum intensity, maximum double bonds and maximum double bonds in the second fatty acid is by default, 0.4 Da, 4 units, 10 counts per second, 8 and 2, respectively.

We further evaluated if this setup enabled identification of the correct lipid species. FAS data of human red blood cells opened in Analyst QS was submitted through the Find Phospholipids script. Q1 mass tolerance was set to 0.4 Th and the thresholds of peak area and intensity to 4 and 10, respectively, and without the smooth option of the spectra. Maximum total double bonds was set to 8 with maximum 2 double bonds in the second fatty acid, and submitted for identification. This clearly allowed identification of correct molecular GPL species (Figure 28) verified by the Calculus software. The precursor ion mass, peak intensity and peak area data of individual GPLs are categorised in their respective columns. Furthermore, in MPIS data, precursor scan and fragment mass columns were included. The respective GPL classes are categorised in the last six columns with species, displayed by their brutto composition.

Normally 50 acyl anions were selected in a single FAS analysis (50 spectra), but massive amounts of data would be generated. Therefore, it was required to structurize the display view of the identified GPLs. We decided to label the identified GPL species depending on how they were identified. For instance, *m/z* 688.8 is identified as PE 32:1 (Figure 28). Since this *m/z* value is detected in both precursor scans of FA 16:1 and FA 16:0, the PE 32:1 can be identified as {16:0;16:1}-PE, and therefore displayed in bold. If the same *m/z* value would only be detected in the precursor scan of FA 16:0 and not FA 16:1, it would be displayed as normal text. If the FA 16:1 precursor scan was not acquired it would be displayed in colour, with or without background to easier distinguish the

different classes. Since masses of various GPL species overlap, in several cases multiple GPLs are suggested for the detected *m/z* value. Identifying the same GPL species in the different FA precursor ion scans, as for the PE 32:1 above, including the particular head group precursor ion scan, clearly can abolish any misidentifications. Therefore combing both HGS and FAS enables correct identification of molecular species.

Figure 28. Screen shot of identified GPLs using the Find Phospholipids script. *M/z* 688.6 is identified as PE 32:1; {16:0/16:1}-PE.

We further wanted to automize the identification process further and enable processing of multiple data files simultaneously. The identification process was done on a single acquired data file or on all files of the *wiff*-file using the Find Phospholipids script. In Analyst QS all acquired data files are saved and indexed in a single *wiff*-file (*e.g.* standard Analyst file type). The individual GPL identifications of one TOF and two FAS data files are displayed in Figure 28. Sample 1 (defined by their *wiff* index number) contains the TOF data and is labeled in black. Samples 2 and 3 are both FAS data and labeled in green. By clicking on the sample number, the individual GPLs detected in that particular file are displayed.

To increase the flexibility in data manipulation an option in the Find Phospholipid script was implemented for exporting the identified data as a tab delimited text file. This text file could also be reopened by the script for further analysis, without any hindrance in the Analyst QS software (allows full data analysis with the script opened).

In conclusion, the GPL identification setup in the Lipid Profiler software readily enables fast, direct and comprehensive identification of GPLs. Applying identification directly on data files opened in Analyst QS significantly increases the flexibility in data handling and verification. In this way the identified lipid species can directly be reviewed with the peaks detected in the mass spectra. User friendly display and manipulation of identified GPL species readily helps in the data interpretation and charting of individual species. Enabling identification processing on multiple files clearly increases the throughput, without loosing the simplicity in the data handling. Possibility to export the identified lipid species together with their mass spectrum data is advantageous for any post data processing, as for instance, quantification.

2.3.4 *Lipid Profiler 1.0 enables monitoring of the relative abundances*

The relative quantification of molecular GPLs was done by spiking an equal amount of the total lipid extract of ^{13}C-labeled lipids from *P. pastoris* into samples which served as internal standard (described in section 2.4.4.1). Increasing the correctness of the quantification, intensities and/or area of peaks of interest are normalized to intensities of three internal standards (^{13}C-labeled lipids of the same class) having *m/z* similar to that of the quantified peak. Thus, the relative changes in the concentration of lipid species can be calculated as:

$$\frac{\left[\frac{(\mathrm{EIp/EIst1})}{(\mathrm{CIp/CIst1})}\ \frac{(\mathrm{EIp/EIst2})}{(\mathrm{CIp/CIst2})}\ \frac{(\mathrm{EIp/EIst3})}{(\mathrm{CIp/CIst3})}\right]}{3} - 1 \times 100\%$$

where EIp and CIp stand for intensities (areas) of experimental and control peaks, respectively; EIst1-EIst3 and CIst1-CIst3 are intensities (areas) of peaks of ^{13}C-labeled internal standards in experimental and in control spectra, respectively. The result is presented in percentage along with the mean standard error. This we included in the Lipid Profiler software. Here we are only considering MPIS data.

We first evaluated how to handle the data and how the workflow should be shaped. The strategy was first to define sample data and control data. The sample information was organized into a tab delimited text file. This file had a one line header followed by a sample list that could be prepared in any text editor program. The full path of the *wiff*-file,

the index of the sample in the *wiff*-file, the index of lipid sample (data with the same sample number are considered to be replicates) and the dilution factor (to correct for differences in amounts of native and labeled fatty acids) were included and considered necessary to enable extraction of the correct data. The control data file was generated in the same way. Since we wanted to quantify according to the calculation formula described above, three replicates of each sample and control were included.

We decided to use a main wizard window – termed Phopsholipid Profiling Criteria - to manipulate all the steps involved in the complex quantification process (Figure 29). First, the lipids to be quantified were defined. A data file could be subjected for GPL identification using the Find Phospholipids script, and selected identified GPLs used for quantification. Another possibility to select GPLs for quantification could be obtained from a previous identification file. We considered that it would be particularly feasible if all data manipulation settings could be saved in a database that then could be reused for other quantification analysis. This would considerably simplify and speed up further quantifications. Therefore, we implemented the option to select and modify an existing settings database, or, alternatively to set up a new one. Next step in the application was to specifying the internal standards. Here, we wanted to include both options of using lipid labeled analogues and/or any synthetic standards as internal standards. The parent ion and precursor ion masses and names of the internal standards were specified. To quantify against summed response of several synthetic standards the user needs to assign the same group name to such standards.
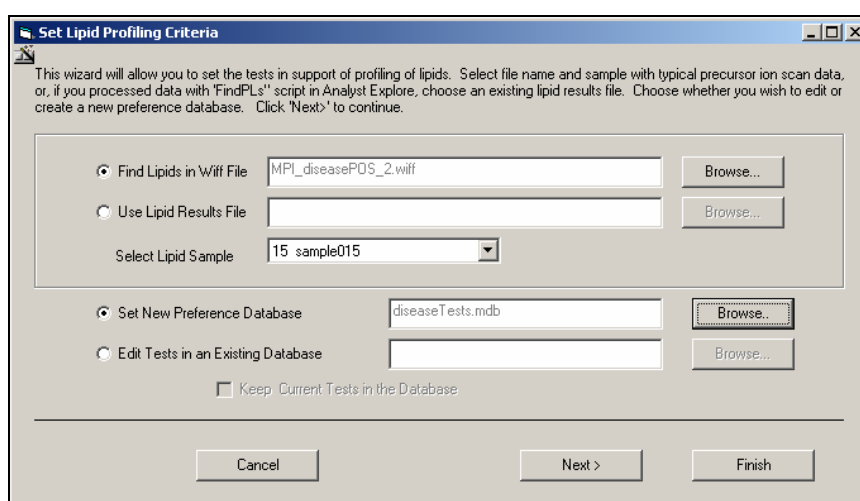
Figure 29. Screen shot of the Set Lipid Profiling Criteria window.

After defining the internal standards, the next step was to select which identified GPLs to be quantified (Figure 30). To simplify the overview we considered tabulating all found lipids. Furthermore, to verify the lipid identification, each data point could be independently reviewed in their particular mass spectra. For each GPL species which should be quantitatively monitored, the name of the test, *e.g. m/z* 688.8 detected by FAS *m/z* 255.5 is FA 16:0/PE 32:1 and the internal standard are set in the last two columns to the right. When all internal standards for the lipids to be monitored have been set the settings are saved in the preference database. This can be reused for other quantification analyses.
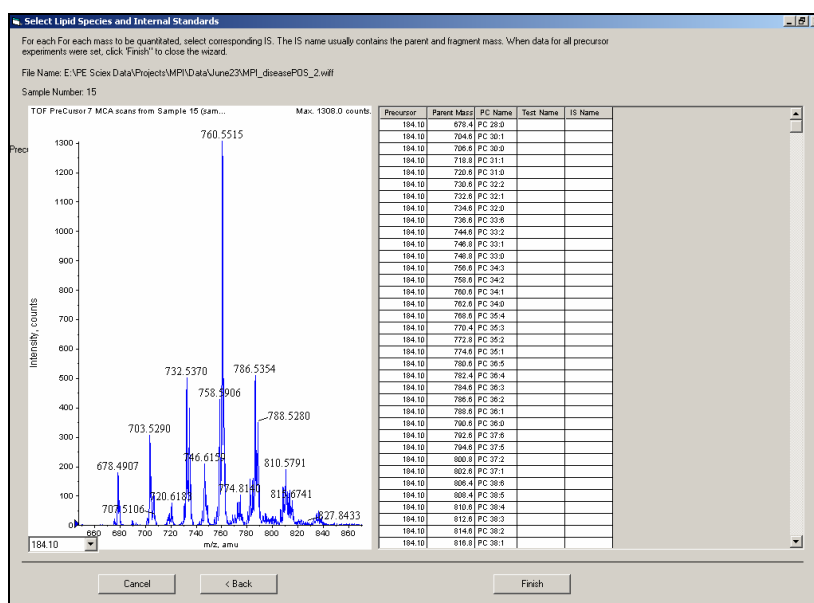
Figure 30. Setting Monitored Lipids and Internal Standards.

Having all data manipulation set, our final goal was to process the data and evaluate a feasible display of the quantification results. This was done in the main window of the Lipid Profiler 1.0 software (Figure 31). The previous defined data and control data files and quantification settings database was selected, and subjected to quantification processing.
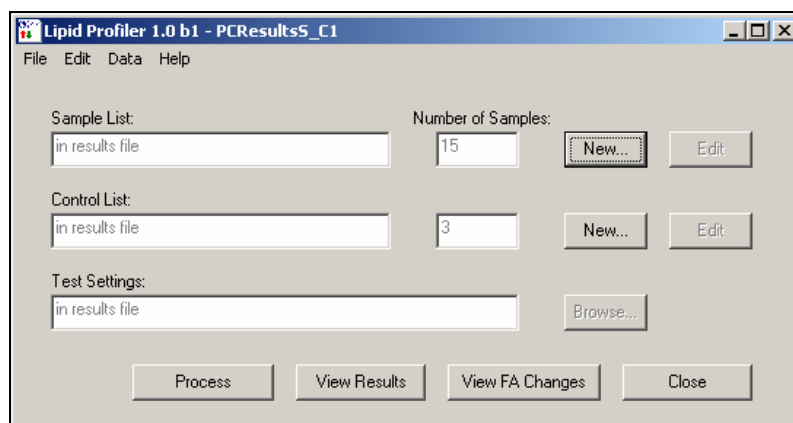
Figure 31. Lipid Profiler 1.0 Main Window.

We considered to enable reviewing of the results in three different ways; 1. sample data, 2. control data and 3. statistics. This allowed us to more easily verify the data used for the quantification. The quantification was performed as the formula described above. For these calculations we used both the peak area and peak intensity values of the selected lipids and standards. The standard deviation and relative standard error of individual calculation were included in the result file. Quantification by peak area was proved to be more correct, with less variation.

Importantly, to avoid any pitfalls in the data processing, we considered including a possibility to display the experimental data. Reviewing the sample data clearly helped us to correct previously made mistakes.

Finally, after completed quantification processing, it is feasible to display the results in a simple fashion. Therefore, we decided to view the results in terms of changes in lipid groups (Figure 32). Changes in the individual fatty acid of a particular lipid could be viewed. Furthermore, since the HGS and FAS analysis can be combined, changes in the individual fragments could be comprehensively viewed. This can further be compared to other samples. Changes in all monitored lipids or samples can be viewed in the same fashion. Here, the differences between calculations by peak area and peak intensity can be displayed. If the results are derived from replicate measurements, they are displayed as RESULT ± SD. The complete result file could further be exported to a text file for further manipulation.
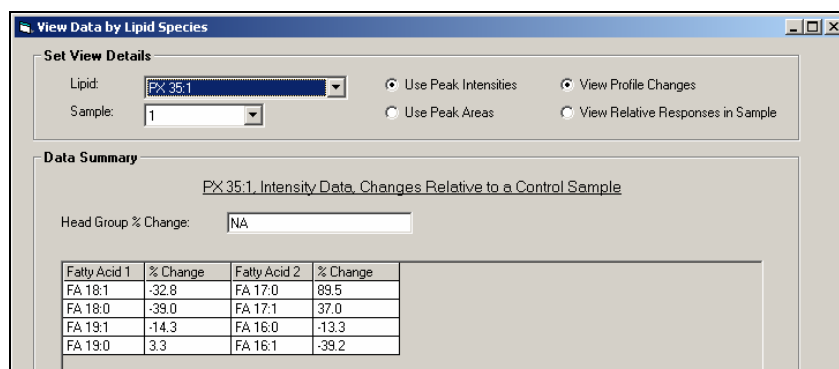
Figure 32. View Lipid Changes

2.4   APPLICATIONS

2.4.1   GPLs of Triton X-100 DRMs of human red blood cells

Preparations of detergent-resistant membranes (DRMs) are valuable for the analysis of biological membranes. DRMs are a most useful starting point for defining membrane subdomains, including cholesterol–sphingolipid rafts. DRMs of for instance MDCK cells does not only comprise of domains of the plasma membranes but are presumably contaminated by domains of other cellular membranes. This definitely complicates the interpretation of the results and therefore this should be done with extreme caution. Plasma membranes can be purified and separated by subcellular fractionation and then used for further studies. Still, this is not optimal since subcellular fractionation does not enable 100% separation of plasma membranes from other cellular membranes and, therefore, other membrane remnants cannot be abolished. On the other hand, red blood cells (RBC) do not contain a nucleus or cytoplasmic organelles. The only lipid membrane in these cells is the plasma membrane. RBC would therefore be suitable for studying plasma membrane DRMs in particular. Previously Salzer et al showed that raft microdomians exist in RBC (Salzer and Prohaska 2001). Equally important, the lipid composition and major molecular species of glycerophospholipids of human RBC have been previously rigorously characterized (Connor, Lin et al. 1997) by a sophisticated analytical routine that involved several TLC separations, hydrolysis of lipids by phospholipase C, derivatization of diradylglycerols by benzoic anhydride followed by quantification of diradylglycerolbenzoates by reversed-phase HPLC (Blank, Robinson et al. 1984). Furthermore, the distribution and quantification in the different GPL classes over the inner

and outer membrane leaflet have thoroughly been studied (Renooij, Van Golde et al. 1976). With all this information in hand, charting of PC and SM in DRMs prepared from RBC would be very informative, revealing insights in lipid organization of, in particular, plasma membrane lipid rafts.

We set out to evaluate the molecular GPL composition of different DRM preparations of RBC. It must be noted that at this point only HGS was available. Total cell membranes (TCMs) of RBC ghosts were obtained by flotation on sucrose step gradients. Fractions were further drawn from the top of the gradient and each fraction, after lipid extraction, was subjected to PIS m/z 184.1 for analysis of PC and SM. The PC and SM profiles of four fractions are illustrated in Figure 33. No significant changes can be observed in any of the fractions analyzed. The heavy fraction (fraction 8) shows similar profiles in both PCs and SMs as the light fraction (fraction 2). Irrespective of the lipid, all lipids show similar distribution throughout the gradient and this suggests that no separation of distinct domains has occurred, *i.e.* that the plasma membrane is not subdivided into sub-compartments that would be expected from what we know about RBC.
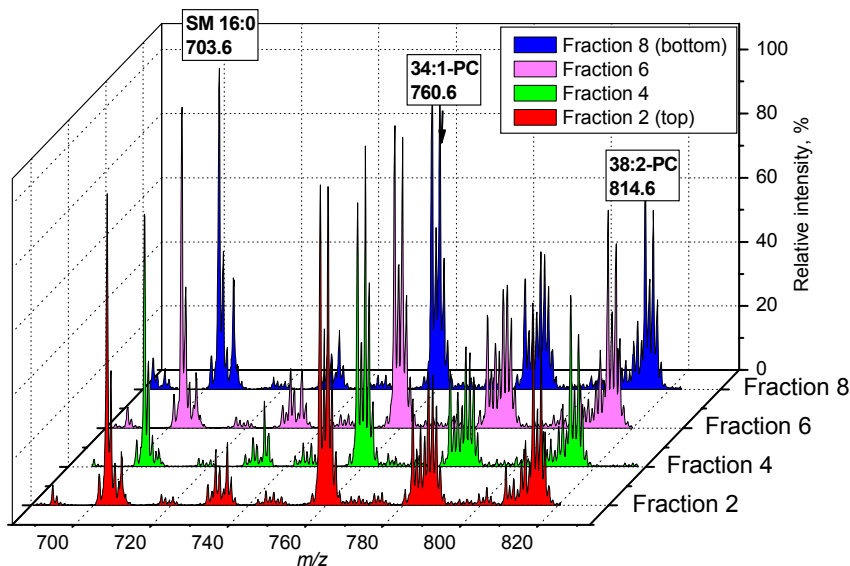
Figure 33. PC and SM species of total cellular membranes of RBC. PC and SM profile of four different fractions obtained by flotation of RBC ghosts without any detergent, *e.g.* TCM. Three peaks are labeled; *m/z* 703.6, SM 16:0; *m/z* 760.6, 34:1-PC; *m/z* 814.6, 38:2-PC. The top fraction (2) is displayed in front (red) whereas the bottom fraction (8) is displayed in back (blue).

Next, floated fractions of RBC ghosts prepared using 1% Triton X-100 were analysed. Both lower fractions, 8 and 6, show more or less similar profiles in PC and SM species whereas the upper fractions clearly show a distinctive PC and SM profile (Figure 34). The latter fractions are significantly enriched in SM in comparison to the lower fractions. Moreover, the upper fractions also contain more saturated PC. This suggests that 1% Triton X-100 clearly disrupts lipid association in RBC. The SM-rich membrane domains, enriched in saturated PC (Figure 35) are insoluble in 1% Triton X-100 likely because of their liquid ordered phase and thus float up to a lower density. In comparison, liquid disordered membranes are soluble in Triton X-100 and will not float upon centrifugation. Taken together, this approach readily documents the particular PC and SM species of plasma membrane DRMs of RBC. Future analyses have to be done in order to obtain more complete profiles in PCs and SMs together with other GPLs of DRMs.
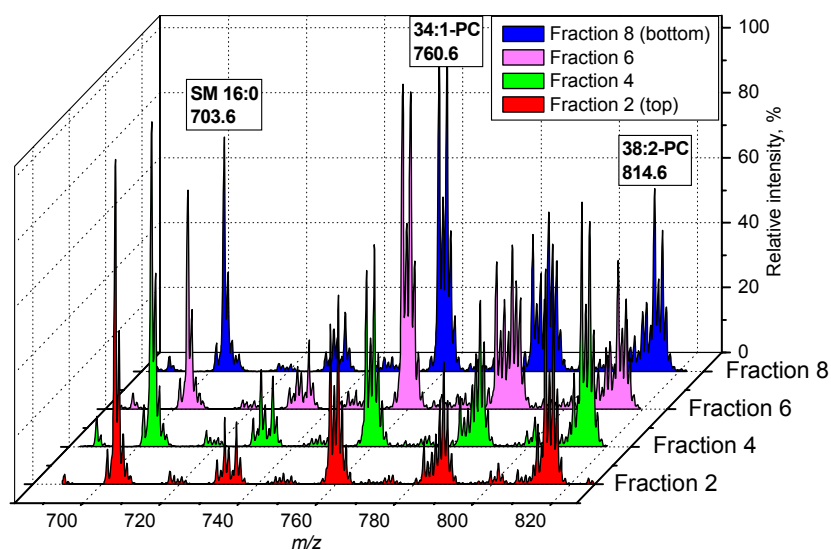
Figure 34. PC and SM species of 1% Triton X-100 DRMs of RBC. PC and SM profile of four different fractions obtained by flotation of RBC ghosts in 1% Triton X-100. Three peaks are labeled; m/z 703.6, SM 16:0; m/z 760.6, 34:1-PC; m/z 814.6, 38:2-PC. The top fraction (2) is displayed in front (red) whereas the bottom fraction (8) is displayed in back (blue).
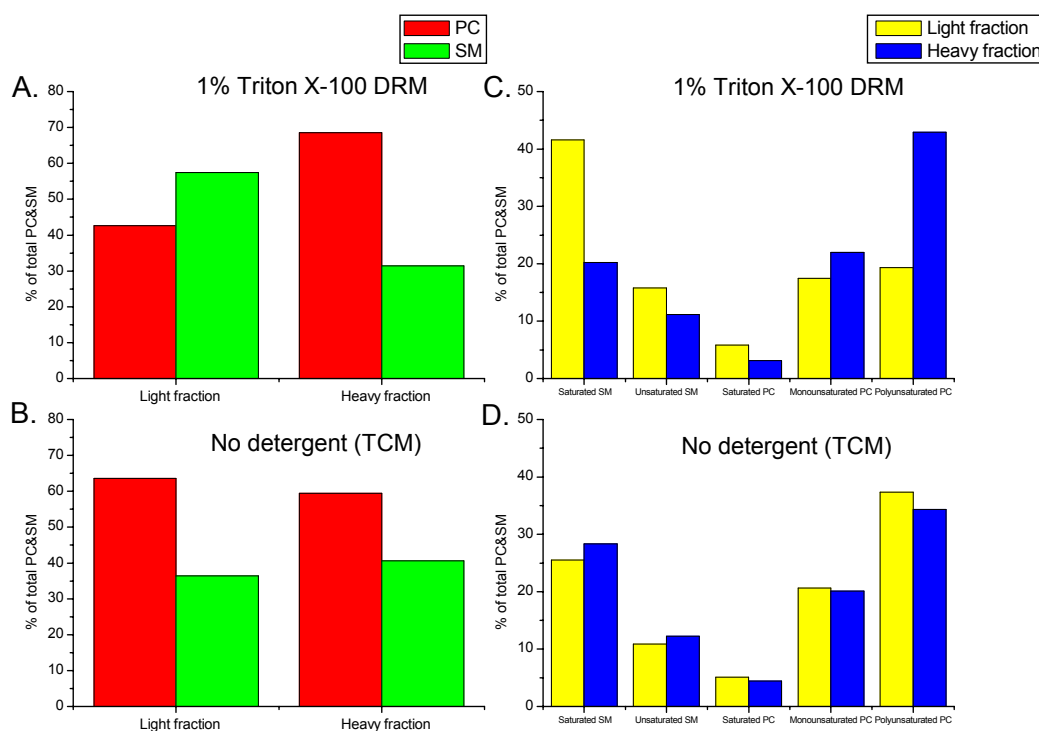
Figure 35. Abundance of PC and SM in 1% Triton X-100 DRMs of RBC. Comparison of the abundance of SM and PC in light and heavy fractions prepared using 1% Triton X-100 (A) and prepared without detergent (B) is shown. The abundance of the individual SM and PC fatty acid constituents was monitored in light and heavy fractions prepared using 1% Triton X-100 (C) and prepared without detergent (D). In A and B, SM and PC were respectively compared to the total sum of PC and SM and presented as %. In C and D, percent fractions of each PC species were determined and grouped into saturated (PC x:y, y=0), monounsaturated (PC x:y, y=1), and polyunsaturated (PC x:y, y=2 or more) PC species (in *x:y*, *x* indicates the total number of carbon atoms of the fatty acid side chains; *y* indicates the number of double bonds). In the same way, percent fractions of each SM species were determined and grouped into saturated (SM x:y, y=0) and unsaturated (SM x:y, y=1 or more).

DRM of 1% Triton X-100 contained approximately two-fold more SM in comparison to the respective light fraction of TCM (Figure 35, A and B). On the other hand, the levels in PC approximately show a completely reversed trend. Thus, DRM contained 60% SM whereas the level of PC was 40%. The decrease in PC in DRM is clearly detected as an increase in the heavy fraction, and vice versa for SM. This indicates that PC is more affected by solubilization in comparison to SM. This is probably due to the high levels of polyunsaturated PC in RBC (Figure 35D) that preferably imbeds in liquid disorder over liquid ordered phases. Notably, close to 30% of the total SM was still found

in the heavy fraction (Figure 35A). DRMs of 1% Triton X-100 were enriched in saturated SM species whereas the abundances in unsaturated (mainly monounsaturated) species were not significantly elevated (Figure 35C). Enrichment of saturated PC was also observed in DRM fraction whereas the level of monounsaturated PC species was not disturbed. On the other hand, polyunsaturated PC species were drastically reduced in the DRM fraction. Interestingly, the distribution of the various SM and PC species was kept very constant throughout the gradient in the TCM preparation (Figure 35D). This clearly indicates that there is no domain separation upon flotation at detergent-free conditions.

2.4.2 Molecular GPLs of Triton X-100 DRMs of MDCK cells

DRM preparation has mainly been approached by the use of mild detergents such as Triton X-100. The floated fractions containing DRMs will contain trace amounts of detergents that are upon lipid extraction, extracted together with the lipids. This will lead to detergent contamination of the samples to be analyzed, and thus substantially complicate any mass spectrometric lipid analysis due to the high chemical background. We previously showed that the high specificity of PIS in QqTOF instruments enables detection of selective lipids (section 2.1.4). Therefore, we decided to evaluate if the current MPIS setup allows comprehensive charting of molecular GPLs of 1 % Triton X-100 DRMs prepared from MDCK cells.

First, PCs were analyzed by PIS *m/z* 184.1. Seventeen PC species, differing in the total number of carbon atoms and/or the total number of double bonds in the fatty acid moieties, were detected using the Lipid Profiler 1.0 software. For each species, its percent fraction of the total PC was calculated by the software. In addition, the relative concentration of each species was determined to allow comparison of the amounts present in total cell membranes (TCM) and Triton X-100 DRMs (Table 5).

Table 5. Relative concentration of MDCK PC species of 1% Triton X-100 DRMs.

[a]Brutto composition	+Precursor ion, *m/z*	Relative abundance	
		Total cell membranes	Triton X-100
PC 30:0	706.5	62.7 ± 5.0	15.7 ± 2.2
PC 31:1	718.5	66.7 ± 0.6	4.4 ± 0.6
PC 31:0	720.5	33.3 ± 2.7	9.5 ± 2.4
PC 32:2	730.5	44.8 ± 4.3	0
PC 32:1	732.5	267.9 ± 16.0	14.9 ± 1.2
PC 32:0	734.5	95.0 ± 3.6	22.0 ± 1.8
PC 33:2	744.5	82.6 ± 2.2	3.0 ± 0.5
PC 33:1	746.5	463.4 ± 7.0	26.3 ± 0.9
PC 34:2	758.5	242.7 ± 12.6	8.6 ± 1.5
PC 34:1	760.5	1344.6 ± 7.1	83.4 ± 5.4
PC 34:0	762.5	139.5 ± 11.9	15.0 ± 1.1
PC 35:2	772.5	187.5 ± 9.1	6.6 ± 1.9
PC 35:1	774.5	99.3 ± 10.8	6.2 ± 0.8
PC 36:3	784.5	73.9 ± 6.5	2.1 ± 0.5
PC 36:2	786.5	725.4 ± 5.7	24.3 ± 2.4
PC 36:1	788.5	435.5 ± 8.8	34.3 ± 2.7
PC 38:3	812.5	62.5 ± 4.6	2.1 ± 0.7

[a] total number of carbon atoms : total number of double bonds

Significant less PC species were detected in DRMs. To visualize the differences in PC distribution, the PC species were grouped according to the degree of saturation of their fatty acid. In total cell membranes, approximately 10% of the PC was saturated, 60% was monounsaturated and 30% polyunsaturated. This ratio was rearranged in Triton X-100 DRMs, comprising approximately 20% saturated, 60% monounsaturated and 20% polyunsaturated PC species.

Dissection of lipid rafts into molecular components will improve understanding of their properties and functions. Comprehensive lipid analysis of DRMs should complement the analysis of DRM protein contents. Therefore, we next evaluated whether molecular GPLs of Triton X-100 DRMs could be charted by FAS. Performing FAS readily allowed detailed profiling of the compositional changes in molecular GPL species (Figure 36). Clear differences were observed between TCM and DRM profiles. For example, 16:0/16:0-PC is hardly detectable in TCM whereas in DRM it is one of the major GPL species, and for the 18:1/18:1 PG this is completely reversed. On the other hand, DRMs contain significant amounts of {13:0;18:0}-PG and {13:0;18:1}-PG. Furthermore, the ratio of the predominant 18:1/18:1-PE and {18:0;18:1}-PE species is reversed in DRM in comparison to TCM. Notably, new unidentified species are also detected in DRM. Here, clearly a similar trend is observed as for PC, with enrichment in saturated GPL species. It must still be underlined that, due to the high accuracy in fragment ion selection, detection of molecular species of detergent-containing samples is made possible. Interestingly, by

further performing ion trap MS^3 analysis on the same samples one would be able to quantify the mol% of positional isomers and thus together with FAS and HGS enable a complete quantification at the molecular species level.
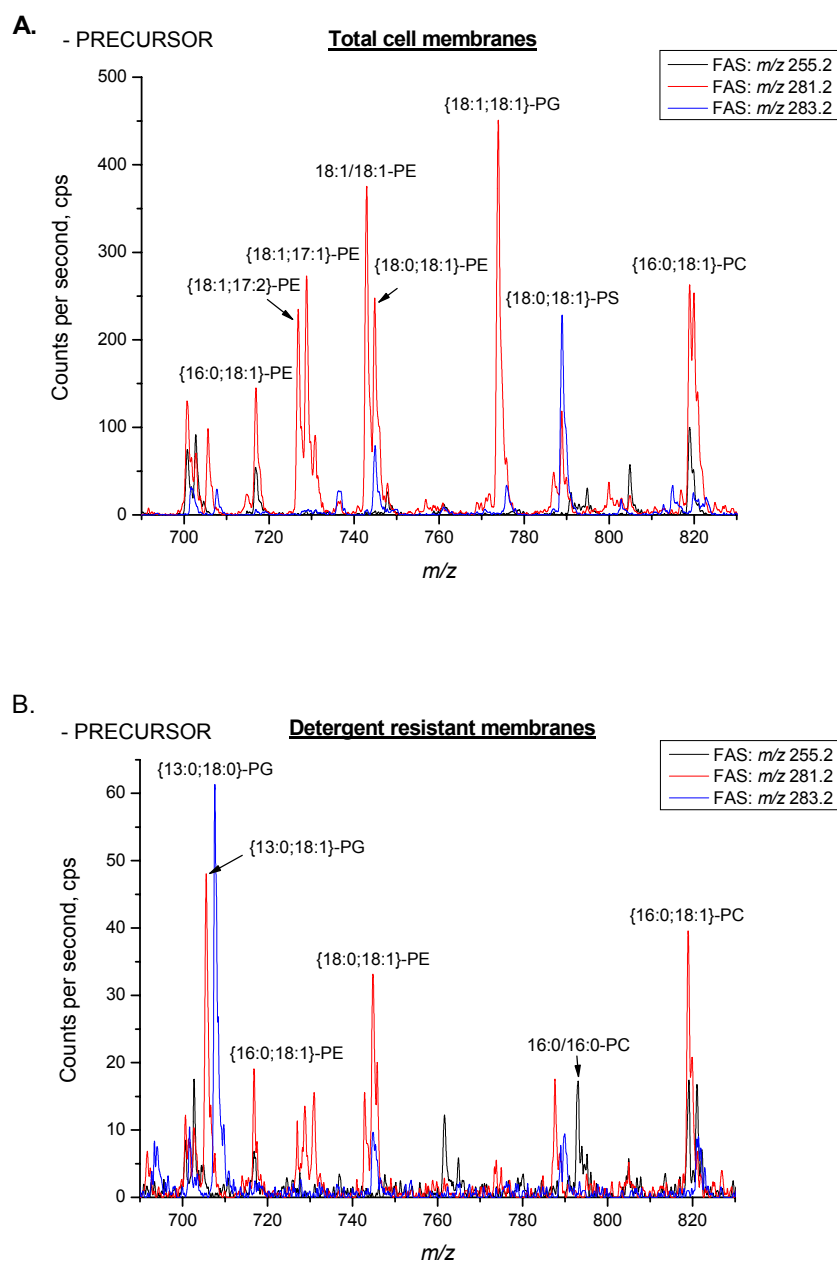
Figure 36. 1% Triton X-100 DRMs of MDCK cells analyzed by FAS. Compositional changes of individual lipid species between Total cell membranes (A) and Detergent resistant membranes (B) are detected

2.4.3   Shotgun Lipidomics – a perspective in automated analysis of molecular GPLs

2.4.3.1 Relative quantification based on isotopic labeled GPLs

To address a variety of biological questions, the lipid analysis methodology should be able to monitor changes in the lipid composition in a quantitative fashion. To this end, a bunch of internal standards (typically, synthetic lipids that do not occur in the living cell) is usually spiked into the analyzed sample. However, individual species within the same lipid class are detected with varying sensitivity (Koivusalo, Haimi et al. 2001). Also, as mentioned previously, conventional lipid extraction procedures, as Bligh & Dyer or Folch, may result in preferential losses of some lipids or even entire lipid classes, depending on the properties of their fatty acid moieties. It is therefore important that internal standards should be almost identical to endogenous lipids of interest, although for many lipid classes such standards are not readily available. Furthermore, this requirement is impossible to meet in conventional mass spectrometric quantification, because multiple peaks of internal standards would be overlapping with peaks of interest in a complex analyte.

Digests of proteins metabolically enriched in stable isotopes are widely employed as internal standards in quantitative proteomics (Gygi, Rist et al. 1999; Oda, Huang et al. 1999; Yao, Freas et al. 2001). It is therefore conceivable that metabolic labeling of cells may also produce internal standards useful for lipid quantification. As a test-bed I analyzed total lipid extracts of *E.coli* cells. The pool of *E.coli* lipids consists of three major classes: PEs, PGs and (in relatively minor amount) cardiolipins (Vance and Vance 1996). Harvesting cells in the medium that contained ^{13}C-glucose, as a single carbon source, enriched ^{13}C isotopes in lipid molecules and resulted in inversed isotopic distribution of their molecular ions and shifted their *m/z* according to the total number of carbon atoms (Figure 37). Notably, this could be accomplished already after 24 hours of labeling. Importantly, ^{13}C atoms were equally incorporated in fatty acids and in head groups of lipids of all classes. Therefore, in the mixture ^{13}C labeled lipids and normal lipids could be detected simultaneously by PIS using the fragment masses specific for the labeled and for the unlabeled head groups, respectively (Figure 37). The characteristic fragment of the head group of PE contains five carbon atoms and therefore its *m/z* was shifted by 5 Da. Therefore, unlabeled PEs were detected by selecting the fragment with *m/z* 196.0, ^{13}C labeled PEs were detected at *m/z* 201.1, and both precursor ion spectra were acquired in parallel. An equal amount of an unfractionated extract of ^{13}C-labeled lipids was spiked into

analyzed samples thus serving as a comprehensive internal standard. Relative changes in the concentration of lipid species were calculated from the ratio of intensities of their ions and ions of internal standards.
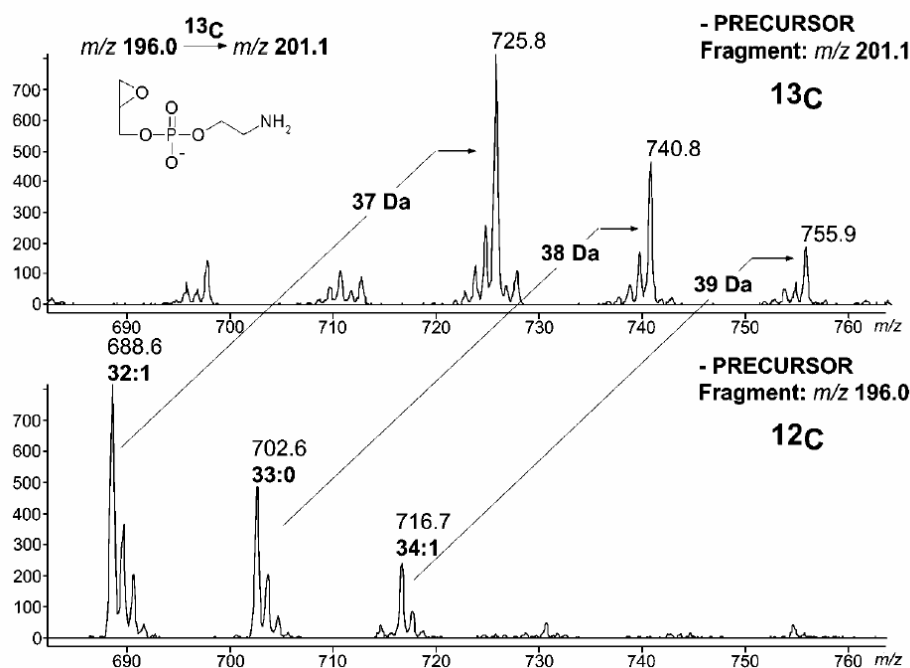
Figure 37. Profile of metabolically labeled PEs from *E. coli* with ^{13}C isotope. Simultaneous detection of labeled and unlabeled forms of PEs by multiple precursor ion scanning. Upon labeling, peaks at *m/z* 688.6 (PE 32:2), 702.6 (PE 33:0), and 716.7 (PE 34:1) (lower panel) were shifted according to the total number of carbon atoms (upper panel). *M/z* of the characteristic fragment of the headgroups (upper panel, inset) increased from *m/z* 196.0 to 201.1 and allowed parallel and independent detection of labeled and unlabeled forms from their mixture.

However, several major classes of phospholipids that are present in mammalian cells are missing in *E.coli*. Methylotrophic yeast *P.pastoris* (Pringle, Broach et al. 1992) offers a broader spectrum of lipids and may utilize methanol as a single source of carbon. By growing *P.pastoris* cells in medium that contained ^{13}C-methanol we generated a mixture of ^{13}C-labeled lipids. Labeling of *P. pastoris* showed similar ^{13}C incorporation as in *E.coli*. As illustrated in Figure 38, growing the methylothropic yeast in ^{13}C-methanol for a subsequent time, approximately 4 weeks, results in close to complete exchange of ^{12}C to ^{13}C isotopes of PC. Therefore, these promising results we decided that from this point on use labeled *P. pastoris* lipids as a comprehensive internal standard in all subsequent experiments with mammalian cells.
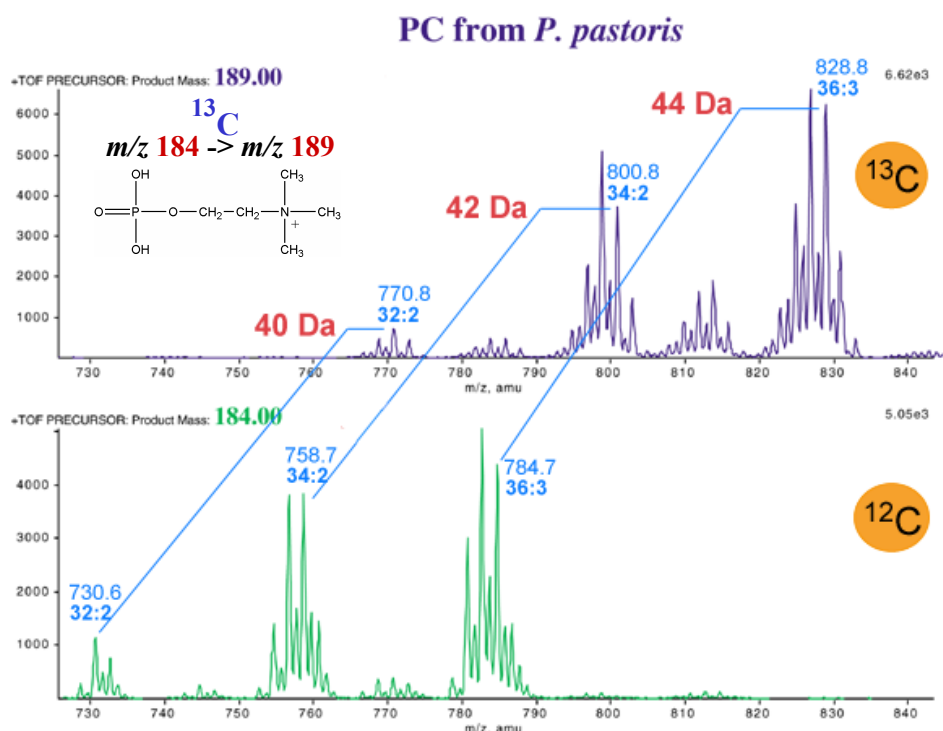
Figure 38. Profile of metabolically labeled PCs from *P. pastoris* with ^{13}C isotope. Simultaneous detection of labeled and unlabeled PC forms by multiple precursor ion scanning. Upon labeling, peaks at *m/z* 730.6 (PC 32:2), 758.7 (PC 34:2), and 784.7 (PC 36:3) (lower panel) were shifted according to the total number of carbon atoms (upper panel). *M/z* of the characteristic fragment of the headgroups (upper panel, inset) increased from *m/z* 184.1 to 189.1 and allowed parallel and independent detection of labeled and unlabeled forms from their mixture.

Quantification demands linearity of the instrument response. To check this in multiple precursor ion scanning (MPIS) mode, the total lipid extract from unlabeled *P.pastoris* cells was proportionally diluted and the aliquots were spiked with equal amounts of the internal standard.

Currently, no neutral loss scanning option, a conventional method of detecting PEs and PSs (Brugger, Erben et al. 1997), is available on QqTOF instruments. To replace it, samples were spiked with 1 mM LiCl and positively charged lithium adducts of the neutral fragments (Hsu and Turk 2000) were selected as characteristic fragment ions in precursor ion scanning (Table 6).

Table 6. Masses of characteristic head group fragment ions. [a] Fragment ions were selected within mass window of (0.1 Da centered at the m/z specified in the table. [b] Model organisms used for generating ^{13}C-labeled internal standards (*E. coli*, *P. pastoris*) lack SMs. Instead, peaks of ^{13}C-labeled PCs were used as internal standards for relative quantification of SMs. [c] Since this fragment ion may also be yielded from PIs and PSs, the identification should be confirmed by fatty acid scanning.

Lipid class	Mode	Cation	Selected Fragment Ions, m/z[a]	
			unlabeled	^{13}C-labeled
Phosphatidylcholines (PCs)	+	H$^+$	184.1	189.1
Sphingomyelins (SMs)	+	H$^+$	184.1	-[b]
Phosphatidylethanolamines (PEs)	+	Li$^+$	148.1	150.1
	-		196.1	201.1
Phosphatidylserines (PSs)	+	Li$^+$	192.1	195.1
Phosphatidylinositols (PIs)	-		241.1	247.1
Phosphatidylglycerols (PGs)	-		153.1[c]	156.1

The instrument response was linear in a 10x intensity range both in negative and positive ion modes. However, special precautions had to be taken to avoid saturation of the MCP detector. To this end the intensities of peaks were carefully monitored during the acquisition and adjusted, if necessary, by varying spraying voltage or the distance between the spraying capillary and the orifice of the mass spectrometer (Chernushevich, Loboda et al. 2001). Due to the high sensitivity of precursor ion scans for m/z 184.1 and 189.1 (detecting of unlabeled and labeled PCs), the trapping feature had to be turned off to avoid saturation, and therefore this scan was performed separately from other precursor ion scans in positive ion mode.

In summary, the combination of MPIS and metabolic isotopic labeling of lipids should allow monitoring of changes in any detectable lipid class with no recourse to synthetic standards.

2.4.3.2 Evaluation of the Advion NanoMate 100

At the moment, each liquid sample was manually infused into the mass spectrometer. Analysis of a larger pool of samples can therefore be very laborious. Nanoelectrospray (nanoES) has been shown to be difficult to automate. This has been attempted by using continuous flow nanoES constructed to enable analysis of multiple samples (Geromanos, Philip et al. 1998). With this technique all samples are sprayed

through the same capillary. This increases the risk for contamination leading to misinterpretation. An interesting automation attempt is the use of an automated, robotic, chip-based nanoelectrospray system, the NanoMate 100 and ESI Chip (Van Pelt, Zhang et al. 2003). Here, the samples are drawn robotically from a 96 well plate and infused into the MS instrument through the nozzle of the ESI Chip. With this approach there are no significant risks of carry-over between samples. Therefore, we decided to evaluate whether if the latter approach would enable automation of the lipid analyses.

A perspective on how the currently developed methodology could be fitted in a automated and fast comprehensive analysis of molecular GPL species of unseparated lipid extracts is demonstrated in Figure 39. We further explored this setup by combining the multiple precursor ion scanning (MPIS) technique in combination with an Advion NanoMate robot mounted on a QqTOF mass spectrometer. The analysis was combined with the Lipid Profiler software enabling automated identification and quantification for fast high-throughput profiling of molecular GPLs in lipid extracts of fatty acid oxidation disorders.
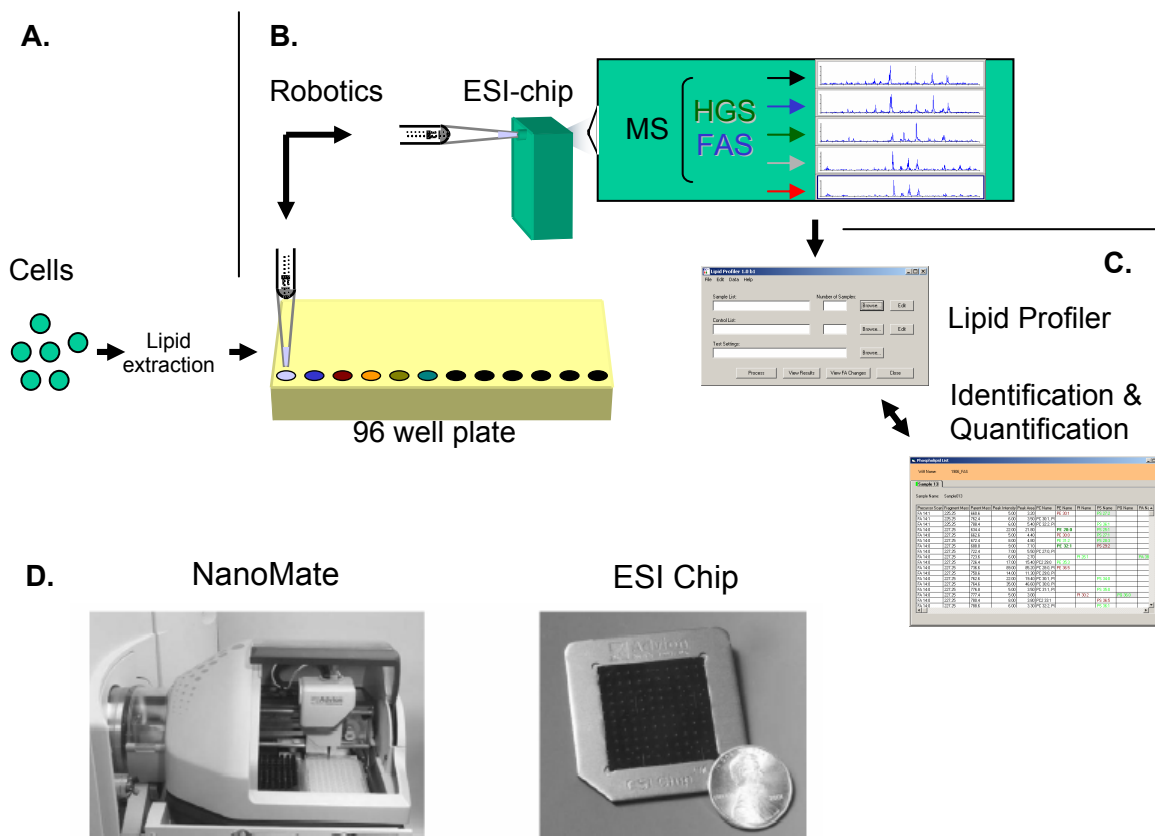
Figure 39. Automated GPL analysis overview. A. Cells of healthy individuals and patients with disorders are subject to total lipid extraction and further processed for MS analysis as described in Experimental Procedures. B. 5µl of analyte, placed in a 96 well microplate, is automatically drawn by the Advion NanoMate 100 robot using a conductive tip. The tip is precisely aligned to the ESI Chip nozzle. The analyte is ionized by the high tip voltage and subjected to HGS and FAS in positive and negative ion mode, respectively. C. Acquired precursor ion scanning spectra are automatically interpreted by the Lipid Profiler software generating tables of identified molecular GPL species. Lipid Profiler further allows user defined and automated quantification analysis of molecular species. D. Photograph of the NanoMate mounted on a mass spectrometer and photograph of the ESI Chip which consists of 100 nanoelectrospray nozzles. The ESI Chip is positioned in front of the mass spectrometer sampling orifice.

First the mounted Advion NanoMate 100 robot system on a QqTOF instrument was evaluated (Figure 39B). We tested the differences between silicone dioxide coated and polypropylene (PP) plastic 96 well plates, the best way of avoiding evaporation of organic solvents and the sensitivity of the approach. 20 µl of a chloroform/methanol mixture in a ratio 1:2 (v/v) were evaporated approximately after 60 min, without sealing, from both plate types. Instead, heat sealing using alu foil showed no significant losses of organic solvent after overnight incubation at ambient temperature from either plate type. On the

other hand, monitoring the signal response of total lipid extracts during different incubation times clearly showed differences between both plate types. Approximately after a 3-hour incubation the sample spraying from the PP plate became drastically unstable and stopped whereas no differences could be observed of the sample spraying from the silicone dioxide coated plate, even after longer incubation times. This is most likely due to the unspecific binding of lipids to the PP material and extraction of polymeric compounds from the plastic. Therefore from this point on we decided to use only 96 well plates made out of borosilicate glass. Neither the conductive sample tip nor the precise alignment of the ESI-Chip showed any decline in the signal response during the complete analysis time. Furthermore, the hydrophobic surface of the ESI-Chip was showed to be stable to organic solvents and no leakage between the nozzles was observed. As the NanoMate 100 showed only a slight decrease in sensitivity in comparison to a QqTOF MS with a mounted conventional nano-ESI ion source, we decided to fix each total lipid extract concentration to 2000 cells/µl.

2.4.3.3 Advion NanoMate 100 and the Lipid Profiler 1.0 automates analysis

We then tested this strategy by using total lipid extracts of skin fibroblasts from healthy patients and from patients suffering from various fatty acid oxidation disorders. We chose here the common trifunctional protein (TFP), respiratory chain complex 1 and 4 (R Chain), very long-chain acyl-CoA dehydrogenase (VLCAD) and long-chain 3-hydroyacyl-CoA dehydrogenase (HOAD) disorders (see reviews (Tyni and Pihko 1999; Solis and Singh 2002). Temporarily cell cultured fibroblasts, in growth medium supplemented with and without fetal calf serum (FCS), were subjected to total lipid extraction and prepared for MS analysis (Figure 39A). First, both control and disorder samples were analyzed in positive ion mode by selecting the fragment ion at *m/z* 184.1 (PIS *m/z* 184.1) for detection of PC and SM species. Each spectrum was submitted to the Lipid Profiler software for PC identification using a threshold of 20 counts per second (cps) or 5 area units corresponding to approximately 5% of the relative peak intensity (Figure 39C). By plotting the abundance of identified PC species of each sample, normalized to the total PC amount, showed no rearrangements in PCs of the FCS supplemented samples of disorders in comparison to the control (data not shown). On the other hand significant rearrangements could be observed in the same samples were grown without FCS (Figure 39, A-E). This is likely due to a down regulation in *de novo* biosynthesis of fatty acids supplemented with FCS, whereas

the lack of external supplement of fatty acids requires a more activated biosynthesis. All disorders showed a similar PC profile pattern but with less evenly distributed PCs in comparison to the control. Notably, different control cells analyzed showed similarities in their PC profiles, thus excluding profile differences due to analysis errors. In the R Chain, VLCAD and HOAD disorders the PCs 32:1, 34:1, 34:2 and 36:2 were the main PCs whereas in TFP these were less prominent, but still showed similar patterns in respect to the others.
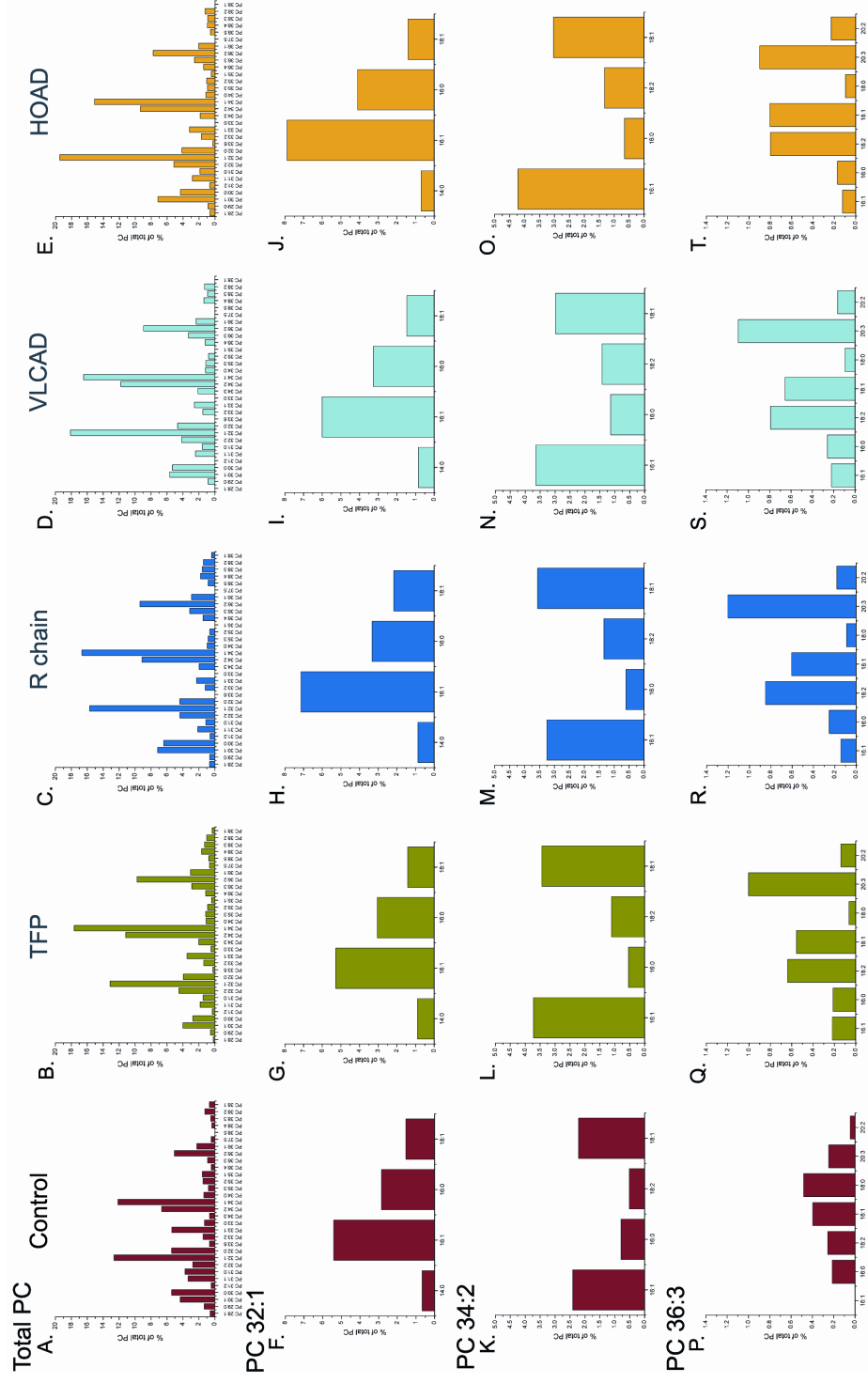
Figure 40. Changes in molecular PCs of fatty acid oxidation disorders. A-E. Abundance of brutto composed PCs detected by PIS *m/z* 184.1. F-J and K-O. Quantity changes in isobaric species of PC 32:1 and PC 34:2 respectively, monitored by FAS. P-T. Quantity changes and interchanged fatty acid distribution in isobaric species of PC 36:3, monitored by FAS. Abundance of PC species was related to the total detected PC monitored by PIS *m/z* 184.1 and FAS, respectively.

84

In contrary to PCs, differences in SM species could be observed in cells grown both with and without FCS, which was more pronounced in the latter (Figure 41). Cells grown in FCS free medium clearly showed larger total amounts of SM in comparison to PC. Interestingly, in FCS free samples, all major SM species and more drastically shorter fatty acid chained species were foremost down regulated in TFP. On the other hand, R chain and VLCAD showed mainly a significant up regulation in the shorter fatty acid chained species in comparison to the control. This was not as pronounced and clear if the cells were supplemented with FCS. In HOAD, SMs did not seem to be as affected as their PCs in either cell medium types.
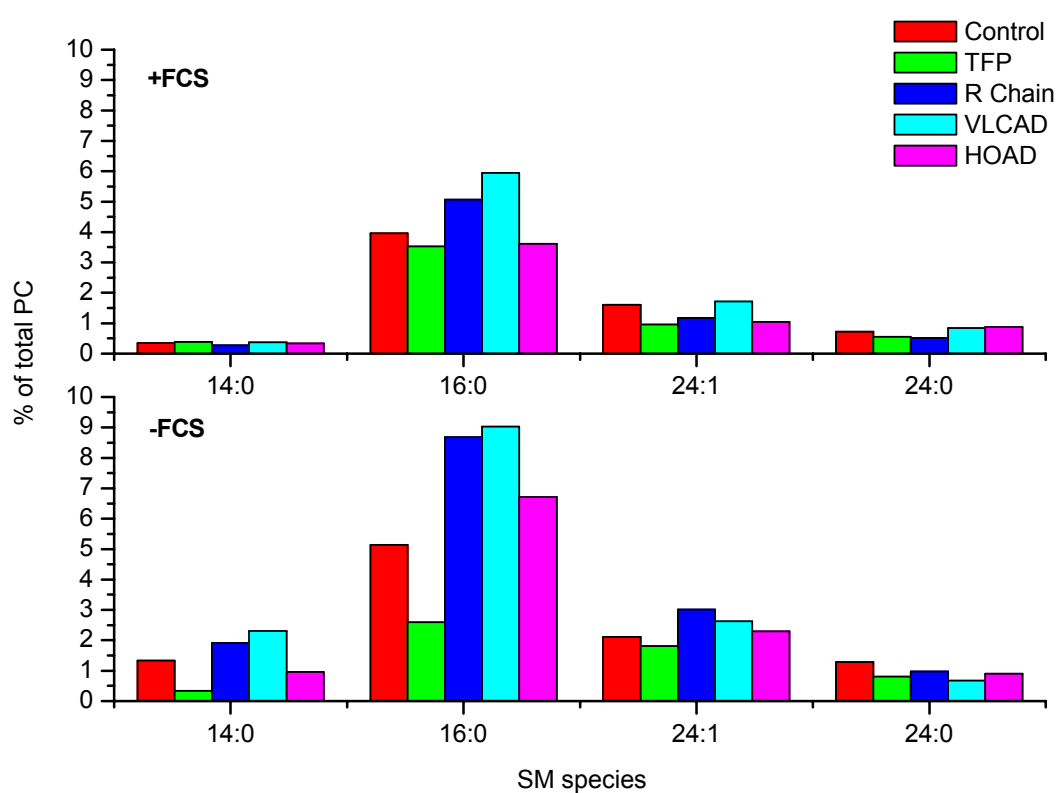
Figure 41. Abundance in SM species of FCS supplemented and non-supplemented cells. The quantity in the most predominant SM species related to the total amount of PC of control and disorder fibroblast cells supplemented with FCS (upper panel). Growing the cells without FCS, results in significantly higher levels of SM species (lower panel).

Next, FAS of the non FCS supplemented samples was performed in negative ion mode for monitoring the changes in the molecular PC species, shown in Figure 40 (A-F), rather than looking at the sum of isobaric molecular species analyzed by PIS *m/z* 184.1. The 30 most common acyl anions were recorded simultaneously and each spectrum was subjected to the Lipid

Profiler software in the same way as described above and the relative abundance in molecular species was normalized to the total amount of PC recorded by FAS. As for PC, PE and PG the dissociation of the *sn*-2 fatty acid is more efficient in comparison to the *sn*-1 fatty acid (Hsu and Turk 2000; Hsu and Turk 2001) and vice versa for PA and PS (Hsu and Turk 2000). Therefore, observed differences in their intensities enable fatty acid positioning at the glycerol backbone. Notably, it does only predict the predominant molecular species and the occurred rearrangements in the attached fatty acids rather than direct quantification of isomeric species, e.g. 14:0/18:1-PC and 18:1/14:0-PC. In this section the predominant molecular species are mentioned. In the case of PC 32:1, consisting of the isobaric species 14:0/18:1-PC and 16:0/16:1-PC, the 16:0/16:1-PC species was increased in R chain, VLACD and HOAD while the 14:0/18:1-PC species was not affected in respect to the control (Figure 40, F-J). Furthermore, the abundance of both species was directly comparable to the abundance of PC 32:1 monitored by PIS *m/z* 184.1. PC 34:2 showed more significant differences in their predominant molecular species (Figure 40, K-O). Similar molar ratios of 16:1/18:1-PC and 18:1/16:1-PC were observed in control as well as in disorders, only with major increase in abundance in the latter. Control cells contained similar levels of 18:2/16:0-PC and 16:0/18:2-PC, while in the disorders the predominant species was 16:0/18:2-PC with increasing abundance. As the degree of saturation increased, more significant changes in molecular species were observed. PC 36:3 in the control cells consisted of 18:2/18:1-PC and 16:0/20:3-PC whereas in the disorder samples this was drastically rearranged. In TFP the major species were 18:1/18:2-PC, 16:0/20:3-PC, 20:2/16:1-PC and 16:1/20:2-PC all increased in abundance in comparison to the control. R chain and VLCAD showed differences in the abundance between the molecular species but otherwise similarities to the TFP. In HOAD equal amounts of 18:1/18:2-PC and 18:2/18:1-PC was observed. 16:0/20:3-PC and 16:1/20:2-PC species were observed at higher and at lower abundance respectively. Interestingly, in all disorders 16:1/20:2-PC was detected, while this was missing in the control, making it a considerably interesting candidate as a disorder screening molecule.

2.4.3.4 New, abolished and rearrangements in molecular species is observed in disorders

FAS enables detection of molecular species of all major GPL classes simultaneously and thus allows monitoring of their relative abundance and prediction of the predominant species. The relative abundance of a section of the GPL molecular species is shown in Table 7. In this small section, many more molecular species of PE and PS were detected in the disorders in comparison to the control, whereas approximately an equal number of molecular species of other GLPs was

detected. Interestingly, both new and missing molecular species were observed in the disorders in respect to the control. Similar observations were also seen among the disorders. For instance, the 18:0/16:0-PE (34:0) was missing from R chain and control, but present in TFP, VLCAD and HOAD. On the other hand 18:0/16:0-PC was present in control, TFP and HOAD, but missing in R chain and VLCAD. 16:0/18:0-PG as well as 18:0/16:0-PA were only present in the control. Furthermore, molecular species belonging to the same lipid class were redistributed differently among each disorder and in comparison to the control. Different patterns of redistribution and types of molecular species were observed among the different lipid classes, both between disorders and in comparison to the control.

Table 7. Section of molecular GPL species of fatty acid oxidation disorders quantified by FAS. In disorders both new (bold text, bold background) and missing (no text, light background) molecular species are observed. Relative abundance monitored by an internal standard is presented.

Relative Abundance

Brutto composition	Fatty acid	diacyl glycerophosphatidylethanolamine					diacyl glycerophosphatidylcholine					diacyl glycerophosphatidylglycerol				
		Control	TFP	R chain	VLCAD	HOAD	Control	TFP	R chain	VLCAD	HOAD	Control	TFP	R chain	VLCAD	HOAD
34:0	FA 16:0		**0.14**		**0.05**	**0.07**	0.07	0.20			0.08	0.03				
	FA 18:0		**0.04**		**0.03**	**0.04**	0.51	0.23			0.26	0.02				
34:1	FA 16:1	0.24	0.54		0.28	0.43	0.04	0.13	0.05							
	FA 16:0	0.23	0.68	0.42	0.30	0.55	0.43	1.53	0.39	0.69	0.77		**0.21**	**0.04**	**0.04**	**0.10**
	FA 18:1	0.47	1.45	0.86	0.68	1.35	0.69	2.79	0.99	0.88	1.22		**0.35**	**0.08**	**0.10**	**0.15**
	FA 18:0	0.07	0.18		0.09	0.17	0.07	0.12	0.02			0.06				
34:2	FA 16:1		**1.30**	**0.54**	**0.68**	**1.19**	0.30	1.42	0.40	0.51	0.77					
	FA 16:0		**0.06**	**0.04**	**0.06**	**0.12**	0.10	0.20	0.07	0.16	0.12					
	FA 18:2		**0.18**	**0.11**	**0.10**	**0.20**	0.06	0.42	0.17	0.20	0.24	0.14				
	FA 18:1		**1.37**	**0.49**	**0.59**	**0.95**	0.27	1.31	0.44	0.41	0.55					
34:3	FA 14:0			**0.03**	**0.06**			**0.08**		**0.01**						
	FA 16:2			**0.02**	**0.04**					0.02	0.04					
	FA 16:1	0.01	0.12	0.05	0.06	0.10	0.04	0.19	0.05	0.08	0.10			0.02		0.06
	FA 18:2	0.02	0.13	0.06	0.07	0.12	0.03	0.16	0.07	0.05	0.09			0.03		0.10
	FA 18:1			**0.04**	**0.02**			**0.10**	**0.04**	**0.04**	**0.06**					
	FA 20:3			**0.02**	**0.02**					0.04						

Brutto composition	Fatty acid	diacyl glycerophosphatidylserine					diacyl glycerophosphatidylinositol					diacyl glycerophosphatic acid				
		Control	TFP	R chain	VLCAD	HOAD	Control	TFP	R chain	VLCAD	HOAD	Control	TFP	R chain	VLCAD	HOAD
34:0	FA 16:0		**0.18**	**0.06**	**0.03**	**0.20**	0.04					0.04				
	FA 18:0		**0.11**	**0.04**	**0.05**	**0.27**						0.02				
34:1	FA 16:1	0.09	0.31		0.15	0.20	0.04									
	FA 16:0	0.18	0.40	0.16	0.20	0.27				**0.02**			**0.04**			
	FA 18:1	0.22	0.62	0.20	0.21	0.30				**0.10**			**0.05**			
	FA 18:0	0.29	0.77		0.40	0.57	0.06									
34:2	FA 16:1		**0.12**	**0.02**	**0.04**	**0.07**	0.02									
	FA 16:0		**0.04**		**0.03**	**0.03**										
	FA 18:2		**0.07**		**0.02**	**0.03**										
	FA 18:1		**0.31**	**0.08**	**0.13**	**0.17**	0.02									

All disorders contained elevated amounts of total PE and PG, whereas the total PC, PS and PI amounts were decreased in comparison to the control cells (Figure 42A). No PA could be detected in R Chain, VLCAD and HOAD. Levels in lipid classes among the disorders were also elevated. TFP contained almost twice the amount of PG as VLCAD whereas the latter contained significant higher levels of PI and PC. On the other hand, HOAD and R chain showed similar levels in each lipid class except for PS. Thus, disorders clearly show differences in their total lipid class level in comparison to the control, but also differences among the disorders are clearly observed. This becomes further pronounced by grouping all molecular species in each lipid class by their degree of saturation (Figure 42B). All disorders contained significantly less amounts of saturated and monounsaturated species, whereas the polyunsaturated species were slightly increased in comparison to the control. Notably, this correlated to the results on PCs detected by PIS m/z 184.1 in Figure 40, showing the correspondence of both analysis modes. Conversely, the amount of saturated PE species was similar in the disorders and the control. The control contained, moreover, additional amounts of monounsaturated species and decreased levels of polyunsaturated species in comparison to disorders. Amounts of monounsaturated PS were highest among all samples except in R chain where polyunsaturated species were predominant. Furthermore, equal amounts of saturated PS species were observed in all samples except for HOAD. Polyunsaturated species were clearly predominant in the PG class with more abundance in the disorders in comparison to the control. Monounsaturated species stayed equal among all samples, whereas in the disorders no saturated species were observed. A similar pattern is detected for PIs except that lesser or equal amounts of both mono- and polyunsaturated species were observed with respect to the control.
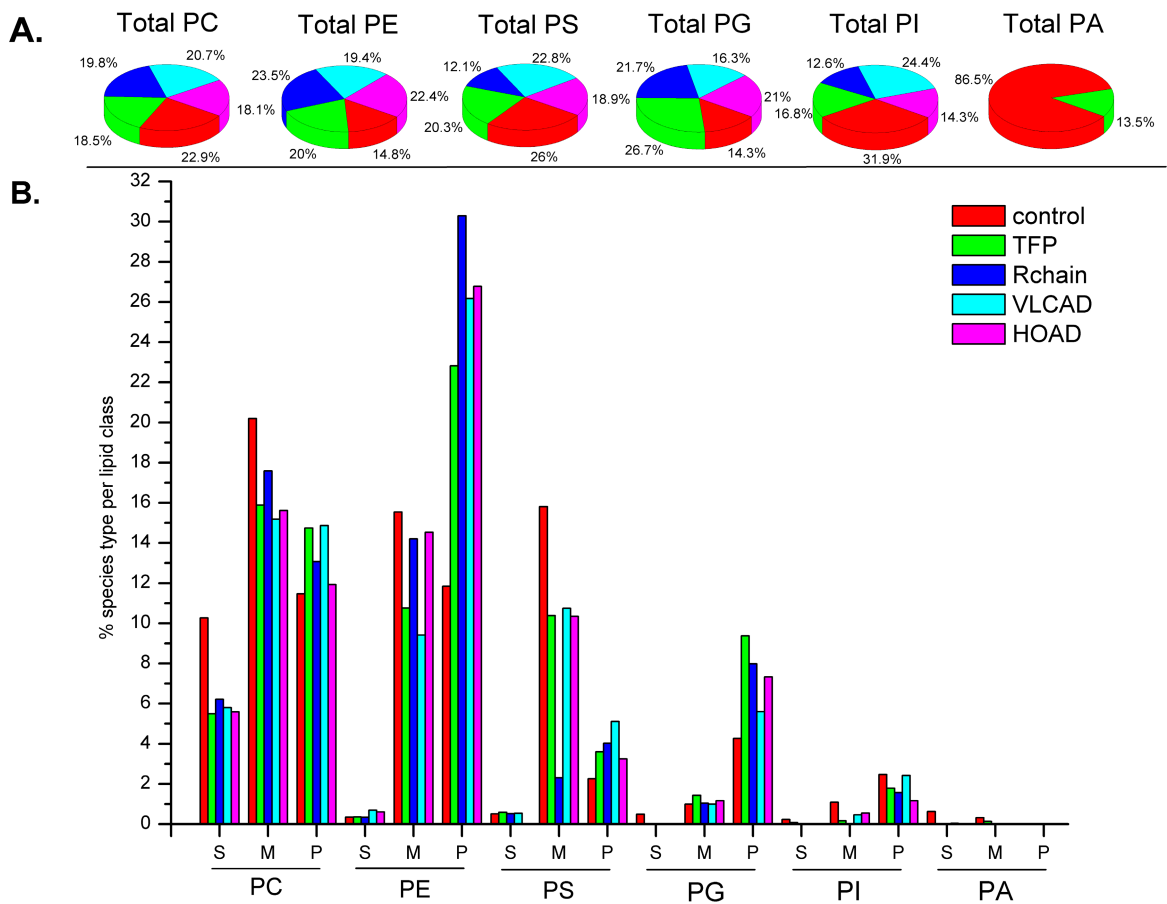
Figure 42. Distribution of GPL classes and types of fatty acid oxidation disorders. A. Abundance of detected GPL classes. Each lipid class was correlated to the total sum of the particular class from all samples. B. Distribution of saturated (S), monounsaturated (M) and polyunsaturated (P) species related to the total level of a particular class.

In conclusion, this strategy clearly demonstrates the feasibility of comprehensive high throughput profiling of molecular GPL species in fatty acid oxidation disorders as the TFP, VLCAD, R Chain and HOAD.

3   DISCUSSION

Multiple precursor ion scanning on a QqTOF instrument significantly improves the analysis of glycerophospholipids. HGS, a variation of MPIS, enables detection of particular lipid species. Since the characteristic head group fragment ions are selected for PIS analysis, it can only reveal the total carbon number and number of double bonds of analyzed GPLs. GPLs have mainly been analyzed in this way on triple quadrupole instruments (Brugger, Erben et al. 1997; Blom, Koivusalo et al. 2001; Pike, Han et al. 2002). Analysis of mixtures of isobaric species, *e.g.* comprising different fatty acid backbones, can not directly be resolved using HGS. This can, for instance, be accomplished by performing MS/MS on the parent ion and monitoring the generated acyl anions. This is not optimal since it requires a second analysis step, which has to be performed on all detected lipids if an unknown lipid mixture is to be analyzed. FAS, another variation of MPIS is advantageous here. By selecting the acyl anions for PIS analysis readily allows detection of molecular GPL species of PE, PS, PI, PG and PA. Predominant molecular species can be determined from the intensity differences of respective fatty acid signals. The position-dependent fatty acid dissociation renders different abundances in *sn*-1 and *sn*-2 acyl anions upon CID (Hsu and Turk 2000; Hsu and Turk 2000; Hsu and Turk 2000; Hsu and Turk 2000; Hsu and Turk 2001). From this intensity difference in acyl anions, positioning of respective fatty acid can be accomplished. Notably, from the acyl anion intensities the molar percentage of positional isomers could not be determined. This is likely due to the way they are generated in their fragmentation cascade. Therefore, the observed intensity differences in the fatty acid signals only reflect the predominant molecular species.

High sensitivity detection of PC is difficult in negative ion mode, in which FAS is performed, due to the quaternary amino group. This can be overcome by adding ammonium acetate or -chloride. This renders negatively charged PC adducts that, upon collision-induced dissociation, produce acyl anions (Han and Gross 1994; Kerwin, Tuininga et al. 1994), which then can be selected for FAS. Since ammonium acetate is normally added for analysis of GPLs, it is not required to separate sample preparations for analysis of molecular PC species from other molecular phospholipids species. Thus, molecular species of all major GPLs can be analyzed by FAS.

A major advantage of a QqTOF instrument is that in enables a virtually unlimited number of PIS to be performed simultaneously. It must be noted that in triple quadrupole

instruments only single PIS can be performed. MPIS enables comprehensive charting of molecular GPL species in single analyses, by combining HGS and FAS. Due to the high accuracy of the time-of-flight analyzer, HGS and FAS can readily be performed on total lipid extracts without any interference from chemical background. Complementary FAS and HGS analyses enable verification of the identity of ambiguous peak assignments. In this way the GPL pool of unknown samples can be profiled and assigned at the molecular level in a single run. There is no need for sample clean-up or purification prior to mass spectrometric analysis. Decreasing the number of sample preparation steps saves both time and minimizes biased losses of lipids. Therefore, this approach is superior to the more conventional lipid analysis methods. These latter methods would, for instance, involve several TLC separations, hydrolysis of lipids by phospholipase C, derivatization of diradylglycerols by benzoic anhydride followed by quantification of diradylglycerol-benzoates by reversed-phase HPLC before information in molecular species are retrieved (Blank, Robinson et al. 1984). Furthermore, the high selectivity of mass spectrometry enables charting of the molecular species of detergent-contaminated samples. By narrowing the *m/z* mass window of the selected fragment ion detection of any particular lipid is facilitated without any interference of overlapping detergent peaks. This clearly is an advantage for analysis of detergent-resistant membranes which contains significant amounts of detergents, *e.g.* Triton X-100. This would not be possible on a triple quadrupole instrument. Normally, in these instruments fragment ions are selected in *m/z* mass window of 3 Da in PIS, which is not accurate enough for selection of lipid fragment ions only. Mass window of the selected choline head group for detection of PC had to be narrowed to 0.1 Da before PC could be distinguished from "parasitic" Triton X-100 cluster ions (Figure 14).

PIS on QqTOF instruments have been limited by the low duty cycle, which can be as low as 5 % for low molecular weight species (Bateman 1998). By introducing ion trapping and bunching technology, it is possible to trap fragment ions of a given *m/z* temporarily in the collision cell which are then released as a short ion packet into the TOF analyzer, thus achieving 100 % duty cycle for any fragment ion (Chernushevich, Loboda et al. 2001). This technology significantly increases the detection sensitivity of GPLs by HGS and FAS. In both modes a 6 to 8-fold signal increase was observed, irrespective of which lipids were analyzed (Figure 8 and 9B). Importantly, the peak profiles in the mass spectrum did not change upon ion enhancement (ion trapping). This finding agrees with the results of Chernuschevic et al (Chernushevich, Loboda et al. 2001)**.** Using ion

enhancement the detection limitation of PCs in HGS was at a low 6 fmol/µL concentration (Figure 15). This is directly comparable to the sensitivity of triple quadrupole instruments. This also shows the advantage of PIS, enabling reliable detection of an isotopically resolved singly charged peak corresponding to the particular lipid. Usually, high mass resolution of a quadrupole time-of-flight instrument helps to distinguish multiply charged peptide ions from ions of chemical noise, which are mostly singly charged, by close inspection of the spectra. However, lipids are also detected as singly charged species and high resolution of the instrument alone does not guarantee confident assignment of peaks. Furthermore, intense singly charged ions of chemical background that dominated the TOF MS spectrum would have provided misleading information regarding the sample identity, if not verified by HGS.

The sensitivity of the various GPLs detected by HGS and FAS were comparable. Detection sensitivity of PC adducts by FAS is slightly decreased in comparison to HGS. This is not surprising since their detection in FAS requires formation of salt adducts (Figure 16). The detection sensitivity of PG, PE and PA standards was comparable in FAS, readily detected at a concentration of 3 µM. To achieve similar intensities of the detected PS and PC standards the concentration needed to be raised approximately 3-fold (Figure 17). Notably this was performed at constant collision energy and analysis of standards comprising the same fatty acid moieties, 18:0/18:1, to normalize ionization efficiency. It was important to measure the exact concentration of individual standard prior to FAS analysis to avoid misinterpretations due to incorrect amounts in individual standards. This result clearly indicates that the generation of acyl anions is collision energy-dependent and slightly variable among the different GPL classes. Collision energy required for analysis of GPLs by HGS is dependent on the nature of their head group (Figure 19) (Brugger, Erben et al. 1997). Therefore, using fixed collision energy will only enable maximal detection of a particular lipid class, whereas lipid classes with different collision energy dependency are only partly detected. By changing the collision energy, the maximal detection (sensitivity) of these lipids can be reached. Therefore, careful ramping of the collision energy optimization should produce similar intensities in the different molecular species of the various classes at the same concentrations shown in Figure 17. More care has to be taken if mixtures comprising different fatty acid backbones are to be analyzed, since the dissociation depends on the type of fatty acids attached (Koivusalo, Haimi et al. 2001). This becomes important for absolute quantification of molecular species, but it is not as

crucial for relative quantification where changes are measured. In summary, sensitive charting of molecular species of total lipid extracts can be performed simultaneously by HGS and FAS from a single sample preparation. The small detection sensitivity differences do not disturb profiling of individual molecular species of different classes. These differences should still be kept in mind during analyses, especially during absolute quantification approaches.

The observed detection sensitivity reflects total lipid extracts of approximately 200-300 cells/μL. Bruegger et al analyzed sample amounts of 1000 cells using a triple quadrupole instrument (Brugger, Erben et al. 1997), which is directly comparable to the current QqTOF setup. From this low number of cells, information on the major part of the existing molecular species can be obtained by FAS and HGS. For less abundant molecular species the number of cells has to be increased. It must be noted that this is dependent on the cell type analyzed, due to their different lipid compositions. Preliminary results show that the current detection sensitivity of phosphatidylinositol phosphate (PIP) and phosphatidyl-inositol bisphosphate (PIP_2) is approximately 20 μM and 40 μM, respectively, which is similar to the results of Wenk et al. (Wenk, Lucast et al. 2003). For their analysis of total lipid extracts the number of cells has theoretically to be raised 10-fold. This has still to be evaluated more thoroughly. Increasing the cell number 10-fold would also enable detection of ceramides and cerebrosides (Liebisch, Drobnik et al. 1999), which are currently detected in similar concentration ranges as the PIP and PIP_2, respectively. Analysis of sialic acid-containing glycolipids would also be possible to chart using MPIS technology, but there are no preliminary data on this. The current MPIS setup would allow theses lipids to be simultaneous recorded together with the molecular GPLs. Still, such analysis approach has to be taken with caution. Analysis of these lipids requires different instrumental settings in comparison to GPLs. A 10-fold increase in the signal intensity of GPLs presumably leads to saturation of the detector. Notably, it requires carefully evaluation of which extraction method enables best recovery of the lipids. For GPLs the Folch method enabled best recovery. Thus, it has still to be evaluated whether a single analysis is possible or whether one has to do two different analyses.

A linear response was observed for all analyzed GPLs in the normal working concentration range (0.5-16 μM) irrespective in which mode they were analyzed (Figure 18). No difference could be observed when standards were analyzed singly or spiked into a total lipid extract. The latter situation reflects a typical analysis condition. This clearly

indicates that molecular species can be quantitatively monitored. Generally, endogenous lipid species have been quantified by the use of synthetic standards (Brugger, Erben et al. 1997; Fridriksson, Shipkova et al. 1999; Blom, Koivusalo et al. 2001; Koivusalo, Haimi et al. 2001; Pike, Han et al. 2002). However, individual species within the same lipid class are detected with varying sensitivity (Koivusalo, Haimi et al. 2001). Also, conventional lipid extraction procedures, such as Bligh & Dyer or Folch, may result in preferential loss of some lipids or even entire lipid classes, depending on the properties of their fatty acid moieties. It is therefore important that internal standards should be almost identical to endogenous lipids of interest, although for many lipid classes such standards are not readily available. Furthermore, this requirement is impossible to meet in conventional mass spectrometric quantification, because multiple peaks of internal standards would be overlapping with peaks of interest in a complex analyte. This can be achieved by metabolic labeling of organisms, such as the methylothropic yeast *P. pastoris* that comprises of similar molecular GPL species as mammalian cells. Harvesting this strain in ^{13}C-methanol for approximately four weeks enables close to complete exchange of all ^{12}C carbons to ^{13}C (Figure 41). This procedure shifts the mass of each specific lipid species by their total number of carbons. At the same time, the selected fragment ions in HGS and FAS are mass shifted dependent on their carbon content and thus will not overlap with the endogenous lipids. Importantly, a comprehensive standard may be spiked into samples before fractionation or extraction and therefore the results would be much less affected by biased losses of the analyzed lipids. However, this method only allows monitoring of *relative changes* in the lipid profile, rather than determining the *absolute concentration* of individual lipids in the sample. If the latter is required it will be necessary to once quantify the standard mixture using an established protocol. Metabolic labeled standard mixtures generated in *P. pastoris* would perfectly suit monitoring of lipids in yeast. Upon metabolic labeling the carbons of sterols and sphingolipids will also be exchanged. This means that this lipid extract can be used to monitor the changes in all lipid types of yeasts. Preliminary results show that yeast sphingolipids can be monitored accurately by MPIS (Ejsing, Ekroos et al.). Sterols can be monitored by PIS as sulfated derivatizate (Sandhoff, Brugger et al. 1999). This would allow monitoring of all yeast lipids using the same analysis technique. MPIS have the potential to enable analysis of all these lipids in a single analysis. Such an analysis would enable one to rapidly and comprehensively monitor changes in a particular yeast lipid pool. In combination with yeast mutants it will be possible to gain insights in how particular lipids are affected upon specific mutations, and thus throw light into

biological roles of lipids and their metabolites. Unfortunately, the metabolic labeled yeast lipid extract will not enable monitoring of mammalian glycolipids. This could be approached by labeling mammalian cells in a similar way. This will be more difficult. To this point, preliminary experiments show insufficient exchange of used isotopes. Thus further analyzes will be required how to optimize the labeling.

The difference in fragment patterns of PC observed in QqTOF MS/MS and ion trap MS^2, MS^3 and MS^4, originate from mechanisms by which the collision energy is transmitted to selected precursor ions and affects the yield of unstable intermediates. It is, therefore, not surprising that the fragmentation of PC adducts in a QqTOF instrument at high collision energy predominantly yielded acyl anion fragments of fatty acids, whereas abundant peaks of de-methylated lysoPCs were observed in MS^3 ion trap spectra.

The inspection of fragmentation pathways by ion trap MS^3 revealed that they have different positional specificity (Figure 22). Neutral loss of fatty acid as ketene accounts for ~58 % of the total intensity of fragment ions and occurs almost exclusively *via* the cleavage of *sn*-2 fatty acid (~99% of ketene fragment ions), thus generating de-methylated 2-lysoPC. Its yield does not depend on the fatty acid moieties, as is evident from the accurate estimation of mol% of isomeric species comprising different combinations of fatty acids (Table 2 and Figure 23). Acyl anion fragments are abundant in MS^3 spectra (~39% of the total fragment ion intensity) and are mostly (although not exclusively!) produced from the *sn*-2 fatty acid (80% of intensity of acyl anion fragments). Neutral loss of free fatty acid appears to be a relatively minor process that accounts for about 2% of the total fragment ion intensity.

Relative (in mol%) quantification of isobaric and isomeric PC species by ion trap MS^3 fragmentation is direct and does not require internal standards. The determination is very specific because of the accurate selection of precursor masses at the MS^2 and MS^3 stages, and therefore is reliable even if applied to total lipid extracts. Furthermore, matching pairs of de-methylated 2-lysoPCs and acyl anion fragments of *sn*-2 fatty acid additionally verify the peak assignment. At the same time, MS^3 fragmentation is poorly suited for the detection of PC precursors in lipid mixtures, as well as for the quantification of PC species with different molecular mass. Since no efficient precursor ion scanning is possible on ion trap mass spectrometers, complementary analysis by QqTOF mass spectrometry and by ion trap mass spectrometry should be used in concert.

Applying FAS on a quadrupole time-of-flight mass spectrometer, and MS^3 fragmentation on the ion trap mass spectrometer, allowed characterization of the molecular composition of PCs. FAS complemented the previously established method of PIS *m/z* 184.1 and not only increased the specificity and the dynamic range of detection, but also allowed identification of the fatty acid moieties and their relative localization on the glycerol backbone of the individual PC molecules. MS^3 fragmentation of precursor ions detected by FAS independently enabled quantitative estimation of the relative amount of their positional isomers. A combination of both mass spectrometric methods is currently the most detailed and comprehensive approach for the characterization of individual molecular species of PCs

A combination of FAS and MS^3 was applied to profile PCs in a lipid extract from MDCK II cells. The conventional analysis by PIS *m/z* 184.1 detected 25 peaks of isobaric PCs (Table 3). Further analysis of the same sample by FAS revealed that they represent 46 species with unique fatty acid composition. MS^3 fragmentation of the most abundant peaks suggested that they are mixtures of positional isomers and therefore the total number of molecular species is close to one hundred. Notably, although no sizeable amount of ether PCs were detected, it could not be excluded that they might be present in the extract (Daniel, Huang et al. 1993), but were masked by more abundant species.

Although PCs of MDCK II cells and human red blood cells have been extensively characterized, no indication of the possible presence of positional isomers has been reported (Renooij, Van Golde et al. 1976). Biochemical studies have shown that fatty acid remodelling is a common phenomenon in eukaryotic organisms (Yamashita, Sugiura et al. 1997), which potentially accounts for the observed presence of isomeric lipid species. Biophysical studies have demonstrated that positional isomers display different types of phase behaviour and have differences in phase transition temperatures (Cunningham, Brown et al. 1998; Keller, Radhakrishnan et al. 2000). Importantly, positional isomers differ in their ability to interact with sterols thus affecting the dynamics of membrane microdomains. With the analytical tools now available the biological role of the observed complexity can be evaluated in molecular detail. Charting the molecular composition of PCs (and, conceivably, of other glycerophospolipids) by mass spectrometry has several advantages over conventional methods. A combination of head group scanning (PIS *m/z* 184.1), FAS and ion trap MS^3 fragmentation provided the most detailed and comprehensive characterization of the molecular composition, including the relative quantification, of individual molecular species. The sensitivity of detection was at the low

picomole – femtomole level. The sample preparation routine was vastly simplified and did not require preliminary separation of lipid classes and individual molecular species, enzymatic digestion or chemical derivatization. In FAS *m/z* of acyl anions can be selected with high accuracy thus increasing the dynamic range and the specificity of detection of corresponding lipid precursors. Therefore, glycerophospholipids comprising fatty acid moieties of possible medical diagnostic interest (such as very long chain fatty acids (Ramanadham, Hsu et al. 2000), fatty acids having odd number of carbon atoms (Sperl, Murr et al. 2000), *etc*.) can be reliably detected and quantified in total extracts in the presence of overwhelming amount of lipids with more prevalent fatty acids moieties. It is therefore conceivable that upon further development this technology will pave the way for high throughput "Shotgun Lipidomics" – the approach, in which molecular species of multiple lipid classes will be identified and quantified by computer processing of a very large number of simultaneously acquired precursor ion scans for *m/z* of characteristic fragments, including (but not limited to) the fragments of head groups and acyl anions of a variety of fatty acids.

FAS and HGS enable a rapid, accurate and comprehensive lipid analysis of total lipid extracts. In a single run a large pool of data can be retrieved. This requires more automated data interpretation. The calculus software enables to quickly, in a manual fashion, identify lipids by matching a determined *m/z* value to the calculated masses of lipids. Since this can be performed through a web-browser, it is easily accessed and is therefore suitable for simple identifications. Lipid Profiler 1.0 software is suitable for more complex data. Lipid Profiler 1.0 software enables, in a simple and fast fashion, automatic identification and quantification of molecular GPL species. Furthermore, this can be directly applied on a large set of data without any subsequent decrease in time spent for these processes. The integration of the software into the data acquiring Analyst QS software makes it enormously flexible in handling and viewing data and results. Enabling both TOF (for identification only) and MPIS data to be processed increases not only the flexibility but also the reliability in the final results. By combing FAS and HGS molecular GPL species can be distinguished and correctly verified. In this way any overlaps in misidentified species can be abolished and therefore increasing dramatically the reliability in quantification. Combining HGS and FAS data in the quantification processing enables detailed monitoring of changes in the individual fragments of GPLs. For instance it allows monitoring the amount and the changes in a particular molecular species to the total

amount of its class detected or to the total GPL amount in the sample, *e.g.* {16:0;16:1}-PC to the total PC amount or GPL amount. Furthermore, changes in intensities in the individual fatty acid signals shows quantitative information in the fatty acid remodelling, *e.g.* suggests the changes in the mol% of positional isomers. Detailed information of changes in individual fatty acids and head group is retrieved that further enables better understanding of lipid processes. Absolute quantification of molecular GPL species is planned to be integrated into the quantification section in the Analyst QS software, in which separate dilution curves, required for absolute quantification, are automatically handled by the software thus enabling a direct and automated quantification. Lipid Profiler software will clearly be a valuable tool in handling the massive amounts of data generated by HGS and FAS.

Detergent-resistant membranes is a most useful starting point for defining membrane subdomains, including cholesterol–sphingolipid rafts, and will remain valuable for the analysis of biological membranes. This approach was therefore chosen as preliminary application for evaluating the current mass spectrometric setup.

The current HGS and FAS setup using the Lipid Profiler software clearly enabled charting of the molecular phospholipid species of isolated DRMs prepared in Triton-X 100 from human red blood cells (RBC) and MDCK cells. The enrichment in the individual lipids in DRMs prepared using 1% Triton X-100 showed similarities in behaviour to MDCK cells, even though the molecular lipid composition of RBC is different from the MDCK cell line. First, MDCK cells contained far less SM species than RBC. Second, the main PCs in MDCK cells were of a monounsaturated nature whereas polyunsaturated species were dominating in RBC. This complicates the comparison of the GPL composition of DRMs between RBC and MDCK cells. It is previously shown that comparison of DRMs of different cell types requires extreme caution to avoid any misinterpretations (Schuck, Honsho et al. 2003). It was possible to find common trends between both preparations. Enriched SM species in DRMs of MDCK cells were also enriched in DRMs of RBC. Saturated SM species, dominated by SM 16:0, were more enriched in comparison to unsaturated SM species. Notable amounts of SM did not partition into DRMs (Figure 35C). A major part of the unsaturated species, and a smaller part of the saturated species, was still found in the soluble fraction. In DRMs of RBC, approximately 20% of the PC was saturated, 40% monounsaturated and 40% polyunsaturated. This correlated to the PC content of DRMs of MDCK cells, which

comprised 20 % more of the monounsaturated and 20% less of the polyunsaturated PCs. This slight difference is not surprising since both cell types comprise significantly different molecular species. Overall it shows that lipids with typical physiochemical nature favour partitioning into DRMs. Saturated GPLs, along with sphingolipids are known to preferentially partition into the liquid-ordered phase (Schroeder, London et al. 1994; Schroeder, Ahmed et al. 1998), whereas polyunsaturated GPL species favors the liquid disorder phase milieu (Antollini and Aveldano 2002). This corresponds to what is expected if raft microdomains were enriched in floated fractions of 1 % Triton X-100. 16:0/16:0-PC was enriched in both DRM preparations. Interestingly, similar observations have been done on DRMs prepared from KB cells (Pike, Han et al. 2002) and of unstimulated RBL-2H3 cells (Fridriksson, Shipkova et al. 1999). On the other hand, by isolating membrane fractions using the non-detergent method of Smart et al. (Smart, Ying et al. 1995) this enrichment was not observed. Furthermore, enrichment in arachidonic acid and plasmenylethanolamine was observed in the latter method, which could not be observed in DRMs of MDCK cells. Notably, this was not evaluated in RBC which comprise significant amounts of ether lipids. This indicates that the non-detergent method of Smart *et* al. isolates different kinds of membranes and/or membrane domains. Future analysis is required for dissecting these differences in more detail. Using FAS allowed charting molecular species of DRMs of MDCK cells. Enrichment was observed in the PEs {16:0;18:1} and {18:0;18:1}. This was also observed in the DRMs of KB cells, but notably not in the non-detergent isolations of the same cells (Pike, Han et al. 2002). Again, this indicates differences between both preparation methods. Notably, a major increase in the PGs {13:0;18:0} and {13:0;18:1} was observed. Saturated and monounsaturated PG species have been shown to be enriched in DRMs of RBL-2H3 cells (Fridriksson, Shipkova et al. 1999). It requires more investigations to understand the reasons for these increases. Taken together, these analyses indicate that RBC comprises raft microdomains. Importantly, DRM of RBC contains only plasma membrane GPLs whereas MDCK cells contain GPLs of various cellular membranes. By preparing DRMs of MDCK plasma membranes might show even more similarities to the DRMs of RBC. Still this should be done with extreme caution to avoid any misinterpretation. A more comprehensive GPL study might reveal more specific changes in molecular GPLs in DRM. For instance, there might be a redistribution in positional isomers in both these states that drastically changes the physiochemical properties of the membranes. Therefore, together with preparations of MDCK cells, HGS and FAS should be combined with ion trap MS^3 analysis of RBC

preparations to completely characterize and quantify the molecular GPLs. The individual profiles should further be carefully compared and applied for pattern recognition.

With the developed MPIS technology on a QqTOF instrument it has become possible to chart PC and SM species of floated fractions contaminated with detergents. Notably, with other available techniques today this is not feasible to the same extent. The high sensitivity of the method allows detailed tracing of individual lipids through out the gradient. This explicitly will give insights into the understanding of the behavior of cellular membranes and of particular interest raft microdomains. Furthermore, this can all be approached in a quantitative fashion thus making the method most valuable. The Lipid Profiler software significantly accelerates the lipid identification and quantification. The possibility to manipulate in a flexible way quantified lipids by the software increases the possibility of tracking changes in particular lipids. However, caution should be taken when drawing conclusions from DRM experiments when comparing results obtained in different ways. Finally, to diminish and avoid any pitfalls, analyses should be done as comprehensively and with as many experimental tools as possible. Here, combination of ion trap MS^3 analysis and QqTOF MS HGS and FAS analysis allows at present the most detailed and comprehensive way of monitoring molecular GPLs quantitatively.

High sensitivity of MPIS would further enable to quantitatively examine the content of cholesterol and glycolipid species. Ongoing experiments show that it is feasible to implement these analyzes in the current setup, and thus enabling the most comprehensive lipid analysis of a membrane preparation in single method. For instance, this will enable analyzing the membrane organization and lipid content of cellular transport vesicles, such as was done for COP I-coated vesicles (Brugger, Sandhoff et al. 2000). In combination with metabolic labeled standards of *P. Pastoris,* lipid and membrane morphogenesis in yeast can be more extensively exploited (Schneiter, Brugger et al. 1999). Thus, it now becomes possible to study how lipids contribute to cellular processes in more detail. The complexity of lipid constituents of membranes is just beginning to be recognized and remain a real challenge for future studies.

Knowledge of how the molecular composition of GPLs changes in fatty acid oxidation disorders as the TFP, VLCAD, R Chain and HOAD disorders, is up to now poorly understood and requires future studies. Our automation strategy clearly demonstrates the feasibility of comprehensive high throughput profiling of their molecular GPL species and thus opening a new way of studying them. Not only is the setup simple, robust, sensitive

and quantitative but it also offers distinct advantages in its speed and automation. The complexity of the molecular GPL species can be monitored in detail, both by identification of the molecular species and by their quantification. Close to complete GPL profiles of fibroblasts from patients are efficiently and easily compared to each other and to GPL profiles of control patients. In this way differences in molecular GPLs between the different disorders and the control can be identified and evaluated. The aim would be to identify marker lipids for prognostic and diagnostic tests. On the other hand, such detailed molecular GPL species information will enormously increase the knowledge of a particular disorder or relationship between disorders, and thus assist in drug development.

These results clearly indicate the possibility to perform automated lipid analysis - Shotgun Lipidomics, with wide variety of applications. Of particular interest will be the investigations of other diseases and disorders to explore the value of detailed lipid analyzes. Finally, integration of this strategy in the fields of biochemistry and cell biology will considerably enhance the input into system biology approaches.

In summary, MPIS technology has clearly brought a new analytical dimension to the field of lipid analysis. Detailed information on the fatty acid composition of individual lipid molecules can now be obtained in parallel with conventional profiling of lipid classes. Thus, it has become possible to identify individual lipid species including their positional isomers, by ion trap MS analysis, rather than charting an intrinsically heterogeneous isobaric subpopulation of molecules, sharing the same number of carbon atoms and double bonds. It must be envisioned that FAS in combination with ion tarp MS^n analysis could become a powerful method for discovering novel lipid classes since detection of lipid species does not rely on preliminary knowledge of their head groups or other radicals. Currently, multiple scanning has been set up only in precursor ion scanning mode. Future technical development will include the implementation of multiple neutral loss scanning that will increase the specificity and sensitivity of detection of various lipid classes. A combination of various methods of scanning, including ion trap MS^n analysis, may help to profile in detail glycolipids and signaling lipids, which do not yield a single distinct fragment ion and therefore are not reliably detectable by any specific scan. Powered by further development of the Lipid Profiler software, comprehensive lipid profiling may eventually match the sensitivity and throughput of the characterization of proteomes and thus provide a more comprehensive view of molecular machines embedded into cellular membranes.

4 MATERIALS AND METHODS

4.1 MATERIALS

4.1.1 Materials

Synthetic GPL and glycosphingolipid standards and corex glass vials with teflon screw caps were purchased from Avanti Polar Lipids, Inc. (Alabaster AL). ^{13}C-glucose was purchased from Martek Biosciences Corp. (Columbia MD), ^{13}C-methanol (99% atom % ^{13}C) from Cambridge Isotope Laboratories (Andover MA). *E.coli* strain BL-21 was kindly provided by G. Stier (EMBL, Heidelberg). *Pichia pastoris* strain SmdII 684 was obtained from Stephen Weeks (EMBL, Heidelberg). YNB medium was purchased from Difco Laboratories, Inc. (Detroit MI). Other components of cell media were obtained from Gibco BRL (Rockville MD). FCS (fetal calf serum) was obtained from PAA Laboratories GmbH (Cölbe). De-lipidated FCS was obtained from Dr. C. Thiele (MPI CBG, Dresden). Chloroform and methanol were LC grade from Merck (Darmstadt, Germany). Perchloric acid was purchased from Sigma Chemical Company (St. Louis MO). Ammonium acetate, ammonium chloride, ammonium molybdate and L-ascorbic acid were purchased from Sigma Chemical Company (St. Louis MO). Phospholipase A_2 (PLA$_2$) from *Crotalus atrox* venom and phospholipase D (PLD) from *Streptomyces chromofuscus* was obtained from Sigma Chemical Company, (St. Louis MO). Triton X-100 was purchased from Perbio. Skin fibroblast cells of patients with fatty acid oxidation disorders were obtained from Sandra Jackson (TU, Dresden). Nanoelectrospray capillaries (brand "short") were purchased from Proxeon Biosystems A/S (Odense, Denmark).

4.1.2 Mass Spectrometers

Modified QSTAR Pulsar *i* quadrupole time-of-flight mass spectrometer (QqTOF) was from MDS Sciex, Concord, Canada, and equipped with a nanoelectrospray ion source from Proxeon Biosystems A/S, Odense, Denmark. A QqTOF was also equipped with a NanoMate 100 from Advion BioSciences, Ithaca NY, USA.

LCQ quadrupole ion trap mass spectrometer was from Finnigan ThermoQuest, San Jose, CA, USA, and equipped with a nanoelectrospray ion source from Proxeon Biosystems A/S, Odense, Denmark.

4.1.3 Calculus and Lipid Profiler 1.0 software

Calculus software was initiated in spring 1999 and programmed by Gustaf Selen at the Åbo Akademi University in Turku, Finland. This software facilitates data processing in support of simple web-based phospholipid identification. The Phyton programming language was used for the Linux operative system. The software was installed and maintained on a Linux server by the computer department at the institute. Calculus can be reached under the intranet address: http://calculus.

Lipid Profiler software was initiated together with MDS Sciex, Concord, Canada, in summer 2002 and programmed by Eva Duchoslav. This software facilitates data processing in support of qualitative and quantitative profiling of lipids by TOF MS and MPIS (HGS and FAS) on QqTOF instruments. Lipid Profiler version 1.0 is compatible with the MS acquiring software Analyst QS 1.0 SP6 and later versions. Microsoft Office (Microsoft Access), version XP is recommended. While Microsoft Access is not needed for data processing, it is required for any customizing the supporting lipid database.

4.2 METHODS

4.2.1 Cell culture

MDCK cell strain II (Louvard 1980) was maintained in supplemented MEM (including 5% FCS, 2 mM glutamine, 100 units/mL penicillin and 100 µg/mL streptomycin) in 5% CO_2 at 37 °C in a humidified incubator. Cells were grown in tissue culture flasks for 3-4 days.

4.2.2 Metabolic labeling of lipids with stable isotopes

E.coli strain BL-21 was grown for 24 hours at 37 °C in 50 ml M9 medium supplemented with 1% Trace elements, 1 mM $MgSO_4$, 0.3 mM $CaCl_2$, 50 µg each of biotin and thiamin

(G.Stier, EMBL, Heidelberg) and 0.4 % ^{13}C-glucose. Cells were spun down, the supernatant was discarded and the pellet was frozen in liquid nitrogen.

P.pastoris cells were continuously grown at 30 °C in YNB medium, without amino acids and ammonium sulfate and were supplemented by 0.4 mg/L biotin and 1% ^{13}C-methanol. At OD 600 = 1.0, a new culture was made by diluting an aliquot by the fresh media 1:100 (v/v) and the procedure was repeated four times. The final culture (P4) was centrifuged for 5 min at 2,000 rpm and 4 °C. The supernatant was discarded and the pellet was frozen in liquid nitrogen.

4.2.3   Preparation of cells

Confluent MDCK II cell monolayers grown on plastic support were washed three times with PBS buffer before being scraped and pelleted in 2 mL Eppendorf tubes for 5 min at 14,000 rcf at room temperature. Cell pellets were snap frozen in liquid nitrogen and stored at -20°C.

Human red blood cells were pooled by centrifugation for 10 min at 200 rcf at 4°C and washed 5 times with cold 150 mM NaCl and 10 mM Tris-Cl, pH 7.5 (TBS). Cells were aliquoted into 2 ml Eppendorf tubes, snap frozen and stored at -80°C.

4.2.4   Detergent extraction and flotation

For flotation on sucrose step gradients, confluent MDCK cells from a 10 cm tissue culture plate (10^7 cells) were washed with homogenization buffer (HB, 250 mM sucrose, 10 mM HEPES, pH 7.4) and collected by scraping and centrifugation at 2000 rpm for 5 min. Cells were resuspended in 500 μL HB containing CLAP (chymostatin, leupeptin, antipain and pepstatin, 25 μg/mL each) and homogenized by passing through a 25 G needle 20 times. This procedure disrupted over 90% of the cells, while the nuclei remained intact. 500 μL HB/CLAP were added containing no detergent or 2% Triton (all % w/v). Extraction was done on ice for 30 min. Samples were adjusted to 42% (w/w) sucrose with 2 ml 56% sucrose in 10 mM HEPES, transferred into SW40 centrifuge tubes (Beckman), overlaid with 8.5 mL 38% and 0.5 mL 5% sucrose/HEPES, and centrifuged at 39,000 rpm (271,000 g) for 18 h. 2.5 mL were collected from the top as the floating fraction.

150 μL RBC pellet was placed in a 2 mL tube and 9 vol (1350 μL) of ice-cold TBS containing 0.5 % Triton X-100 was added. The mixture was incubated on ice for 20 min and further centrifuged for 10 min at 15,000 g and 4 °C. The pellet was resuspended in 400 μL 60 % sucrose prepared in TBS and the % of the sucrose concentration was adjusted to a final of 40 % by adding 200 μL TBS containing 0.5% Triton X-100, and thoroughly mixed. The mixture was transferred into a SW60Ti centrifuge tube (Beckman), overlaid with 2.2 mL 30 % and 1.2 mL 10% sucrose/TBS, and centrifuged at 230,000 g for 17 h and 4 °C. 10 400 μL fractions were collected from the top.

4.2.5 Hydrolysis by Phospholipase A$_2$

Synthetic PC standards and their mixtures were hydrolysed by PLA$_2$ as described by Kates ((Kates 1986)). Briefly, 500 nmol of dried PC standard was dissolved in 800 μL diethyl ether/MeOH 99:1 (v/v) and mixed with 450 μL of aqueous solution containing 40 mM calcium chloride, 20 mM Tris-HCl pH 8.0 and 7 μg PLA$_2$. Mixtures were vigorously vortexed for 5 hours and then dried in a vacuum concentrator. Dried samples were extracted and prepared for mass spectrometric analysis as described below.

4.2.6 Hydrolysis by Phospholipase D for preparation of PA standard

600 nmol of dried PC standard was dissolved in 500 μL diethyl ether and mixed for 5 min. 415 μL of 0.1 M Tris and 0.3 M CaCl$_2$ pH 8.0 and 85 μL of PLD (584 U) was added followed by 30 min mixing at 30 °C. 500 μL diethyl ether was added and followed by short mixing and centrifugation at 500 rpm for 5 min at 20 °C. The ether phase was transferred to a new tube. The former solution was remixed with 750 μL of fresh diethyl ether followed by centrifugation at 500 rpm for 5 min at 20 °C. Diethyl ether phases were pooled and dried down in a vacuum concentrator. The final PA standard was re-dissolved in 1.5 mL CHCl$_3$/MeOH 1:2 (v/v) and stored at –20 °C.

4.2.7 Phosphorous determination

Phosphorous assay was performed as described by Rouser (Rouser, Fkeischer et al. 1970). Briefly, dried lipids were dissolved in 300 μL perchloric acid and shortly mixed. The lipids

were destructed at 180 °C for 60 min followed by a cooling down period at room temperature. Cooled lipid solution was placed at 50 °C and 1 mL water was added followed by 5 min incubation. 800 µL of a mixture containing 1.25% ammonium molybdate and 5% L-ascorbic acid was added and mixed followed by 10 min incubation at 105 °C. The sample was cooled down and the adsorption was spectrophotometrically read at 810 nm. The phosphate concentration was obtained by correlating the value to a calibration curve prepared from samples of known total phosphate concentration.

4.2.8   Extraction of lipids

Lipid extraction was performed according to Folch (Folch 1957). Briefly, 500 µL methanol was added to 75 µL of pelleted cells and vortexed for 10 min, followed by addition of 1 mL chloroform and vortexing for another 10 min. The sample was centrifuged for 5 min at 14,000 rpm at room temperature. The supernatant was transferred to a new tube and 300 µL H_2O was added followed by stirring the mixture for another 10 min. Samples were centrifuged at 500 rpm for 5 min at 20 °C. The lower phase (organic) was transferred to a new tube and washed with $CHCl_3$/MeOH/H_2O 3:48:47 (v/v/v). The phases were separated and the organic phase was transferred to a new tube. The sample was dried in a vacuum concentrator and stored at –20 °C.

Efficiency of the lipid extraction method according to Folch (Folch 1957) was compared to the method described by Bligh & Dyer (Bligh and Dyer 1959). Briefly, in the latter, 500 µl of aqueous sample was mixed briefly, followed by addition of 500 µl of chloroform, and mixed briefly. 500 µl of water was added followed by short mixing. The mixture was centrifuged 10 min at 500 g_{av} and room temperature. The lower organic phase was transferred to a new glass tube (B). 500 µl chloroform was added to the former tube followed by short mixing and centrifuged 10 min at 500 g_{av} and room temperature. The lower organic phase was pooled with the organic phase in glass tube B. 2000 µl water was added to tube B and mixed briefly and centrifuged as above. The lower organic phase was transferred to a new tube and dried in a vacuum concentrator and stored at –20 °C.

4.2.9 Sample preparation for mass spectrometric analysis

The concentration of synthetic GPL standards in stock solutions was determined by the phosphorous assay. Standards were prepared in different concentrations and molar ratios (only for PC) in $CHCl_3$/MeOH 1:2 (v/v) containing 5 mM ammonium acetate or ammonium chloride. Dried total lipid extracts were dissolved in 50-100 µL $CHCl_3$/MeOH 1:2 (v/v). Prior to mass spectrometric analysis, sample aliquots were diluted 5 to 10-fold in chloroform/methanol (1:2) containing an ammonium salt at a final concentration of 5 mM.

Cell-cultured skin fibroblasts from patients suffering from fatty acid oxidation disorders were obtained from Sandra Jackson (TU-Dresden). The cells were harvested in de-lipidated medium supplemented with or without FCS. Washed cell pellets were extracted and prepared for mass spectrometric analysis as described above. The final sample concentration was set to 2000 cells/µL.

4.2.10 Quadrupole time-of-flight mass spectrometry

Precursor ion scanning was performed on a modified QSTAR Pulsar *i* quadrupole time-of-flight mass spectrometer with a nanoelectrospray ion source. TOF analyzer was calibrated in MS/MS mode using 250 fmol/µL solution of 1,2-dilignoceroyl-*sn*-glycero-3-phosphocholine (DGPC) in methanol/chloroform 2:1 (v/v), containing 5 mM ammonium acetate at a set collision energy of 38 eV in positive ion mode. The fragment ion of the head group (brutto formula $C_5O_4H_{15}NP$, *m/z* calc 184.0733) and the intact molecular ion (brutto formula $C_{56}O_8H_{113}NP$, *m/z* calc 958.8198) were used as low and high *m/z* reference masses. Calibration in negative ion mode was performed in a similar way using a synthetic PE standard.

PIS experiments were performed in both positive and negative ion modes typically using a dwell time of 100 msec (5 scans x 20 ms) at a step size 0.2 or 0.1 Da at unit resolution of the Q1 quadrupole. Peak enhancement (trapping of fragment ions in the collision cell) was applied according to the instructions of the manufacturer and was controlled *via* either TOF Tune (on Macintosh) or Analyst QS (on PC) software. For multiple precursor ion scanning trapping conditions were determined experimentally to achieve best transmission of all monitored fragment ions (*e.g.*, in the *m/z*-range 153 to 283 in negative ion mode).

The list of masses of the characteristic head group fragments is provided in Table 6 (see reference Brugger, Erben et al. 1997 for their chemical structures and reference Cheng and Gross 2000 for the review of mechanisms of lipid fragmentation). For instance, the characteristic fragment ion of phosphorylcholine, m/z 184.1, was selected for detection of PCs and SMs in positive ion mode (PIS m/z 184.1). G_{M1} and G_{M3} gangliosides were monitored by selecting the characteristic fragment ion of sialic acid, m/z 290.1, in negative ion mode. Cerebrosides were monitored by selecting the characteristic fragment ion m/z 264.0 in positive ion mode. For FAS of GPL standards, precursor ion spectra of the two acyl anion fragments of the fatty acid moieties were acquired. For FAS analysis of lipid extracts, precursor ion spectra were simultaneously acquired for 30-50 acyl anion fragments of fatty acid moieties, containing 12 to 22 carbon atoms and 0 to 6 double bonds. Collision energy was set at 40 eV in positive and negative ion mode, unless specified otherwise. Fragment ions were selected within a m/z window of 0.15 Da. Peak intensities were maintained below 750 counts/per scan to avoid saturation of the detector. FAS spectra were interpreted using a beta-version of LipidProfiler 1.0 software, (MDX Sciex, Concord, Canada).

In negative ion mode multiple precursor ion scanning experiments with lipids from oleic acid labeled MDCK cells following m/z of acyl anions of the fatty acids were selected: 253.2 (16:1); 255.2 (16:0); 269.2 (^{13}C-labeled 16:1); 271.2 (^{13}C-labeled 16:0); 277.2 (18:3); 279.2 (18:2); 281.2 (18:1); 283.2 (18:0); 295.2 (^{13}C-labeled 18:3); 297.2 (^{13}C-labeled 18:2); 299.2 (^{13}C-labeled 18:1); 301.2 (^{13}C-labeled 18:0); 303.2 (20:4); 311.2 (20:0); 323.2 (^{13}C-labeled 20:4); 331.2 (^{13}C-labeled 20:0).

4.2.11 Advion NanoMate 100

A NanoMate 100 from Advion BioSciences was used as an automated nanoelectrospray ionization source for mass spectrometry. 25 μL sample was transferred to each well of a 96 well plate made out of polypropylene or coated with silicone dioxide (SUN-Sri, Wilmington NC, USA). Heat-seal from ABgene (Epsorn, UK) was used with Combi Termo-Sealer from ABgene (Epsorn, UK) to seal the 96-well sample plate. The heat was applied for approximately 3 seconds. 5 μL of sample was aspirated from a 96 well plate with a conductive pipette tip and infused through an ESI chip nozzle. The inlet pressure and the spray voltage were 0.1 psi and 1.0 KV for positive mode or 0.3 psi and 1.2KV for negative mode. Contact closure started 5 seconds after the sample flow. Samples were

infused one after another in automatic mode. FAS and HGS were performed on a QqTOF instrument as described above.

4.2.12 Ion trap mass spectrometry

Ion trap mass spectrometry was performed together with Ute Bahr at the Johann Wolfgang Goethe-University in Frankfurt, Germany. MS^n fragmentation on a quadrupole ion trap was performed on a quadrupole ion trap mass spectrometer LCQ equipped with a nanoelectrospray ion source. About 3 μL of the analyte were loaded into laboratory-made, gold-coated glass capillaries and sprayed at a voltage of 900-1000 V. The temperature of the heated transfer-capillary was 180°C, the capillary voltage was -15 V, and the tube lens was -15 V. Spectra were averaged over 10-50 scans, each scan consisting of 3 microscans. For MS^2 and MS^3 fragmentation, precursor ions were selected using an isolation width of 5 Da and 2 Da, respectively. The relative collision energy was set between 16-22%.

4.2.13 Quantitative monitoring of changes in lipid profile

Respective FAS and HGS data from different samples were acquired at similar total ion counts. Peak areas of detected molecular GPL species by FAS were exported from the Lipid Profiler software and manipulated in Microsoft Excel. For monitoring changes and relative abundance in lipid classes, the peak areas of molecular species of a particular class were summed and related to the total peak area of all detected molecular species. For monitoring changes and relative abundance in a molecular species, its peak area was related to the total peak area of the particular lipid class. PC and SM species were calculated together if not otherwise mentioned.

4.2.14 Quantitative monitoring of changes in lipid profile using standards

An equal amount of the total unseparated extract of ^{13}C-labeled lipids from *Pichia pastoris* was spiked into samples and served as the internal standard. The ^{13}C labeled lipid mixture was diluted so that intensities of labeled and unlabeled lipid peaks were similar. For quantification, intensities of peaks of interest were normalized to intensities of three

internal standards (^{13}C labeled lipids of the same class) having similar *m/z* as the quantified peak. Relative changes in the concentration of lipid species were calculated as:

$$\frac{\left[\dfrac{(EI_p/EI_{st1})}{(CI_p/CI_{st1})} + \dfrac{(EI_p/EI_{st2})}{(CI_p/CI_{st2})} + \dfrac{(EI_p/EI_{st3})}{(CI_p/CI_{st3})}\right]}{3} - 1 \quad \times 100\%$$

EI*p* and CI*p* stand for intensities of experimental and control peaks, respectively; EI*st1*-EI*st3* and CI*st1*- CI*st3* are intensities of peaks of ^{13}C-labeled internal standards in experimental and in control spectra, respectively. The result is presented in percentage along with the mean standard error.

5   REFERENCES

Akesson, B., J. Elovson, et al. (1970). "Initial incorporation into rat liver glycerolipids of intraportally injected (9,10-3H2)palmitic acid." Biochim Biophys Acta **218**(1): 44-56.

Anderson, R. G. (1998). "The caveolae membrane system." Annu Rev Biochem **67**: 199-225.

Antollini, S. S. and M. I. Aveldano (2002). "Thermal behavior of liposomes containing PCs with long and very long chain PUFAs isolated from retinal rod outer segment membranes." J Lipid Res **43**(9): 1440-9.

Arvidson, G. A. (1968). "Biosynthesis of phosphatidylcholines in rat liver." Eur J Biochem **5**(3): 415-21.

Baburina, I. and S. Jackowski (1998). "Apoptosis triggered by 1-O-octadecyl-2-O-methyl-rac-glycero-3- phosphocholine is prevented by increased expression of CTP:phosphocholine cytidylyltransferase." J Biol Chem **273**(4): 2169-73.

Balcarova-Stander, J., S. E. Pfeiffer, et al. (1984). "Development of cell surface polarity in the epithelial Madin-Darby canine kidney (MDCK) cell line." Embo J **3**(11): 2687-94.

Bateman, R. H. C., R.; Hoyes, J. B.; Gilbert, A. J.; Langridge, J. I.; Malone, K.; Bordoli, R. S. (1998). Orlando FL **42**.

Beckedorf, A. I., C. Schaffer, et al. (2002). "Mapping and sequencing of cardiolipins from Geobacillus stearothermophilus NRS 2004/3a by positive and negative ion nanoESI- QTOF-MS and MS/MS." J Mass Spectrom **37**(10): 1086-94.

Bevers, E. M., P. Comfurius, et al. (1983). "Changes in membrane phospholipid distribution during platelet activation." Biochim Biophys Acta **736**(1): 57-66.

Blank, M. L., M. Robinson, et al. (1984). "Novel quantitative method for determination of molecular species of phospholipids and diglycerides." J Chromatogr **298**(3): 473-82.

Bligh, E. G. and W. J. Dyer (1959). "A Rapid Method of Total Lipid Extraction and Purification." Canadian Journal of Biochemistry and Physiology **37**(8): 911-917.

Blom, T. S., M. Koivusalo, et al. (2001). "Mass spectrometric analysis reveals an increase in plasma membrane polyunsaturated phospholipid species upon cellular cholesterol loading." Biochemistry **40**(48): 14635-44.

Bohuslav, J., T. Cinek, et al. (1993). "Large, detergent-resistant complexes containing murine antigens Thy-1 and Ly-6 and protein tyrosine kinase p56lck." Eur J Immunol **23**(4): 825-31.

Boumann, H. A., M. J. Damen, et al. (2003). "The two biosynthetic routes leading to phosphatidylcholine in yeast produce different sets of molecular species. Evidence for lipid remodeling." Biochemistry **42**(10): 3054-9.

Brindley, D. N., A. Abousalham, et al. (1996). ""Cross talk" between the bioactive glycerolipids and sphingolipids in signal transduction." Biochem Cell Biol **74**(4): 469-76.

Brooks, S., G. T. Clark, et al. (2002). "Electrospray ionisation mass spectrometric analysis of lipid restructuring in the carp (Cyprinus carpio L.) during cold acclimation." J Exp Biol **205**(Pt 24): 3989-97.

Brown, D. A. and E. London (1998). "Structure and origin of ordered lipid domains in biological membranes." J Membr Biol **164**(2): 103-14.

Brown, D. A. and E. London (2000). "Structure and function of sphingolipid- and cholesterol-rich membrane rafts." J Biol Chem **275**(23): 17221-4.

Brown, D. A. and J. K. Rose (1992). "Sorting of GPI-anchored proteins to glycolipid-enriched membrane subdomains during transport to the apical cell surface." Cell **68**(3): 533-44.

Brugger, B., G. Erben, et al. (1997). "Quantitative analysis of biological membrane lipids at the low picomole level by nano-electrospray ionization tandem mass spectrometry." Proc Natl Acad Sci U S A **94**(6): 2339-44.

Brugger, B., R. Sandhoff, et al. (2000). "Evidence for segregation of sphingomyelin and cholesterol during formation of COPI-coated vesicles." J Cell Biol **151**(3): 507-18.

Callahan, M. K., P. M. Popernack, et al. (2003). "Phosphatidylserine on HIV envelope is a cofactor for infection of monocytic cells." J Immunol **170**(9): 4840-5.

Cheng, C. and M. L. Gross (2000). "Applications and mechanisms of charge-remote fragmentation." Mass Spectrom Rev **19**(6): 398-420.

Chernushevich, I. (2000). "Duty cycle improvement for a quadrupole time-of-flight mass spectrometer and its use for precursor ion scans." Eur J Mass Spectrom **6**(6): 471-479.

Chernushevich, I. V., A. V. Loboda, et al. (2001). "An introduction to quadrupole-time-of-flight mass spectrometry." Journal of Mass Spectrometry **36**(8): 849-865.

Cole, R. B. (2000). "Some tenets pertaining to electrospray ionization mass spectrometry." Journal of Mass Spectrometry **35**(7): 763-772.

Connor, W. E., D. S. Lin, et al. (1997). "Abnormal phospholipid molecular species of erythrocytes in sickle cell anemia." J Lipid Res **38**(12): 2516-28.

Cui, Z., M. Houweling, et al. (1996). "A genetic defect in phosphatidylcholine biosynthesis triggers apoptosis in Chinese hamster ovary cells." J Biol Chem **271**(25): 14668-71.

Cui, Z., J. E. Vance, et al. (1993). "Cloning and expression of a novel phosphatidylethanolamine N- methyltransferase. A specific biochemical and cytological marker for a unique membrane fraction in rat liver." J Biol Chem **268**(22): 16655-63.

Cunningham, B. A., A. D. Brown, et al. (1998). "Ripple phase formation in phosphatidylcholine: Effect of acyl chain relative length, position, and unsaturation." Physical Review E **58**(3): 3662-3672.

Daniel, L. W., C. Huang, et al. (1993). "Phospholipase D hydrolysis of choline phosphoglycerides is selective for the alkyl-linked subclass of Madin-Darby canine kidney cells." J Biol Chem **268**(29): 21519-26.

DeLong, C. J., P. R. Baker, et al. (2001). "Molecular species composition of rat liver phospholipids by ESI-MS/MS: the effect of chromatography." J Lipid Res **42**(12): 1959-68.

DeLong, C. J., Y. J. Shen, et al. (1999). "Molecular distinction of phosphatidylcholine synthesis between the CDP- choline pathway and phosphatidylethanolamine methylation pathway." J Biol Chem **274**(42): 29683-8.

Devaux, P. F. (1991). "Static and dynamic lipid asymmetry in cell membranes." Biochemistry **30**(5): 1163-73.

Drevot, P., C. Langlet, et al. (2002). "TCR signal initiation machinery is pre-assembled and activated in a subset of membrane rafts." Embo J **21**(8): 1899-908.

Ehehalt, R., P. Keller, et al. (2003). "Amyloidogenic processing of the Alzheimer beta-amyloid precursor protein depends on lipid rafts." J Cell Biol **160**(1): 113-23.

Ejsing, C. S., K. Ekroos, et al. unpublished.

Ekroos, K. and A. Shevchenko (2002). "Simple two-point calibration of hybrid quadrupole time-of-flight instruments using a synthetic lipid standard." Rapid Commun Mass Spectrom **16**(12): 1254-5.

Emmett, M. R. and R. M. Caprioli (1994). "Micro-Electrospray Mass-Spectrometry - Ultra-High-Sensitivity Analysis of Peptides and Proteins." Journal of the American Society for Mass Spectrometry **5**(7): 605-613.

Exton, J. H. (1994). "Phosphatidylcholine breakdown and signal transduction." Biochim Biophys Acta **1212**(1): 26-42.

Fadok, V. A., D. R. Voelker, et al. (1992). "Exposure of phosphatidylserine on the surface of apoptotic lymphocytes triggers specific recognition and removal by macrophages." J Immunol **148**(7): 2207-16.

Folch, J. M., Lees, M., Sloane-Stanley, G. H. (1957). "A simple method for the isolation and purification of total lipids from animal tissue." J. Biol. Chem. **226**: 497-509.

Fridriksson, E. K., P. A. Shipkova, et al. (1999). "Quantitative analysis of phospholipids in functionally important membrane domains from RBL-2H3 mast cells using tandem high-resolution mass spectrometry." Biochemistry **38**(25): 8056-63.

Fuller, S., C. H. von Bonsdorff, et al. (1984). "Vesicular stomatitis virus infects and matures only through the basolateral surface of the polarized epithelial cell line, MDCK." Cell **38**(1): 65-77.

Geromanos, S., J. Philip, et al. (1998). "InJection adaptable fine ionization source ('JaFIS') for continuous flow nano-electrospray." Rapid Commun Mass Spectrom **12**(9): 551-6.

Glish, G. L. and R. W. Vachet (2003). "The basics of mass spectrometry in the twenty-first century." Nature Reviews Drug Discovery **2**(2): 140-150.

Gygi, S. P., B. Rist, et al. (1999). "Quantitative analysis of complex protein mixtures using isotope-coded affinity tags." Nat Biotechnol **17**(10): 994-999.

Han, X. and R. W. Gross (1994). "Electrospray ionization mass spectroscopic analysis of human erythrocyte plasma membrane phospholipids." Proc Natl Acad Sci U S A **91**(22): 10635-9.

Han, X. L. and R. W. Gross (1995). "Structural Determination of Picomole Amounts of Phospholipids Via Electrospray Ionization Tandem Mass Spectrometry." Journal of the American Society for Mass Spectrometry **6**(12): 1202-1210.

Hansson, G. C., K. Simons, et al. (1986). "Two strains of the Madin-Darby canine kidney (MDCK) cell line have distinct glycosphingolipid compositions." Embo J **5**(3): 483-9.

Heikinheimo, L. and P. Somerharju (2002). "Translocation of phosphatidylthreonine and -serine to mitochondria diminishes exponentially with increasing molecular hydrophobicity." Traffic **3**(5): 367-77.

Hsu, F. F. and J. Turk (2000). "Characterization of phosphatidylethanolamine as a lithiated adduct by triple quadrupole tandem mass spectrometry with electrospray ionization." J Mass Spectrom **35**(5): 595-606.

Hsu, F. F. and J. Turk (2000). "Characterization of phosphatidylinositol, phosphatidylinositol-4- phosphate, and phosphatidylinositol-4,5-bisphosphate by electrospray ionization tandem mass spectrometry: a mechanistic study." J Am Soc Mass Spectrom **11**(11): 986-99.

Hsu, F. F. and J. Turk (2000). "Charge-driven fragmentation processes in diacyl glycerophosphatidic acids upon low-energy collisional activation. A mechanistic proposal." J Am Soc Mass Spectrom **11**(9): 797-803.

Hsu, F. F. and J. Turk (2000). "Charge-remote and charge-driven fragmentation processes in diacyl glycerophosphoethanolamine upon low-energy collisional activation: a mechanistic proposal." J Am Soc Mass Spectrom **11**(10): 892-9.

Hsu, F. F. and J. Turk (2001). "Studies on phosphatidylglycerol with triple quadrupole tandem mass spectrometry with electrospray ionization: Fragmentation processes

and structural characterization." Journal of the American Society for Mass Spectrometry **12**(9): 1036-1043.

Hunt, A. N., G. T. Clark, et al. (2002). "A comparison of the molecular specificities of whole cell and endonuclear phosphatidylcholine synthesis." FEBS Lett **530**(1-3): 89-93.

Huwiler, A., T. Kolter, et al. (2000). "Physiology and pathophysiology of sphingolipid metabolism and signaling." Biochim Biophys Acta **1485**(2-3): 63-99.

Igbavboa, U., J. Hamilton, et al. (2002). "A new role for apolipoprotein E: modulating transport of polyunsaturated phospholipid molecular species in synaptic plasma membranes." J Neurochem **80**(2): 255-61.

Ikonen, E. (2001). "Roles of lipid rafts in membrane transport." Curr Opin Cell Biol **13**(4): 470-7.

Ivanova, P. T., B. A. Cerda, et al. (2001). "Electrospray ionization mass spectrometry analysis of changes in phospholipids in RBL-2H3 mastocytoma cells during degranulation." Proc Natl Acad Sci U S A **98**(13): 7152-7.

Iverson, S. J., S. L. Lang, et al. (2001). "Comparison of the Bligh and Dyer and Folch methods for total lipid determination in a broad range of marine tissue." Lipids **36**(11): 1283-7.

Kates, M. (1986). Techniques of lipidology . In RH Burdon & PH van Knippenberg (eds), Laboratory Techniques in Biochemistry and Molecular Biology. A. E. S. B.V.

Kawai, K., M. Fujita, et al. (1974). "Lipid components of two different regions of an intestinal epithelial cell membrane of mouse." Biochim Biophys Acta **369**(2): 222-33.

Keller, S. L., A. Radhakrishnan, et al. (2000). "Saturated phospholipids with high melting temperatures form complexes with cholesterol in monolayers." Journal of Physical Chemistry B **104**(31): 7522-7527.

Kennedy, E. P. and S. B. Weiss (1956). "Function of Cytidine Coenzymes in the Biosynthesis of Phospholipides." Journal of Biological Chemistry **222**(1): 193-213.

Kent, C. (1995). "Eukaryotic phospholipid biosynthesis." Annu Rev Biochem **64**: 315-43.

Kerwin, J. L., A. R. Tuininga, et al. (1994). "Identification of molecular species of glycerophospholipids and sphingomyelin using electrospray mass spectrometry." J Lipid Res **35**(6): 1102-14.

Koivusalo, M., P. Haimi, et al. (2001). "Quantitative determination of phospholipid compositions by ESI-MS: effects of acyl chain length, unsaturation, and lipid concentration on instrument response." J Lipid Res **42**(4): 663-72.

Kovatchev, S. and H. Eibl (1978). "The preparation of phospholipids by phospholipase D." Adv Exp Med Biol **101**: 221-6.

Kurzchalia, T. V., P. Dupree, et al. (1992). "VIP21, a 21-kD membrane protein is an integral component of trans-Golgi-network-derived transport vesicles." J Cell Biol **118**(5): 1003-14.

Kuypers, F. A., P. Butikofer, et al. (1991). "Application of liquid chromatography-thermospray mass spectrometry in the analysis of glycerophospholipid molecular species." J Chromatogr **562**(1-2): 191-206.

Lands, W. E. M. and P. Hart (1965). "Metabolism of glycerolipids. 6. Specificities of acyl coenzyme A - phospholipid acyltransferases." J Biol Chem **240**(5): 1905-&.

Larsen, A., S. Uran, et al. (2001). "Collision-induced dissociation of glycero phospholipids using electrospray ion-trap mass spectrometry." Rapid Commun Mass Spectrom **15**(24): 2393-8.

Levery, S. B., M. S. Toledo, et al. (2001). "Comparative analysis of glycosylinositol phosphorylceramides from fungi by electrospray tandem mass spectrometry with

low-energy collision-induced dissociation of Li(+) adduct ions." <u>Rapid Commun Mass Spectrom</u> **15**(23): 2240-58.

Liebisch, G., W. Drobnik, et al. (1999). "Quantitative measurement of different ceramide species from crude cellular extracts by electrospray ionization tandem mass spectrometry (ESI-MS/MS)." <u>J Lipid Res</u> **40**(8): 1539-46.

London, E. and D. A. Brown (2000). "Insolubility of lipids in triton X-100: physical origin and relationship to sphingolipid/cholesterol membrane domains (rafts)." <u>Biochim Biophys Acta</u> **1508**(1-2): 182-95.

Louvard, D. (1980). "Apical membrane aminopeptidase appears at site of cell-cell contact in cultured kidney epithelial cells." <u>Proc Natl Acad Sci U S A</u> **77**(7): 4132-6.

Madore, N., K. L. Smith, et al. (1999). "Functionally different GPI proteins are organized in different domains on the neuronal surface." <u>Embo J</u> **18**(24): 6917-26.

Manes, S., G. del Real, et al. (2003). "Pathogens: raft hijackers." <u>Nat Rev Immunol</u> **3**(7): 557-68.

March, R. E. (1997). "An introduction to quadrupole ion trap mass spectrometry." <u>Journal of Mass Spectrometry</u> **32**(4): 351-369.

Matlin, K. S. and K. Simons (1984). "Sorting of an apical plasma membrane glycoprotein occurs before it reaches the cell surface in cultured epithelial cells." <u>J Cell Biol</u> **99**(6): 2131-9.

McEvoy, L., P. Williamson, et al. (1986). "Membrane phospholipid asymmetry as a determinant of erythrocyte recognition by macrophages." <u>Proc Natl Acad Sci U S A</u> **83**(10): 3311-5.

Morris, H. R., T. Paxton, et al. (1996). "High sensitivity collisionally-activated decomposition tandem mass spectrometry on a novel quadrupole / orthogonal-acceleration time-of-flight mass spectrometer." <u>Rapid Commun. Mass Spectrom.</u> **10**: 889-896.

Oda, Y., K. Huang, et al. (1999). "Accurate quantitation of protein expression and site-specific phosphorylation." <u>Proc Natl Acad Sci USA</u> **96**: 6591-6596.

Okuyama, H., K. Yamada, et al. (1975). "Accepton concentration effect in the selectivity of acyl coenzyme A: U aclglycerylphosphorylcholine acyltransferase system in rat liver." <u>J Biol Chem</u> **250**(5): 1710-3.

Pessin, J. E. and M. Glaser (1980). "Budding of Rous sarcoma virus and vesicular stomatitis virus from localized lipid regions in the plasma membrane of chicken embryo fibroblasts." <u>J Biol Chem</u> **255**(19): 9044-50.

Pike, L. J., X. Han, et al. (2002). "Lipid rafts are enriched in arachidonic acid and plasmenylethanolamine and their composition is independent of caveolin-1 expression: a quantitative electrospray ionization/mass spectrometric analysis." <u>Biochemistry</u> **41**(6): 2075-88.

Pringle, J., J. Broach, et al., Eds. (1992). <u>The molecular and cellular biology of the yeast Saccharomyces: gene expression</u>, Cold Spring Harbor Laboratory Press.

Ramanadham, S., F. Hsu, et al. (2000). "Electrospray ionization mass spectrometric analyses of phospholipids from INS-1 insulinoma cells: comparison to pancreatic islets and effects of fatty acid supplementation on phospholipid composition and insulin secretion." <u>Biochim Biophys Acta</u> **1484**(2-3): 251-66.

Rauvala, H. (1976). "Isolation and partial characterization of human kidney gangliosides." <u>Biochim Biophys Acta</u> **424**(2): 284-95.

Renooij, W., L. M. Van Golde, et al. (1976). "Topological asymmetry of phospholipid metabolism in rat erythrocyte membranes. Evidence for flip-flop of lecithin." <u>Eur J Biochem</u> **61**(1): 53-8.

Rodriguez-Boulan, E. and W. J. Nelson (1989). "Morphogenesis of the polarized epithelial cell phenotype." Science 245(4919): 718-25.

Roper, K., D. Corbeil, et al. (2000). "Retention of prominin in microvilli reveals distinct cholesterol-based lipid micro-domains in the apical plasma membrane." Nat Cell Biol 2(9): 582-92.

Rouser, G., S. Fkeischer, et al. (1970). "Two dimensional then layer chromatographic separation of polar lipids and determination of phospholipids by phosphorus analysis of spots." Lipids 5(5): 494-6.

Salzer, U. and R. Prohaska (2001). "Stomatin, flotillin-1, and flotillin-2 are major integral proteins of erythrocyte lipid rafts." Blood 97(4): 1141-3.

Sandhoff, R., B. Brugger, et al. (1999). "Determination of cholesterol at the low picomole level by nano-electrospray ionization tandem mass spectrometry." J Lipid Res 40(1): 126-32.

Scheiffele, P., A. Rietveld, et al. (1999). "Influenza viruses select ordered lipid domains during budding from the plasma membrane." J Biol Chem 274(4): 2038-44.

Scheiffele, P., M. G. Roth, et al. (1997). "Interaction of influenza virus haemagglutinin with sphingolipid-cholesterol membrane domains via its transmembrane domain." Embo J 16(18): 5501-8.

Schneiter, R., B. Brugger, et al. (1999). "Electrospray ionization tandem mass spectrometry (ESI-MS/MS) analysis of the lipid molecular species composition of yeast subcellular membranes reveals acyl chain-based sorting/remodeling of distinct molecular species en route to the plasma membrane." J Cell Biol 146(4): 741-54.

Schroeder, R., E. London, et al. (1994). "Interactions between saturated acyl chains confer detergent resistance on lipids and glycosylphosphatidylinositol (GPI)-anchored proteins: GPI-anchored proteins in liposomes and cells show similar behavior." Proc Natl Acad Sci U S A 91(25): 12130-4.

Schroeder, R. J., S. N. Ahmed, et al. (1998). "Cholesterol and sphingolipid enhance the Triton X-100 insolubility of glycosylphosphatidylinositol-anchored proteins by promoting the formation of detergent-insoluble ordered membrane domains." J Biol Chem 273(2): 1150-7.

Schuck, S., M. Honsho, et al. (2003). "Resistance of cell membranes to different detergents." Proc Natl Acad Sci U S A 100(10): 5795-800.

Shevchenko, A., I. Chernushevich, et al. (1997). "Rapid 'De Novo' peptide sequencing by a combination of nanoelectrospray, isotopic labeling and a quadrupole/time-of-flight mass spectrometer." Rapid Commun. Mass Spectrom. 11: 1015-1024.

Simons, K. and E. Ikonen (1997). "Functional rafts in cell membranes." Nature 387(6633): 569-72.

Simons, K. and D. Toomre (2000). "Lipid rafts and signal transduction." Nat Rev Mol Cell Biol 1(1): 31-9.

Simons, K. and G. van Meer (1988). "Lipid sorting in epithelial cells." Biochemistry 27(17): 6197-202.

Singer, S. J. and G. L. Nicolson (1972). "The fluid mosaic model of the structure of cell membranes." Science 175(23): 720-31.

Smart, E. J., Y. S. Ying, et al. (1995). "A detergent-free method for purifying caveolae membrane from tissue culture cells." Proc Natl Acad Sci U S A 92(22): 10104-8.

Solis, J. O. and R. H. Singh (2002). "Management of fatty acid oxidation disorders: A survey of current treatment strategies." Journal of the American Dietetic Association 102(12): 1800-1803.

Sperl, W., C. Murr, et al. (2000). "Odd-numbered long-chain fatty acids in propionic acidaemia." Eur J Pediatr **159**(1-2): 54-8.

Steen, H., B. Kuster, et al. (2001). "Detection of tyrosine phosphorylated peptides by precursor ion scanning quadrupole TOF mass spectrometry in positive ion mode." Anal Chem **73**(7): 1440-8.

Tanaka, Y. and A. J. Schroit (1983). "Insertion of fluorescent phosphatidylserine into the plasma membrane of red blood cells. Recognition by autologous macrophages." J Biol Chem **258**(18): 11335-43.

Tyni, T. and H. Pihko (1999). "Long-chain 3-hydroxyacyl-CoA dehydrogenase deficiency." Acta Paediatrica **88**(3): 237-245.

van Heusden, G. P., C. P. Reutelingsperger, et al. (1981). "Substrate specificity of lysophospholipase-transacylase from rat lung and its action on various physical forms of lysophosphatidylcholine." Biochim Biophys Acta **663**(1): 22-33.

van Meer, G. and K. Simons (1982). "Viruses budding from either the apical or the basolateral plasma membrane domain of MDCK cells have unique phospholipid compositions." Embo J **1**(7): 847-52.

Van Pelt, C. K., S. Zhang, et al. (2003). "A fully automated nanoelectrospray tandem mass spectrometric method for analysis of Caco-2 samples." Rapid Commun Mass Spectrom **17**(14): 1573-8.

Vance, D. and J. Vance (1996). "New Comprehensive Biochemistry Volume 31: Biochemistry of Lipids, Lipoproteins and Membranes." Amsterdam: Elsevier Science B.V.

Waite, K. A. and D. E. Vance (2000). "Why expression of phosphatidylethanolamine N-methyltransferase does not rescue Chinese hamster ovary cells that have an impaired CDP-choline pathway." J Biol Chem **275**(28): 21197-202.

Walkey, C. J., L. Yu, et al. (1998). "Biochemical and evolutionary significance of phospholipid methylation." J Biol Chem **273**(42): 27043-6.

Wenk, M. R., L. Lucast, et al. (2003). "Phosphoinositide profiling in complex lipid mixtures using electrospray ionization mass spectrometry." Nat Biotechnol **21**(7): 813-7.

Wilm, M. and M. Mann (1996). "Analytical properties of the nanoelectrospray ion source." Analytical Chemistry **68**(1): 1-8.

Xiao, Y. J., B. Schwartz, et al. (2001). "Electrospray ionization mass spectrometry analysis of lysophospholipids in human ascitic fluids: comparison of the lysophospholipid contents in malignant vs nonmalignant ascitic fluids." Anal Biochem **290**(2): 302-13.

Xie, Y., T. C. Gibbs, et al. (2002). "Role for 18:1 lysophosphatidic acid as an autocrine mediator in prostate cancer cells." J Biol Chem **277**(36): 32516-26.

Yamashita, A., T. Sugiura, et al. (1997). "Acyltransferases and transacylases involved in fatty acid remodeling of phospholipids and metabolism of bioactive lipids in mammalian cells." J Biochem (Tokyo) **122**(1): 1-16.

Yao, X., A. Freas, et al. (2001). "Proteolytic 18O labeling for comparative proteomics: model studies with two serotypes of adenovirus." Anal Chem **73**(13): 2836-42.

6 PUBLICATIONS

Ekroos, K., Chernushevich, I.V., Simons, K., Shevchenko, A.

> Quantitative Profiling of Phospholipids by Multiple Precursor Ion Scanning on a Hybrid Quadrupole Time - of -Flight Mass Spectrometer.
> *Analytical Chemistry.* 2002*,* **74**, 941-949.

Shuck, S., Honsho, M., Ekroos, K., Shevchenko, A, Simons, K.

> Resistance of cell membranes to different detergents.
> *Proc Natl Acad Sci U S A.* 2003 May 13; **100**(10), 5795-5800.

Ekroos, K.*, Ejsing, S.C.*, Bahr, U., Karas, M., Simons, K., Shevchenko, A.
(* equal contribution)

> Charting molecular composition of phosphatidylcholines by Fatty Acid Scanning and ion trap MS(3) Fragmentation.
> *Journal of Lipid Research.* 2003 Aug 16; [Epub ahead of print]

Ekroos K, Shevchenko A.

> Simple two-point calibration of hybrid quadrupole time-of-flight instruments using a synthetic lipid standard.
> *Rapid Communication of Mass Spectrometry.* 2002; **16**(12), 1254-1255.

Ekroos, K., Jackson, S., Duchoslav, E., Hao, Z., van Pelt, C.K., Simons, K., Shevchenko, A.

> Comprehensive glycerophospholipid profiling of human disorders by Shotgun Lipidomics.
> (2003; submitted)

Erklärung

Die vorliegende Arbeit wurde im Zeitraum von Juli 1999 bis October 2003 am Max-Planck Insitut für Molekyläre Zellbiologie und Genetik im den Arbeitsgruppen von Dr. Andrej Shevchenko und Prof. Dr. Kai Simons angefertigt. Es haben keine früheren erfolglosen Promotionsversuche stattgefunden. Die Promotionsordnung der Fakultät Mathematik und Naturwissenschaften der TU Dresden erkenne ich an.

Kim Ekroos

Dresden, den 9. October 2003

Versicherung

Hiermit versichere ich, dass ich die vorliegende Arbeit ohne unzulässige Hilfe Dritter und ohne Benutzung anderer als der angegebenen Hilfsmittel angefertigt habe. Die aus fremden Quellen direkt oder indirekt übernommen Gedanken sind als solche kenntlich gemacht. Die Arbeit wurde bisher weder im Inland noch im Ausland in gleicher oder ähnlicher Form einer anderen Prüfungsbehörde vorgelegt.

Kim Ekroos

Dresden, den 9. October 2003